

The effects of operationally relevant head supported mass on neck  
muscle activity during a rapid scanning task

by

Laura Anne Healey

A thesis  
presented to the University of Waterloo  
in fulfilment of the  
thesis requirement for the degree of  
Master of Science  
in  
Kinesiology

Waterloo, Ontario, Canada, 2019

© Laura Anne Healey 2019

## **Authors Declaration**

I hereby declare that I am the sole author of this thesis. This is a true copy of the thesis, including any required final revisions, as accepted by my examiners.

I understand that my thesis may be made electronically available to the public.

## Abstract

The addition of head supported mass, specifically night vision goggles (NVGs), is widely accepted as a key contributor to neck trouble among armed forces rotary wing pilots (Harrison et al., 2009). In fact, nearly 80% of rotary wing pilots in Canada report neck pain (Chafe & Farrell, 2016). However, speculation remains about the pathway by which added head supported mass may link to underlying injury pathways. The objective of this study was to probe how mass, moment of inertia, and range of motion changes associated with NVG use interdependently affect neck muscle activity. Specific research questions probed how range of motion, mass, and moment of inertia would affect co-contraction, integrated EMG, mean EMG, and peak EMG. The overarching aim of this work was to inform design specifications for an optimized helmet, that specifically considers the helmets use as a head supported mass mounting platform.

Thirty participants performed a rapid, reciprocal scanning task, akin to a scanning task performed by pilots. Participants donned four different operationally relevant head supported mass conditions: (1) helmet only (hOnly), (2) helmet, NVGs and a battery pack (hNVG), (3) helmet, NVGs, battery pack, and traditional lead counterweight (hCW), (4) helmet, NVGs, battery pack, and a lead counterweight fitted inside the posterior of the helmet (hCWL). A laser pointer was attached to the NVGs directly in line with participant's field of view allowing them to acquire solar panel targets set up in yaw (left and right) and pitch (up and down) trajectories in both near (35° arc) and far (70° arc) amplitudes. They were asked to acquire as many targets as possible in twenty seconds in both the yaw and pitch trajectories, in each of the helmet and amplitude conditions. Electromyography (EMG) was collected bilaterally on the sternocleidomastoid, upper neck extensors and upper trapezius. However, after processing only the sternocleidomastoid and upper neck extensors were analyzed. Kinematics were collected to

determine the head-trunk velocity, and solar panel data were recorded to determine performance measures such as time to acquire target, and number of targets acquired.

Results showed that HSM condition had a small, but significant effect on co-contraction in the yaw trajectory, where counterweighted conditions (hCW and hCWL) required significantly higher co-contraction than non-counterweighted conditions (hOnly and hNVG). Further, target amplitude had a main effect on integrated EMG and mean EMG, as well as peak EMG and co-contraction. Interestingly, target amplitude also had a significant main effect on mean velocity, where mean velocity was significantly higher at far amplitudes. Increased angular velocity may explain differences in EMG caused by target amplitude. Finally, helmet moment of inertia did not have a main effect on peak EMG. Overall, the results from this study suggest that increased range of motion may be one of the most detrimental effects caused by NVGs. Long term it is suggested designers consider increasing the field of view of NVGs to reduce the range of motion required to perform a scanning task. Alternatively, designers can implement cockpit design changes that reduce the need to move through a wide range of motion. For current helmet designers looking to make immediate changes it is suggested that mass be decreased to limit neck muscle co-contraction requirements.

## Acknowledgements

This thesis would not have been possible without the support and guidance from so many people. First, to my supervisor Dr. Steve Fischer, who introduced me to biomechanics in second year, and who has continued to foster and encourage an environment of curiosity and learning ever since. Thank you for your constant support, guidance, and motivation throughout my academic career!

Thank you to my supervisory committee members, Dr. Jack Callaghan and Dr. Duane Cronin. Your input challenged me to be a better student and researcher and has helped shape this thesis into what it is now. I appreciate your guidance and support throughout this project.

A special thank you to the large team involved in this project, in particular Aaron Derouin for all the project advice and for providing me with the tools and technology necessary for this project. To Amanda Calford for being there for every data collection and helping me with my processing. Without you this project would not have been possible. Thank you to my OBEL lab mates and friends Dan, Nathalie, Sarah, Justin, Sheldon, and Chris for always being around to help trouble shoot, chat, or provide a laugh.

To all my friends who got me through these two years with laughter, late night chats, and a few drinks, you all mean more to me than I can put in words. To Claragh Pegg, my lab mate, first friend at UW, roommate, mentor, and all-around life coach. Thank you for always being there for me and providing me with support, guidance and endless laughter. To Bhillie Luciani, who was my friend before we even met, and who has ridden this wave with me from day one. From 612 labs to late night ice-cream runs, thank you for being beside me for every amazing, and not so amazing minute of this adventure. To Dan Armstrong, who sat (literally) behind me throughout this whole process. Thank you for letting me endlessly pester you with my questions,

absurd ideas, random memes, and for never failing to make me laugh (or occasionally cry). To Taylor Winberg, thank you for the stellar basketball lessons, endless ice cream sammies, and always being there for an all-around good time.

To the coolest dudes ever: Mike Glinka, Lauren Minty, Graham Mayberry, and Dustin Maier. Thank you for being your cool, adventurous, outgoing, open, and loving selves, and for always reminding me of the importance of work-life balance. I'll never forget all the adventures, late-night deck sing-alongs, and weird parties we had, you truly made my time in Waterloo special (and providing me with somewhere to live was also a bonus!). To Dustin Maier, a particularly cool dude, thank you for your constant love and support. Thank you for always providing me with advice and encouragement when I needed it, but also motivation and drive to help me stay on track, I couldn't have done this without you. I am so excited for all the adventures and memories to come with all of you.

Finally, a special thank you to my parents, Lindsay and Larry, and my brother, David (Goby) for supporting me throughout this journey. Your love and support mean the world to me and I would not have made it this far without your encouragement.

# Table of Contents

<b>Authors Declaration.....</b>	<b>ii</b>
<b>Abstract .....</b>	<b>iii</b>
<b>Acknowledgements .....</b>	<b>v</b>
<b>List of Figures .....</b>	<b>x</b>
<b>List of Tables .....</b>	<b>xiv</b>
<b>List of Abbreviations .....</b>	<b>xv</b>
<b>1. Introduction .....</b>	<b>1</b>
<b>1.1 Neck pain and injury among rotary wing pilots.....</b>	<b>1</b>
<b>1.2 Purpose.....</b>	<b>Error! Bookmark not defined.</b>
<b>1.3 Research objective .....</b>	<b>6</b>
<b>1.4 Research questions and hypotheses.....</b>	<b>6</b>
<b>2. Literature Review .....</b>	<b>8</b>
<b>2.1 Anatomy.....</b>	<b>8</b>
<b>2.1.1 Cervical spine .....</b>	<b>8</b>
<b>2.1.3 Musculature .....</b>	<b>9</b>
<b>2.2 Rotary wing pilots.....</b>	<b>11</b>
<b>2.2.1 Flight Schedules .....</b>	<b>11</b>
<b>2.2.2 Operational environment.....</b>	<b>11</b>
<b>2.2.3 Job demands.....</b>	<b>12</b>
<b>2.2.4 Common concerns and neck trouble findings in rotary wing pilots .....</b>	<b>15</b>
<b>2.3 Head supported mass.....</b>	<b>16</b>
<b>2.3.1 The helmet .....</b>	<b>16</b>
<b>2.3.2 The helmet system .....</b>	<b>16</b>

2.4 Biomechanics of neck injury within an aircrew context.....	20
2.4.1 Added mass .....	21
2.4.2 Increased postural deviation to maintain required field of view .....	25
2.4.3 Moment of inertia.....	28
2.5 Design considerations .....	30
<b>3. Methods .....</b>	<b>32</b>
3.1 Subjects .....	32
3.2 Instrumentation .....	32
3.2.1 Electromyography.....	32
3.2.2 Motion Capture.....	34
3.2.3 Head supported mass .....	36
3.2.4 VTAS .....	38
3.3 Experimental design .....	39
3.4 Protocol .....	40
3.5 Processing.....	42
3.5.1 VTAS .....	42
3.5.2 Kinematics .....	43
3.5.3 Operationalizing events.....	45
3.5.4 EMG .....	47
3.6 Dependant Measures .....	48
3.6.1 Co-contraction.....	48
3.6.2 Muscular effort.....	49
3.6.3 Peak EMG .....	50
3.6.4 Mean velocity .....	50
3.7 Statistical analysis .....	50
<b>4. Results.....</b>	<b>52</b>
4.1 Research Question 1: Co-Contraction Ratio .....	52
4.2 Research Question 2: Total Muscular Demand.....	57
4.2.1 Integrated EMG .....	57
4.2.2 Mean EMG.....	60
4.3 Research Question 3: HSM and Peak Muscular Activation .....	63



4.3 Kinematics.....	66
4.4 Performance Measures .....	70
<b>5. Discussion .....</b>	<b>71</b>
5.1 Key Findings .....	71
5.2 Co-Contraction .....	71
5.3 Total muscular effort .....	74
5.4 Peak muscular activity.....	75
5.5 Implications and suggestions .....	77
5.6 Limitations .....	80
5.7 Future Directions .....	82
<b>6. Conclusions.....</b>	<b>83</b>
<b>References .....</b>	<b>84</b>
<b>Appendix A: More on kinematic processing .....</b>	<b>90</b>
<b>Appendix B: Visualization of cutting turns .....</b>	<b>91</b>
<b>Appendix C-1: Upper trapezius example - pitch.....</b>	<b>92</b>
<b>Appendix C-2: Upper trapezius example - yaw .....</b>	<b>93</b>
<b>Appendix D: Full Performance Measures .....</b>	<b>94</b>

## List of Figures

<b>Figure 1:</b> A conceptual model demonstrating possible pathways of injury caused by NVGs .....	3
<b>Figure 2:</b> Cockpit of a Griffon CH-146 Helicopter .....	12
<b>Figure 3:</b> Forde et al. (2011) defined posture comfort zones .....	13
<b>Figure 4:</b> Flying pilot’s percent of total scanning during spend in ROM zones (Tack et al. 2014) .....	14
<b>Figure 5:</b> Comparison between percent of time spend in neutral, mild, and severe neck postures during day and NVG flying. (Forde et al., 2011) .....	14
<b>Figure 6:</b> Location of added equipment COM and its weight .....	17
<b>Figure 7 :</b> A helmet system with NVGs engaged .....	17
<b>Figure 8:</b> Shift in COM with various helmet configurations. A: the head alone, B: the helmet alone, C: NVGs, D: NVGs and CW. From Forde et al. (2009).....	19
<b>Figure 9:</b> Flying pilot average neck reaction forces. From Tack et al. 2014.....	22
<b>Figure 10:</b> Flying pilot average resultant neck torque. From Tack et al. 2014 .....	23
<b>Figure 11:</b> Main effect of helmet on compressive forces at C5-C6 (Barrett, 2016) .....	23
<b>Figure 12:</b> Neck muscle moment arms for the upper and lower cervical regions, the head and neck in the upright neutral position. Moment arms are averaged over muscle subvolumes. A, flexion-extension; B, axial rotation; and C, lateral bending. Adapted from Vasavada .....	26
<b>Figure 13:</b> Normalized active, passive, and total force-length curves. Modified from Patten and Fregly, 2017.....	27
<b>Figure 14:</b> Diagram of the Delsys Trigno mini sensors .....	33
<b>Figure 15:</b> EMG electrode placement A) sternocleidomastoid B) Upper neck extensors C) Upper trapezius.....	34

<b>Figure 16:</b> Reflective marker placement on the participant .....	35
<b>Figure 17:</b> Reflective marker placement on the Gentex HGU-56/P helmet.....	35
<b>Figure 18:</b> Solar panel interaction with the laser pointer. A) target is active but has not been hit with the laser pointer; B) target has been hit with the laser pointer; C) laser pointer has been on target for at least 300ms indicating a successful acquisition.....	39
<b>Figure 19:</b> VTAS target set-up A – yaw 70 °; a – yaw 35 °; B – pitch 70 °; b – pitch 35 °; C – off-axis 70° ; c – off-axis 35° .....	39
<b>Figure 20:</b> Comparison of study seating vs. real seating. A – Car chair with 4-point harness used in study; B – Pilot seat inside a Griffon Helicopter .....	41
<b>Figure 21:</b> Depiction of study protocol and approximate time allocation.....	42
<b>Figure 22:</b> Example VTAS data with labels depicting TAT (time to acquire target – time from one acquisition the next) and HT (honing time – time from the blue to green) .....	43
<b>Figure 23:</b> Local coordinate systems of the head (black) with the origin between the centre of the ears, and trunk (red) with the origin between T10 and the zyphiod process .....	44
<b>Figure 24:</b> An example of operationalizing events based on kinematics and VTAS data in the yaw trajectory. The black trace is head-trunk angular velocity (deg/s) about the z-axis with peaks in velocity indicated with red dots. Green dashed lines indicate where targets have been acquired. ....	45
<b>Figure 25:</b> Example of operationalizing events (turn left, turn right, starting, and honing) for UNER, UNEL, SCML, and SCMR in the yaw trajectory.....	46
<b>Figure 26:</b> Average CCR and NAIEMG ( $\pm$ 1SD) for each HSM condition in the pitch trajectory .....	53

**Figure 27:** Average CCR and NAIEMG ( $\pm 1SD$ ) at each HSM condition in the yaw trajectory. Different letters indicate statistical difference between conditions .....53

**Figure 28:** The effect of amplitude on CCR  $\pm 1SD$  in both the pitch and yaw trajectories. \* Indicates significant differences .....55

**Figure 29:** Amplitude by HSM condition interaction on CCR in the yaw trajectory. Error bars represent 95% confidence intervals. \* Indicates statistical significance.....57

**Figure 30:** The effect of amplitude on integrated EMG  $\pm 1SD$  in both the pitch and yaw trajectories. \* Indicates statistical significance .....58

**Figure 31:** Mean differences in iEMG  $\pm 1SD$  for each muscle between HSM conditions in the pitch trajectory. \* indicates significant differences .....59

**Figure 32:** Mean differences in iEMG  $\pm 1SD$  for each muscle between HSM conditions in the yaw trajectory. \* Indicates significant differences .....60

**Figure 33:** The effect of amplitude on mean EMG  $\pm 1SD$  in all muscles in both the pitch and yaw trajectories. \* Indicates significant differences .....61

**Figure 34:** The effect of HSM condition on mean EMG  $\pm 1SD$  in the pitch trajectory .....62

**Figure 35:** The effect of HSM condition on mean EMG  $\pm 1SD$  in the yaw trajectory .....62

**Figure 36:** Amplitude by condition interactions for starting in the SCML, SCMR and UNEL, and acquiring in the SCML .....65

**Figure 37:** The effect of amplitude on mean velocity in the pitch and yaw trajectories.....66

**Figure 38:** The effect of HSM condition on mean velocity in the yaw trajectory.....67

**Figure 39:** Amplitude by condition interaction effect on mean velocity in the yaw trajectory. Error bars represent 95% confidence interval .....68

**Figure 40:** The effect of amplitude on TAT (time to acquire target).....70

**Figure 41:** Updated potential causal pathways of injury. Highlighted boxes indicate findings from the current study. ....79

**Figure 42:** The effect of amplitude on TAT (time to acquire target) and HT (honing time) in the pitch and yaw trajectories .....94

**Figure 43:** The effect of amplitude on number of targets acquired and error rate in the pitch and yaw trajectories .....95

**Figure 44:** The effect of HSM condition on TAT (time to acquire target) in the pitch and yaw trajectories. Different letters indicate conditions are significantly different. ....96

## List of Tables

<b>Table 1:</b> Origin, insertion, and action of principal superficial muscles in the neck.....	10
<b>Table 2:</b> COM shift and mass moment of inertia in different head mass configurations.....	29
<b>Table 3:</b> Participant demographics.....	32
<b>Table 4:</b> Characteristics of Delsys Trigno mini sensors.....	33
<b>Table 5:</b> HSM conditions and associated mass and relative moment of inertia. <b>A)</b> Gentex HGU-56P helmet <b>B)</b> 3D printed NVGs <b>C)</b> Mock NVGs <b>D)</b> battery pack <b>E)</b> traditional CW <b>F)</b> counterweight liner .....	37
<b>Table 6:</b> Pairwise comparisons for the effect of HSM condition on CCR. * Indicates significant differences .....	54
<b>Table 7:</b> Mean differences of the condition by amplitude interaction effect on CCR .....	56
<b>Table 8:</b> Main effects of amplitude on mean EMG for each muscle in the pitch and yaw trajectories .....	61
<b>Table 9:</b> The effect of amplitude on peak muscular activation.....	64
<b>Table 10:</b> Amplitude by condition interaction for mean velocity in the yaw trajectory .....	69

## List of Abbreviations

HSM .....	Head supported mass
CW.....	Counterweight
NVG .....	Night vision goggle
hOnly .....	Helmet only
hNVG .....	Helmet and night vision goggles
hCW .....	Helmet and counterweight
hCWL.....	Helmet and counterweight liner
EMG .....	Electromyography
COM .....	Centre of mass
UNE .....	Upper neck extensors
SCM .....	Sternocleidomastoid
UT .....	Upper trapezius
MVC .....	Maximum voluntary contraction
VTAS .....	Visual target acquisition system
CCR .....	Co-contraction ratio
TAT .....	Time to acquire target
HT .....	Honing time
NAIEMG .....	Normalized average integrated EMG
iEMG .....	Integrated EMG

# **1. Introduction**

## **1.1 Neck pain and injury among rotary wing pilots**

Neck injury and chronic neck pain disable a substantial number of Canadian Armed Forces Aircrew at any given time. In 2014, 80% of the Royal Canadian Air Force 146 Griffon Helicopter aircrew reported chronic neck pain, and 78 aircrew were grounded due to neck injury at some point in their career (Chafe & Farrell, 2016). In a global context, 58% of the United States Army report neck trouble related to flying, compared to 57% in Sweden (Ang & Harms-Ringdahl, 2006), 43% in the Netherlands (van den Oord, 2010), 38-81% in the United Kingdom, and 29% in Australia (Thomae et al, 1998). Further, in Canada 15% of pilots have been grounded at least once in their career due to flight-related neck pain (Adam, 2004). The impact of neck trouble among pilots is extensive. Neck trouble can affect performance and reduce operational readiness, compromising the pilot, their crew, and the mission. Additionally, there are large financial costs due to loss of manpower and litigation (Salmon et al., 2011). Consequently, there is a strong need to address this problem and reduce neck trouble among rotary wing aircrew pilots.

Unfortunately, the exact mechanism(s) causing aircrew neck pain remains unknown. However, helmets and additional head supported mass (HSM) have widely been accepted as key contributors (Adam, 2004; Manoogian et al., 2006; Harrison et al., 2007). In the past 30 years, technological advances have led to an increase in HSM with additional devices being mounted on the helmet such as night vision goggles (NVGs), heads up displays (HUD), counterweights (CW) and chemical threat masks (Manoogian et al., 2006). This additional equipment affects the distribution of mass, increasing force and torque on the neck, thereby affecting multiple static



and dynamic characteristics of the head and neck system when cruising in the aircraft at altitude and when performing rapid head movements as required to navigate the helicopter (Forde et al., 2011; Manoogian et al., 2006).

Notably, NVGs have been found to be particularly concerning (Harrison et al., 2007; Wickes, Scott, Greeves, 2005; & Thuresson, Ang, Linder, & Harms-Ringdahl, 2005). In fact, neck strain has affected 90% of aircrew logging at least 150 hours of night flying (Adam, 2004) and NVG users experience a 45% greater chance of head and neck injury compared with non-NVG users (Shannon & Mason, 1997). NVGs are the most commonly used head supported device (following the helmet) and are critical for mission effectiveness, however, they appear to come at a large cost for pilots.

Despite a wide body of evidence suggesting that NVGs and their subsequent effect on the overall HSM is likely the key contributor to neck pain among rotary wing aircrew, little has been done to mitigate the problem. Some authors suggest that a CW is beneficial as it will counter-balance the forward weight of the NVGs (Harrison et al., 2009), however the effectiveness of this approach remains uncertain (Farrell et al., 2014; McKinnon et al., 2016). In the field, pilots are also divided on the usefulness of a CW and use is often based on personal preference (Fischer et al., 2013). This is not surprising, as the current CW solution is not standardized, and pilots will simply add a lead block on the posterior of the helmet, increasing both the moment of inertia and the mass (Fischer et al., 2013; Farrell et al., 2016). While theoretically a simple CW solution would be effective when seated upright and static, in reality, pilots are rarely static and must move their heads through a wide range of postures, possibly making the CW ineffective and even harmful. There is an opportunity to seek alternative counter

balancing mechanisms that would effectively mitigate the effects of the NVGs, reducing neck trouble among helicopter aircrew.

Before an optimized helmet / CW system can be developed, leading causes of neck trouble must first be better understood. It is hypothesized that NVGs generate three main mechanical challenges in dynamic situations (**Figure 1**). First, the use of NVGs adds mass, increasing loading on the cervical spine and creating a flexor moment about the atlanto-occipital joint. The neck extensors must activate to balance the flexor moment in addition to contracting to stabilize the head. As a result of the added forward positioned mass, neck trouble could be related to an increase in the resulting in a cumulative loading on the cervical spine and/or to an increase in the sustained low-level muscle activity in the neck extensors, often referred to as the Cinderella hypothesis (Hagg, 1991; Hogdon et al., 1997). Second, NVGs reduce the pilots field of vision from 140° to 40° (Craig et al., 1997), requiring pilots to move through a larger range of motion and adopt more extreme postures to scan the same area. At end ranges of motion muscle fascicles are lengthened, putting them at a mechanical disadvantage and reducing their force production capability. In turn, there is an increased relative muscular demand which may also lead to damage of microstructures and an overexertion injury (Forde et al., 2011, Tack et al., 2014). Third, the location of the NVGs increases the moment of inertia. This will result in a change in resistance to angular motion therefore requiring larger muscle forces to stop and start the head. Increased muscle forces result in increased stress (force per unit area), which over time, can exceed tissue tolerance and possibly result in an overexertion injury or pain due to tissue damage (Kumar, 2001). The effect of NVGs and CWs on the development of neck trouble is likely multifactorial, making injury pathways difficult to understand. However, isolating potential pathways will provide insight to prioritize what factors are most important to consider

for novel helmet designs that may mitigate flight related neck trouble. Understanding how HSM, particularly the change in mass, moment of inertia, and posture, as a result of donning NVGs and CWs, impacts neck function (neck muscle activity) will provide critical insight to further probe the likelihood of potential mechanisms of injury. By increasing knowledge about the plausible injury pathways, we will be better informed to not only design safe and effective interventions (e.g., modified helmets) that maximize performance, but also minimize injury risk.

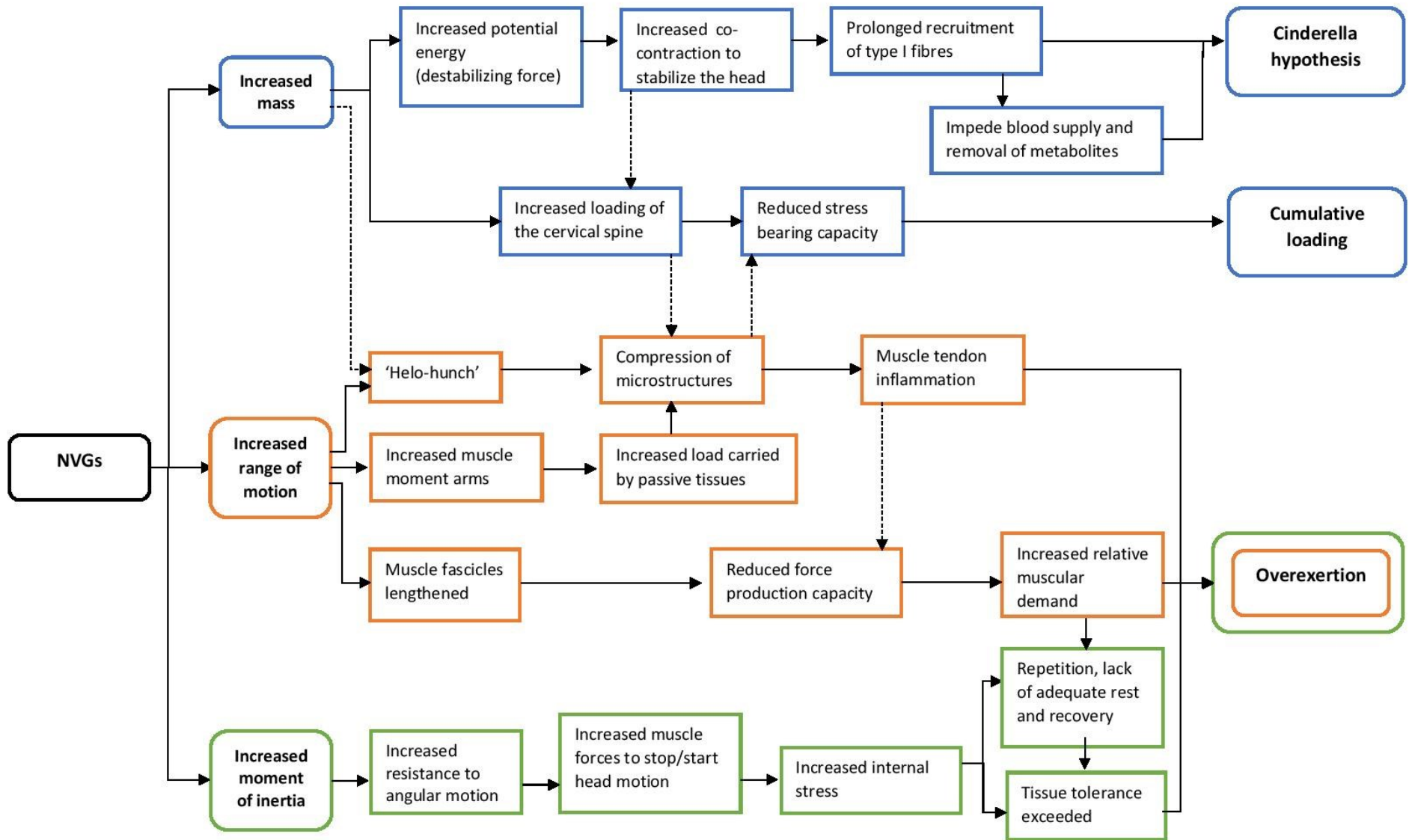


**Figure 1:** A conceptual model demonstrating possible pathways of injury caused by NVGs

The primary purpose of this research was to provide insight into the effects of operationally relevant HSM conditions on neck function during the performance of a rapid, reciprocal visual target acquisition task. Specifically, the aim was to probe how increased mass, moment of inertia, and posture interpedently affect neck function. This thesis assessed participants as they performed rapid head movements under different operationally relevant HSM configurations using equipment including a helmet (hOnly), NVGs (hNVG), a traditional CW (hCW) and a novel CW built into the helmet liner as developed to reduce the moment of inertia relative to a traditional CW configuration (hCWL).

### **1.3 Research objective**

The main objective of this research was to understand the effect of HSM and its configuration on neck function by probing how mass, moment of inertia and posture effect outcome measures that have been implicated in injury pathways. The following research questions will be addressed to meet this objective.

### **1.4 Research questions and hypotheses**

**Research question 1:** Does increased operationally relevant HSM increase *co-contraction* of the neck muscles during the performance of a rapid reciprocal visual target acquisition task.

**Hypothesis 1:** There will be a main effect of condition on co-contraction where post-hoc testing will reveal increases in co-contraction with conditions where head supported mass was increased (e.g., hOnly < hNVG < hNVG+CW = hNVG+CWL).

**Research question 2a:** When range of motion is increased, does *total muscular demand* increase during starting and acquiring phases of a rapid reciprocal visual target acquisition task.

**Research question 2b:** If so, is there an interaction effect of *total muscular demand* between range of motion and head supported mass condition.

**Hypothesis 2:** There will be a main effect of range of motion where muscular demand will be larger at larger target amplitudes. There will also be an interaction effect between range of motion and head supported mass condition where difference in muscular demand will only be detected between conditions that have altered moment of inertia properties when tested in the larger amplitude (e.g., at smaller amplitude:  $h_{\text{Only}} = h_{\text{NVG}} = h_{\text{CW}} = h_{\text{CWL}}$ ; and at larger amplitude  $h_{\text{Only}} < h_{\text{NVG}} = h_{\text{CWL}} < h_{\text{CW}}$ ).

**Research question 3:** Does increased moment of inertia increase *peak muscular activation* required to accelerate and decelerate the head during the performance of a rapid reciprocal visual target acquisition task.

**Hypothesis 3:** There will be a main effect of condition on peak muscular demands where post-hoc testing will reveal increases in peak muscular activation during starting and acquiring phases with conditions with increases in moment of inertia (e.g.,  $h_{\text{Only}} < h_{\text{NVG}} = h_{\text{CWL}} < h_{\text{CW}}$ ).

## **2. Literature Review**

### **2.1 Anatomy**

#### **2.1.1 Cervical spine**

The cervical spine is made up of seven vertebrae. They are the smallest and most fragile of the spine (Marieb, 1998). The three main functions are as follows: support the weight of the head, allow the head to move, and protect the nervous system. Swartz, Floyd, and Cendoma (2005) report the full range of motion is approximately 80° to 90° of flexion, 70° of extension, 20° to 45° of lateral flexion and up to 90° of rotation. However, movement is quite complex, and each vertebrae contributes differently to the movement of the head and neck system.

#### **Atlas and axis**

The first cervical vertebra, also known as the atlas, articulates with the occiput of the skull creating a cradle for the head (Swartz, Floyd & Cendoma, 2005; Bogduck & Mercer, 2000). The atlas is strictly responsible for flexion and extension (i.e. nodding) with a range of motion around 15° to 20°. No rotation or lateral flexion is possible between the occiput and atlas due to the depth of the atlantal sockets where the occiput condyles articulate (Swartz, Floyd & Cendoma, 2005). The second cervical vertebra, known as C2, or the axis, articulates with the atlas and bears the weight of the head through the lateral atlanto-axial joints (Bogduck & Mercer, 2000). The atlanto-axial junction allows the head to rotate from side to side. The range of motion of this joint has been reported as low as 32° in cadavers and up to 75.2° using radiographic techniques. The rotation about this joint accounts for 50% of the rotation in the cervical spine.

## **Cervical column**

The rest of the cervical vertebrae (C3-C7) are referred to as the cervical column. These vertebrae resemble more typical vertebrae with key features such as a body anteriorly, and a neural arch composed of pedicles and laminae posteriorly. Vertebrae are separated by intervertebral discs and articulate with each other creating joints similar to saddle joints. Each joint is capable of rotation and flexion motion, but not lateral flexion. Lateral flexion of the cervical spine is possible due to coupled rotational movement of each segment. All the joints in the cervical spine work together to move the neck, but the movement of the neck does not necessarily reflect the movement at each individual vertebra. Therefore, a vertebra may reach its end range of motion in either flexion or extension before the neck is fully flexed or extended (Swartz, Floyd and Cendoma, 2005). Van Mareren et al. (1990) used high-speed cineradiography to determine that flexion and extension begins at the lower cervical spine, followed by the occiput, atlas and axis, and finally C3-C4. Because we cannot assume uniplanar movement of the cervical spine, it is very difficult to understand individual cervical spine movements by observing the motion of the head alone.

### **2.1.3 Musculature**

Muscle and ligament involvement in head stabilization and movement is very complex and differs based on the position of the head and the motion involved (Adam, 2004). It is estimated that the osteoligamentous system contributes 20% of mechanical stability which the surrounding neck musculature contributes 80% (Panjabi et al., 1998). Ligaments typically contribute to stability at end ranges (Harms-Ringdahl et al. 1986) while muscles provide dynamic support throughout the neutral and mid-range of motion (Falla, 2004).



There are over 20 muscle pairs that aid in stabilizing and moving the head and neck. Ligaments also play a key role in the cervical spine, resisting tensile or distractive forces. Further increasing the complexity of the head neck system, the responses of the ligaments and muscles of the neck differ depending on the position and magnitude of the load (Yoganandan et al., 2001).

Larger superficial muscles are the most commonly considered in the HSM literature. They include the sternocleidomastoid, upper trapezius, and splenius capitis (Alem & Baranzaji, 2006; Pousette et al. 2016; Harrison et al. 2009). The origin, insertion, and action of these muscles are explained in **Table 1**. Smaller and deeper muscles are more often considered in modeling studies due to their inaccessibility. However, smaller and deeper muscles, like the longus capitis and longus coli, play an important role in stabilizing the cervical spine against gravity (Yughdtheswari & Reddy. 2012).

**Table 1:** Origin, insertion, and action of principal superficial muscles in the neck

<b>Muscle</b>	<b>Origin</b>	<b>Insertion</b>	<b>Action</b>
<b>Sternocleidomastoid</b>	Manubrium of the sternum and clavicle	Superior nuchal line (anterior portion) and mastoid process of temporal bone	Flexes the head and rotates the head to the contralateral side
<b>Splenius capitis</b>	Lower half of ligamentum nuchae and spinous processes from C6-T2	Superior nuchal line (lateral portion) and mastoid process of temporal bone	Extends the spine and bends the neck and neck to the ipsilateral side
<b>Upper trapezius</b>	External occipital protuberance, medial third of the superior nuchal line of the occipital bone, and spinous processes of C7	Lateral third of the clavicle, acromion and scapular spine of the scapula	Tilt and turn the head, shrug, steady the shoulders, and twist the arms

## **2.2 Rotary wing pilots**

There are two pilots that sit in the cockpit to operate the Royal Canadian Airforce 146 Griffon Helicopter, the flying pilot, and non-flying pilot (co-pilot) (Fischer et al. 2013). The roles and job demands are similar between the pilot and co-pilot in all rotary wing aircrew. The job of a pilot is complex and multidimensional, placing both physical and mental demands on the individual.

### **2.2.1 Flight Schedules**

At minimum, pilots in the Canadian Armed Forces are required to complete 50 training hours every six months. Specifically, training must include 8 hours of night flying with at least 5 of those hours with NVGs. On average, a training flight lasts from 1.5-2.5 hours, however, an actual flight can last up to 3.5 hours before a refuel is required. Fischer et al. (2013) reported that crew members normally fly between 200 to 300 hours per year with about 25% of those hours spent flying with NVGs.

### **2.2.2 Operational environment**

From an ergonomics standpoint, the cockpit is poorly designed. Both pilot and co-pilot are harnessed in their seats and have limited overhead space mainly restricted by the rotor brake and communication cables (Fischer et al. 2013). Lack of open space requires awkward and extreme postures when performing scanning and searching tasks (Forde, 2011). Both pilots are required to reach controls that are placed in front of them on the dash, as well as above their heads (**Figure 2**). Further, pilots are exposed to a low level sinusoidal vibration generated by the rotor blades, with random jolts from air turbulence or quick aircraft maneuvers (Bulter, 1992).



**Figure 2:** Cockpit of a Griffon CH-146 Helicopter

### 2.2.3 Job demands

In the CH-146 Griffon helicopter the main responsibility of the pilot is to fly the helicopter while the co-pilot is primarily responsible for monitoring the MX-15 Vision system (Fischer et al. 2013). Both the pilot and co-pilot are required to move their head, neck, and body to operate aircraft controls and to scan the outside environment, frequently tilting and turning their heads. The co-pilot experiences additional side-bending to monitor to MX-15 Vision system. The small cabin combined with scanning task requirements results in ergonomically unfavourable positions and cause the neck to be slightly rotated and often flexed (Lopez et al., 2001). This position has been referred to as the ‘helo-hunch’, and has long been understood as a risk factor for neck, back, and leg pain (Phillips, 2011). In fact, in a 2014 DRDC report it was

found that pilots have significantly less neck strength when axially rotated with flexion or extension compared to neutral flexion or extension (Callaghan et al., 2014). Multiple authors have reported that NVGs contribute the ‘helo-hunch’ posture. Both Tack et al (2014) and Forde et al (2011) reported postures throughout a flight and determined that, based on comfort zones used by Forde et al. (2011) (**Figure 3**), a larger percent of the time is spent in mild to severe axial rotation and lateral bend postures when wearing NVGs, while more time is spent in neutral positions in day conditions (**Figures 4-5**). Throughout a flight, compression, resultant torque, and posterior shear have been found to best represent the physical demands affecting neck strain (Tack et al., 2014). The main concerns affected pilot’s ability to meet job demands, reported by CH-146 Griffon helicopter aircrew, are the weight and moment of inertia of the helmet (specifically from NVGs), postural requirements, and vibration of the aircraft (Fischer et al., 2013).

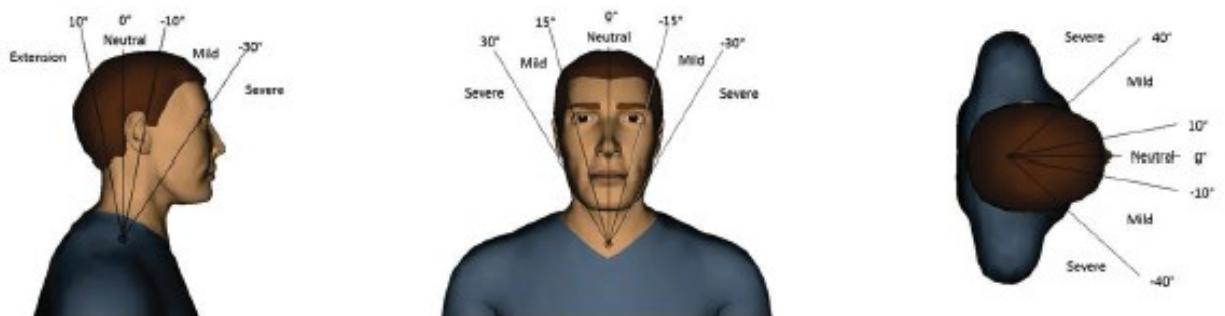


**Figure 3:** Forde et al. (2011) defined posture comfort zones

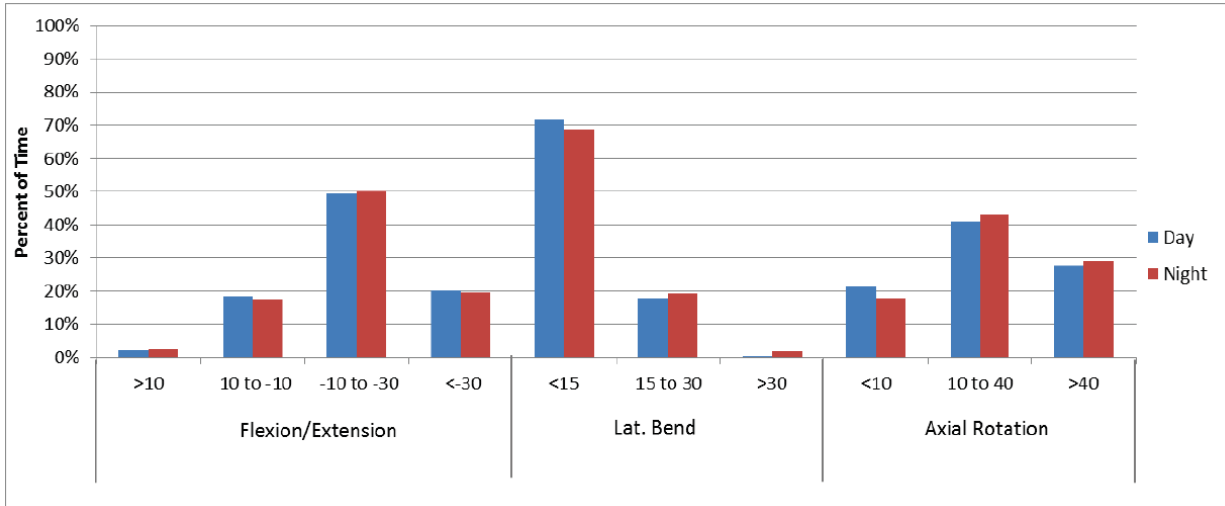


**Figure 4:** Flying pilot's percent of total scanning during spend in ROM zones (Tack et al. 2014)

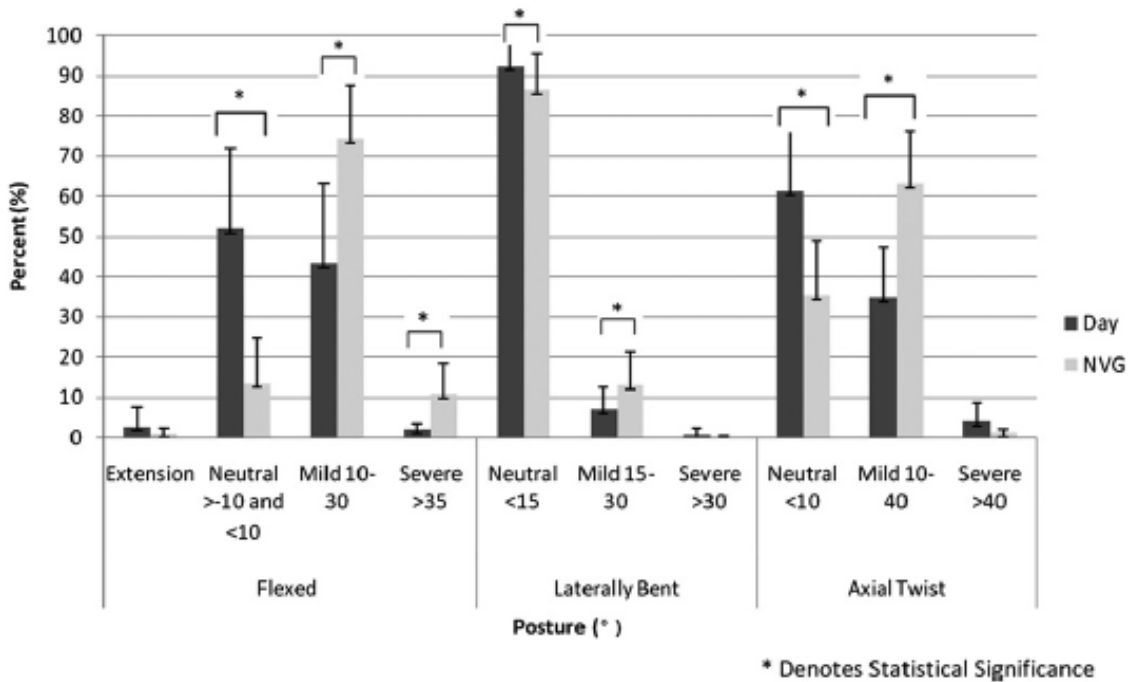


**Figure 5:** Comparison between percent of time spend in neutral, mild, and severe neck postures during day and NVG flying. (Forde et al., 2011)

#### **2.2.4 Common concerns and neck trouble findings in rotary wing pilots**

Neck trouble in pilots has been reported to vary from minor neck pains, aches, and strains, to more severe cases of cervical spine arthritis. While neck strain is among the most commonly reported injury among helicopter pilots (Adam, 2004), the term has not been clearly operationalized, and specificity of this injury is limited. In general, neck strain occurs when muscle or tendon fibres of the neck tear either by stretching too far, or due to repetitive trauma (Altizer, 2003). Failure to take breaks or neglecting to stretch before and after exercising the muscles can also lead to straining. This can occur on a spectrum of severity, from micro-tears to a complete rupture. Ligaments can also be injured, usually caused by a wrench or twist (Altizer, 2003). Symptoms can include aches, pain, and dysfunction and they may become chronic, lasting long after a flight (Adam, 2004).

In more severe cases, the cervical spine can be injured. Out of all military personnel, helicopter pilots are the most likely to have spondylitis, spondylarthritis, osteophytic spurring or arthrosis deformans in the spine, and are at increased risk of developing premature cervical arthritis (Aydog, et al., 2004, Landau et al. 2006). In fact, cervical disc degeneration was found in 50% of helicopter pilots, a greater percentage than transport pilots and fighter pilots (Landau et al. 2006). Aydog et al. (2004) took X-rays of 732 male flight personnel (helicopter, jet, and transport aircraft pilots) and 202 controls over a one year period. It was found that helicopter pilots had a significantly higher number of cervical osteoarthritic changes compared to the controls and the other flight groups. In total 19% of helicopter pilots had cervical disc changes over the year, with 13.84% exhibiting osteoarthritis, 3.14% with decreased lordosis, 1.25% with avulsion fracture, and 1.25% with ligament calcification.

## 2.3 Head supported mass

### 2.3.1 The helmet

The main purpose of the helmet is to protect the head from impact injury and blows to the head due to rapid deceleration or acceleration, falling debris, and other flight hazards (Harrison et al., 2015). Since helmets are primarily designed for blast and impact protection, there is often less regard for ergonomic factors such as mass and distribution of mass. A Gentex HGU 56P helmet weighs 1.4 kg and shifts the centre of mass (COM) 0.5 cm posterior and 7 cm inferior from the heads' natural COM (Forde et al., 2011).

### 2.3.2 The helmet system

Together, the helmet and the devices added onto the helmet are referred to as the helmet system. Common items mounted on the helmet include night vision goggles (NVGs), heads up display (HUD), chemical threat masks, and counterweights (CW). While these devices provide useful and often critical aid to pilots, they all add additional off-centre mass on the head and neck system, increasing head borne load and moment of inertia (**Figure 6**).

#### *Night vision goggles*

NVGs are the most commonly used equipment mounted on the helmet (Harrison et al., 2007) (**Figure 7**). During night missions and missions with poor environmental conditions, pilots rely on NVGs for a safe and successful sortie (Harrison et al., 2007). However, while NVGs are a critical tool for pilots, they are widely accepted as a main contributor to neck trouble amongst rotary wing pilots (Harrison et al., 2007; Wickes, Scott, Greeves, 2005; Thuresson, 2005; & Thuresson, Ang, Linder, & Harms-Ringdahl, 2005). Adding NVGs to the helmet system increases HSM by ~0.6 kg and shifts the COM of the head anteriorly and superiorly increasing the moment on the neck and destabilizing the head (Butler, 1996; Thuresson et al., 2005). Further

complicating the problem, NVGs restrict a pilot's field of vision from 140 degrees to 40 degrees, essentially eliminating their peripheral vision (Craig et al., 1997).

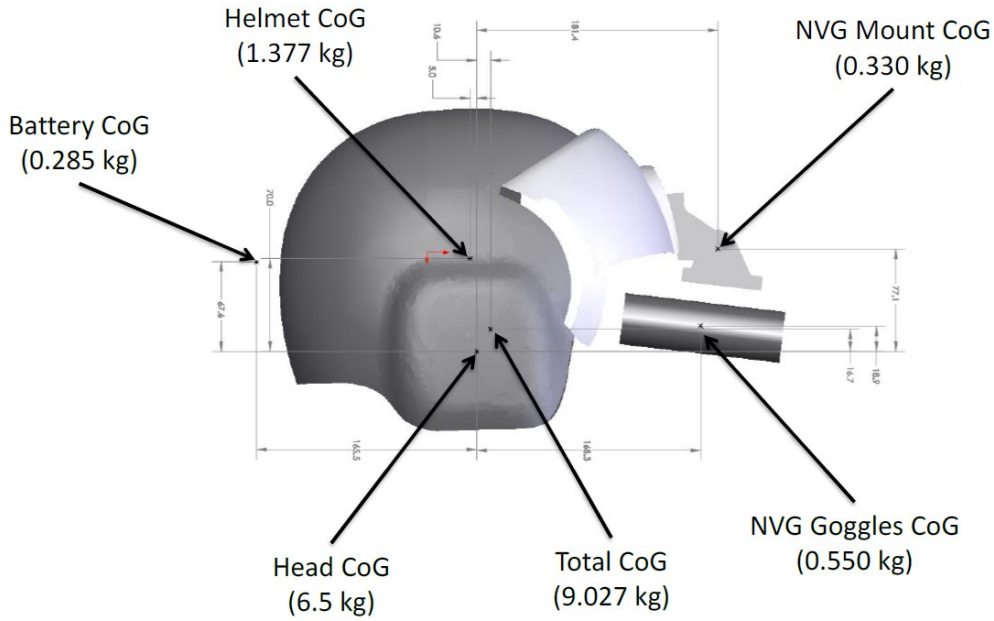


**Figure 6:** Location of added equipment COM and its weight



**Figure 7 :** A helmet system with NVGs engaged



A 2004 survey by Adam sought to determine the rate and severity of neck strain experienced by CH-146 Griffon pilots and flight engineers. After interviewing 196 Griffon aircrew (employ NVGs) and 85 Sea King aircrew (do not employ NVGs) it was found that Griffon pilots experienced significantly more neck pain than pilots of the Sea King. Griffon pilots indicated that the use of NVGs were a primary contributor to their neck pain and the evidence supported that 90% of pilots who logged over 150 hours of night flying (with NVGs) in their career report neck trouble. Similar findings in the Netherlands by van den Oord (2010) showed that pilots who self-reported neck pain had significantly more flying hours than those who were asymptomatic. Of the pilots who reported neck pain, about half attributed their neck pain to NVG use.

### *Counterweights*

In an attempt to balance the moment on the neck caused by the forward weight of the NVGs, many pilots chose to employ a CW system to offset the weight of NVGs and bring the COM closer to its natural location (**Figure 8**). A CW is often a lead block inserted at the back of the helmet into the pocket between the helmet and the NVG battery pack.

Despite multiple research attempts, there is still debate over whether CW use mitigates the effect of NVGs and reduces injury, or compounds the problem. Harrison et al. (2007) reported less metabolic and hemodynamic stress in the trapezius when a CW was used during night flights. Further, Thuresson et al. (2005) showed that in both a neutral and 20 degrees flexed position muscle activity increased when NVGs were added, and decreased when a CW was added, suggesting that a CW is beneficial in static postures. However, Harms-Ringdahl et al (1999) and Farrell et al (2016) both determined that while using a CW was beneficial when the head and neck are in a neutral position, as postures deviate from neutral the benefits decreased

and even became harmful. Other evidence suggests that use of a CW is not beneficial nor harmful (Callaghan et al., 2014). Overall, the effectiveness of a CW in dynamic flight is still unknown.

While the use of CWs is widespread, there is still no standardization. Harrison et al. (2007) is one of the only authors who provides guidelines around CW use, which states that pilots who chose to use a CW are bound by an upper limit of 0.65kg. Other authors have reported weights ranging anywhere from 0.35kg (Thuresson et al. 2003) to 0.9kg (Fischer et al., 2013), and many authors do not provide information on CW mass. Overall, there is a wide variety and individualization in both weight and the placement of the weight chosen by the pilot (Fischer et al., 2013).

Due to the lack of standardization of the CW, there is reason to believe that a CW system can be redesigned. However, first it is important to better understand possible causal factors predisposing aircrew to neck pain so that these factors can be mitigated in an optimized CW design.



**Figure 8:** Shift in COM with various helmet configurations. A: the head alone, B: the helmet alone, C: NVGs, D: NVGs and CW. From Forde et al. (2009)

## 2.4 Biomechanics of neck injury within an aircrew context

In general, neck pain and related musculoskeletal injury is often multifactorial, suggesting that there are a number of factors that contribute to its development (van den Oord, 2010; Forde et al., 2011). Rotary wing pilots are faced with a number of ergonomically unfavourable conditions, all which likely interact in some manner to contribute to neck pain and injury. Since it has been widely suggested that the NVG system (NVG + CW) are of most concern, it is important to understand what changes the NVG system make on the head and neck system. We postulate there are three main effects that the NVG system imposes on the head and neck system: 1 – increased mass, 2 – increased postural deviation to maintain required field of view, 3 – increased moment of inertia. A fourth factor that is important to consider is vibration, which has been cited as a contributing factor for neck pain and is therefore worth discussing.

**Figure 1** provides a conceptual model to demonstrate how the first three factors may influence injury mechanisms such as cumulative loading and overexertion. This section will explore the biomechanical impact of these changes and their possible mechanisms of injury

### 2.4.1 Added mass

#### *Cumulative loading*

Increased external loading on the cervical spine by donning an NVG and CW may be a key contributor to flight-related neck pain (Murray et al., 2016). The cervical spine supports the head (approximately 40 N), but also must withstand substantial compressive loads *in vivo* due to muscle co-activation forces required to balance the head (Patwardhan et al., 2000). During activities of daily living the compressive load on the cervical spine is estimated to range from 120 to 1200 N (Choi et al., 1997; Patwardhan et al., 2000). Work by Farrell in 2016 showed that aircrew experience elevated neck loads up to 20 times greater than office workers.

In a report for Defence Research and Council Canada Tack et al. (2014) had 12 pilots wear a full-body inertial motion suit (X-Sens) and complete tasks common to a pilot in a helicopter. Using a basic static single segment model, torques, joint angles, and reaction forces about the C7-T1 joint were calculated. Results for reaction forces and torque in different positions during day (without NVGs) and night (with NVGs) are presented in **Figures 9 and 10**. It was determined that resultant forces and resultant torque values were higher during each task when NVGs were worn, suggesting that it may increase a pilot's likelihood of a cumulative load injury. While this study was limited to reaction forces, research from Barrett (2016) calculated bone on bone compressive forces at C5-C6 for different head loads using an EMG-driven model (**Figure 11**). Interestingly, this research found no significant difference between a helmet with NVGs and a helmet with NVGs + CW. However, both a helmet and NVGs and a helmet with NVGs + CW resulted in significantly higher compression forces (about 100N more) than wearing the helmet only. Further, not wearing a helmet produced significantly less compression

than all the HSM conditions. High C5-C6 compression with HSM must be sustained over long hours of flight, implicating cumulative load as a mechanism for injury.

It is important to note the limitations to both these studies. First, the research from Tack et al. (2014) used a number of assumptions including C7-Tragion length, head COM location, head mass and location of the tragion. Further, with only the X-Sens system, they were limited to calculating reaction forces and could not determine internal forces and therefore the compression on the spine. The work by Barrett (2016) provides valuable information, however only static postures were assessed and it is likely that HSM will have a large impact during dynamic movement. Ideally, future research should combine dynamic movements with modeling efforts in order to fully understand the effects of HSM on the head and neck system.

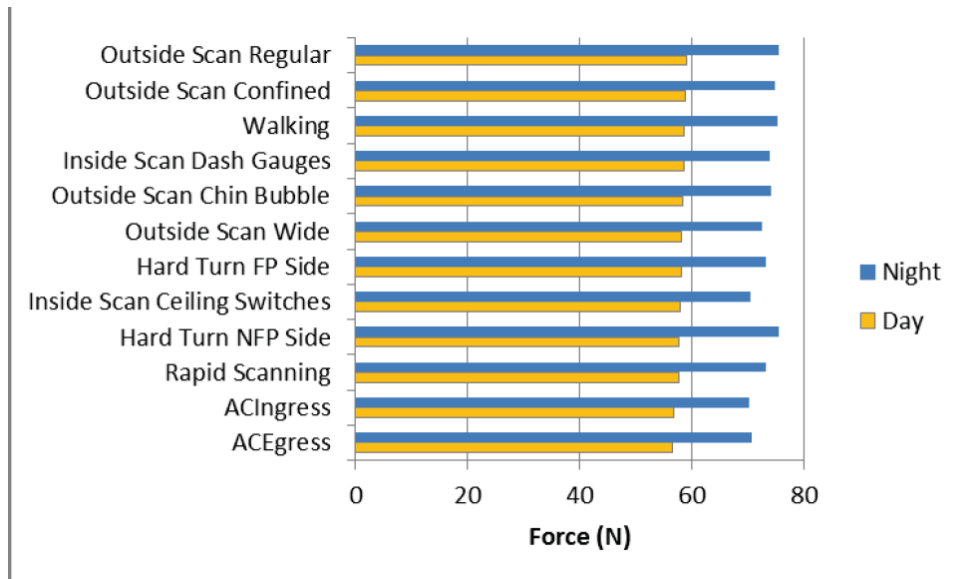


**Figure 9:** Flying pilot average neck reaction forces. From Tack et al. 2014

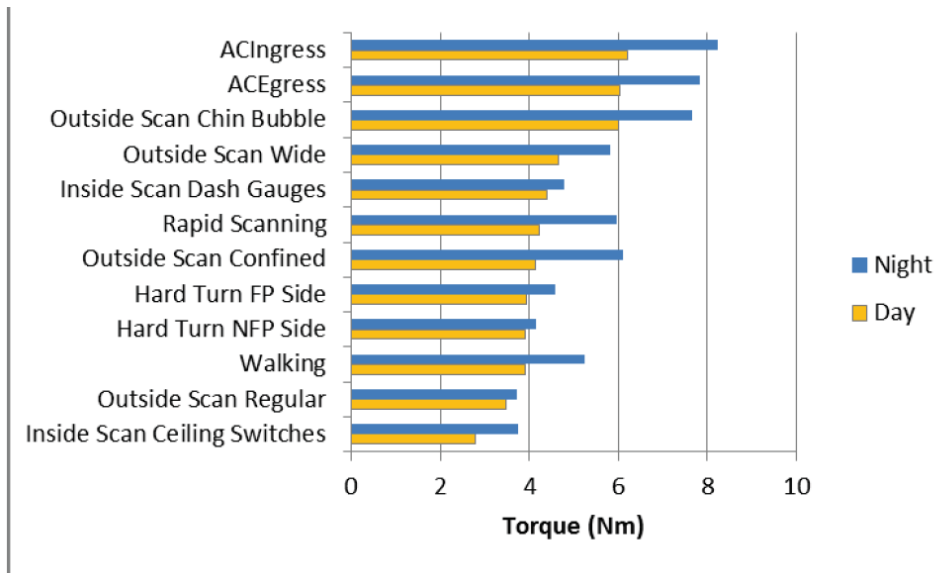


**Figure 10:** Flying pilot average resultant neck torque. From Tack et al. 2014

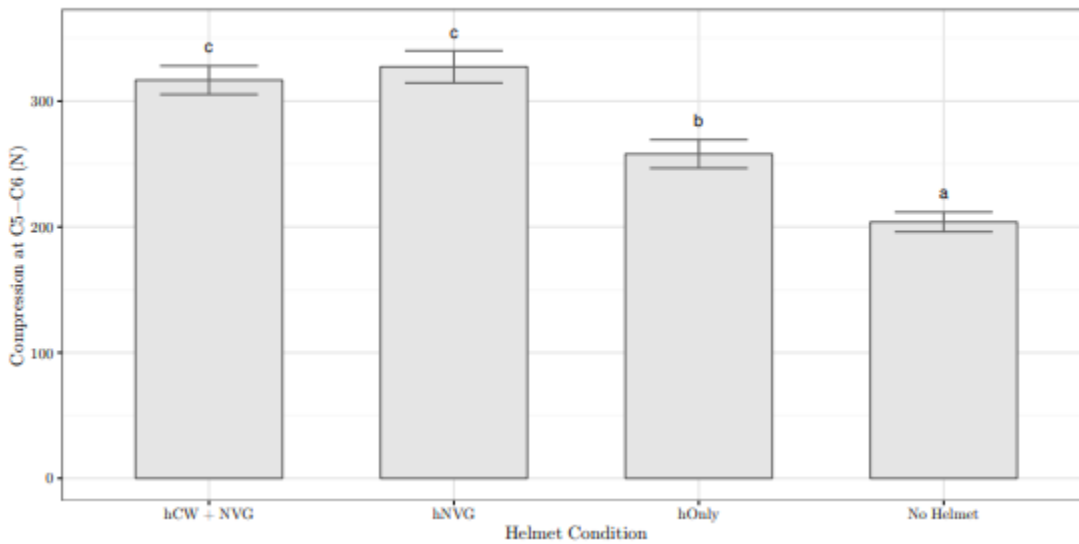


**Figure 11:** Main effect of helmet on compressive forces at C5-C6 (Barrett, 2016)

### *Cinderella hypothesis*

The “Cinderella hypothesis” offers an alternative explanation for how added mass may result in injury. Added off-centre mass on the helmet creates a destabilizing force on the head. A load moment can be stabilized with muscle forces, or alternatively, tension of passive connective tissues (Harms-Ringdahl et al., 2007). Interestingly, Pozzo et al. (1989) showed that cervical musculature activation will compensate for added head supported mass and maintain kinematics. In fact, Dibb (2013) showed that the spine can be statically loaded up to 40% of acute failure load before kinematics change. This suggests that neck musculature is working very hard to constantly keep the head balanced even before kinematic changes become noticeable. The “Cinderella Hypothesis” (Hagg, 1991) provides a possible explanation for how this constant low-level muscle activity may lead to injury.

The Cinderella hypothesis is based on Henneman’s size principal and postulates that low level activity can result in injury since type I fibres are the first to be recruited and the last to be turned off. With little to no rest, type I fibres could be overworked and this may result in fibre injury, resulting in neck pain. Supporting evidence shows that sustained muscle activity as low as 5% can cause ischemic muscular pain and localized muscle fatigue (Sjogaard et al. 1986). Low level static muscle contractions could also put pilots at risk of cumulative trauma and repetitive strain injuries (Sjogaard and Jensen, 2006).

Multiple authors have assessed neck muscle activity in common pilot postures while wearing HSM, as well as during flight, and confirm that there are sustained low level contractions throughout the entire flight. Hogdon et al (1997) found that paraspinal muscles exhibit tonic activity while pilots are in flight. This means that the small supporting muscles of the neck are in a continuously contracted state. Murray et al. (2016) collected muscle activity

from the upper neck extensor (UNE), upper trapezius (UT) and sternocleidomastoid (SCM) during a sortie and found that the UNE had a sustained muscle activity of 10% maximum voluntary contraction (MVC). Injury resulting from these low level, sustained contractions throughout a 1.5-3 hour flight may be explained by the Cinderella hypothesis.

#### **2.4.2 Increased postural deviation to maintain required field of view**

##### *Overexertion*

The moment-generating capacity of a muscle is the product of its moment arm and maximum isometric force (Vasavada et al. 1998). The moment arm is defined as the perpendicular distance from a muscle's line of action to the axis of rotation. Moment arms, and therefore moment-generating capacity of a muscle, can change with posture. The complex nature of head and neck anatomy can make it difficult to calculate the moment arm of a muscle, however many authors have used modeling techniques to estimate the length in different postures. Vasavada et al. (1998) used a biomechanical model to determine how moment arms affect the moment-generating capacities of individual neck muscles. Moment arm lengths in the upright neutral position are presented in **Figure 12**. They found that during extension the moment arm of the sternocleidomastoid increases dramatically, doubling the flexion moment-generating capacity. The moment arms of the semispinalis capitis, trapezius, and splenius increase up to 2-3cm from flexed to extended postures. For lateral bending sternocleidomastoid, trapezius, and the lateral portion of the splenius increased up to 3cm. As moment arms change through different postures, a muscles moment-production capacity also changes. When a muscle moment-generating capacity increases, a larger torque is put on the axis of rotation.



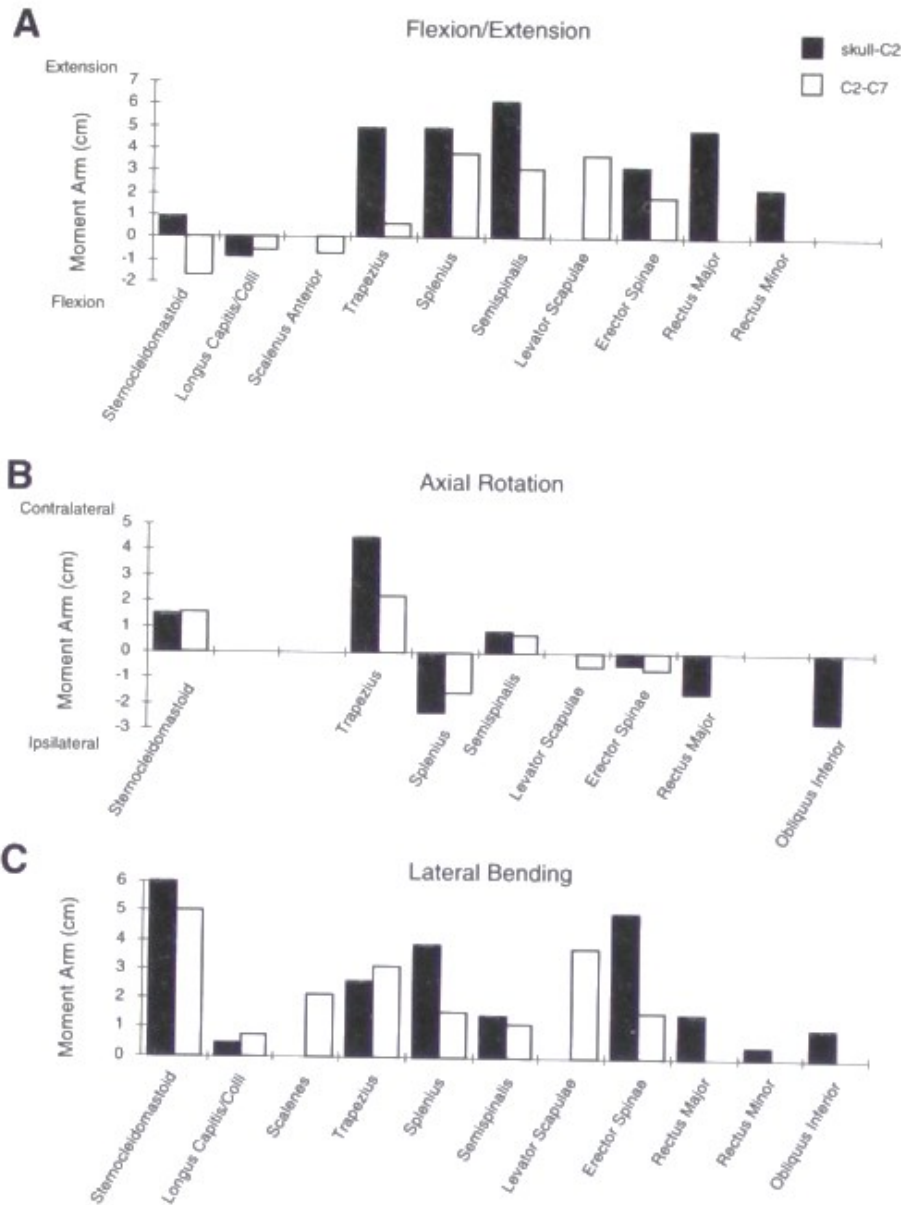


**Figure 12:** Neck muscle moment arms for the upper and lower cervical regions, the head and neck in the upright neutral position. Moment arms are averaged over muscle subvolumes. A, flexion-extension; B, axial rotation; and C, lateral bending. Adapted from Vasavada

Force-production capacity reduces as muscle fascicles are lengthened. Muscles have an optimal length where their force-producing capabilities are highest and the largest number of cross-bridges can be formed (**Figure 13**). Above this length active force production decreases

and more load is carried by passive tissues. Below this length there is too much overlap between cross-bridges resulting in less force producing capability. Vasavada et al. (1998) determined that in a resting position fascicles are within 15% of their optimal length. However, throughout the neck's ROM, more than half the neck muscles decrease to 80% of maximum force producing capability, with some muscles decreasing more than 50% of their capability. At a lower capacity muscles will be working much harder to balance and maintain control of the head.

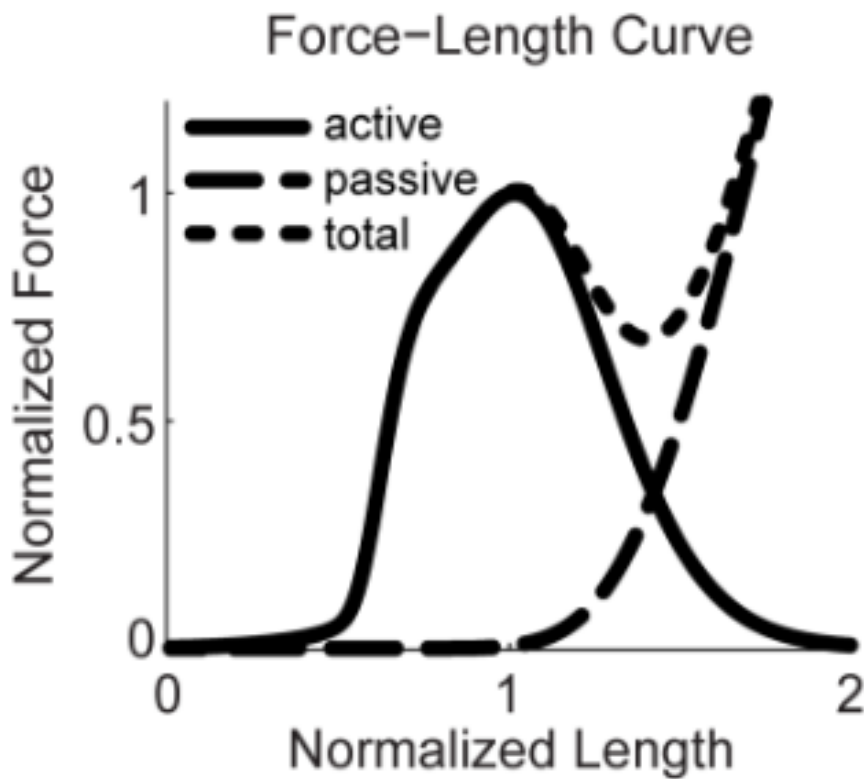


**Figure 13:** Normalized active, passive, and total force-length curves. Modified from Patten and Fregly, 2017

Multiple authors agree that posture has a marked effect on muscle activity. In one study, Thuresson et al. (2003) collected muscle activity in the upper neck across a number of static postures while pilots wore a helmet, helmet and NVGs, and a helmet, NVGs and a CW. They found that muscle activity in the upper and lower neck was significantly higher during neck

flexion combined with ipsilateral rotation than most other postures with all types of head mounted equipment. They concluded that the increased internal loading caused by different positions had a larger impact on EMG activity than the load of the equipment alone. Results from Callaghan (2014) were similar, where posture effected muscle activity and neck strength (83) more than the helmet configuration conditions (5). It has also been suggested that there is no difference in muscle activity between cruising in a neutral posture with NVGs and without NVGs (Murray, 2016). Considering this body of evidence, it is plausible that the postural changes associated with NVG use to maintain field-of-view could be a leading causal factor towards the development of aircrew neck pain.

At extreme ranges of motion, joints are at the largest mechanical and physiological disadvantage (Kumar, 2001). Extreme postures will change the force and moment-generating capacity of the muscle, increasing the exertion necessary to complete scanning tasks. These extreme or awkward postures may lead to compression of the microstructures, which increase the force requirements of the task, and contribute to muscle tendon inflammation. Together, the increased demand from a larger moment-producing capacity and the decrease in force-producing capacity in extreme postures put the soft tissue of the neck at risk of overexertion injury.

### **2.4.3 Moment of inertia**

#### *Overexertion*

A large concern amongst rotary wing aircrew is the shift in COM and increased moment of inertia that results from added HSM (**Table 2**). Moment of inertia increases when off-centre mass is added, and results in an increased resistance to angular motion. Therefore, adding NVGs and CWs to the helmet system will increase the moment of inertia and will likely require larger

muscle forces to start, stop, and stabilize the head. In fact, a helmet system with NVGs, batteries and a CW has four times the resistance to motion in the flexion/extension plane and six times the resistance in side to side rotation compared to the head alone (Fischer et al., 2013). Similar to extreme postures, an increased moment of inertia may result in an overexertion injury due to the increased muscle forces required to move the head. Overexertion injury occurs when tissue tolerance capacity is exceeded and can occur through a combination of exertion, repetition, and lack adequate recovery (Kumar, 2001).

**Table 2:** COM shift and mass moment of inertia in different head mass configurations

Condition	Mass (kg)	Centre of Mass from C7 (cm)			Mass Moment of Inertia (kg·cm <sup>2</sup> )		
		x	y	z	x	y	z
Head & helmet	6.06	0.96	13.69	0.00	349.52	310.65	365.18
Head, helmet & NVG	7.00	2.68	13.47	0.00	369.91	613.14	637.02
Head, Helmet, NVG & CW	7.90	0.58	13.76	0.00	396.33	902.02	960.98

#### 2.4.4 Vibration

Vibration is widely implicated in the etiology of back pain in helicopter aircrew and is important to consider (Shananan & Reading, 1984). Vibrations at the seat of a rotary wing aircraft range from 3-3.5Hz (Smith, 2004), however head motion can be increased above this vibration level due to body sensitivity in this region (Paddan & Griffin, 1988). Vibration largely affects head pitch motion, thereby increasing the load on the head and neck muscles (Butler, 1992). Vibration has also been found to degrade performance. In F-15 fighter aircraft low frequency buffeting (7-8.5Hz) was associated with slower target lock-on (Smith, 2006). Further,

whole body vibration has been associated with increased fatigue, chronic pain, and degenerative disease. Added mass, moment of inertia and posture all influence the vibration experienced. This is reason to believe that vibration acts synergistically with increased mass, moment of inertia, and postures to results in neck pain.

## **2.5 Design considerations**

The design of current helmet system is not optimized to maximize performance and to reduce injury risks, while also serving as a mounting platform for technologies like NVGs. In fact, few design limits are published at all, beyond those specific to blast and impact requirements. However, the United States Air Force has suggested that the maximum allowable helmet mass is 2.5kg. Further, work by Alem, Butler, and Albano (1995) showed that pilot performance is best with a weight-moment of 78Ncm, suggesting an upper limit of 90 Ncm for long duration flights. Other authors have suggested that helmets should minimize the moment of inertia by minimizing mass and symmetrically balancing the load as close to the head's natural centre of gravity as possible (Ivancevic & Beagley, 2004). However, few studies have quantified both performance in a dynamic situation, such as vigilance, and metrics associated with injury risk under different HSM conditions.

The CW provides an excellent opportunity for design optimization as it serves only one function, to balance the head, and therefore can easily be manipulated without much restriction. With improved insight about how specific factors, such as mass, MOI and posture might relate to neck injury, we can provide useful information to designers to help optimize the CW to reduce injury and improve performance. For example, it is important to know whether mass or moment of inertia has a larger impact on performance and function to inform future helmet system optimization and design. A smaller amount of weight could be added at a larger distance away

from the centre of mass to balance the mass of the NVGs if minimizing mass is a priority.

Alternatively, a larger mass could be added closer to the head to balance the mass of the NVGs if minimizing moment of inertia is a higher priority. Finally, if posture demonstrates the largest effect, designers may want to prioritize other, non-CW solutions to mitigate aircrew neck pain.

### 3. Methods

#### 3.1 Subjects

Fifteen male and fifteen female participants were recruited from a convenient university population. Participants were excluded if they had any previous history of neck pain, neck injury, concussions, vertigo, or dizziness or fainting during exercise. Participants were also required to have colour vision. Eligibility was determined prior to the collection day and informed consent was acquired on the collection day. Participant demographics are presented in **Table 3** below. Anthropometrics measurements are based on the Cheverud et al., 1990. This study was reviewed by the University Of Waterloo Office Of Research Ethics Committee (ORE 400080) and received approval prior to data collection.

**Table 3:** Participant demographics

	Age (years)	Height (cm)	Weight (lbs)	Head circumference (cm)	Head length (cm)	Neck circumference (cm)	Sitting height (cm)
Females (n = 15)	23 ± 4	168.0 ± 6.3	154.6 ± 41.4	53.3 ± 1.7	18.9 ± 1.1	58.9 ± 3.9	86.9 ± 3.7
Males (n = 15)	26 ± 4	181.4 ± 7.7	195.7 ± 29.4	58.0 ± 1.8	20.5 ± 0.8	62.9 ± 3.4	92.5 ± 4.2
<b>Total (n= 30)</b>	<b>25 ± 4</b>	<b>144.7 ± 9.7</b>	<b>175.0 ± 41.0</b>	<b>56.6 ± 2.2</b>	<b>19.7 ± 1.2</b>	<b>35.7 ± 3.5</b>	<b>89.7 ± 4.8</b>

#### 3.2 Instrumentation

##### 3.2.1 Electromyography

Surface EMG was recorded at 2000Hz using wireless Trigno mini sensors (Delsys, Natick MA) (**Figure 14**) bilaterally from the sternocleidomastoid (SCM), upper trapezius (UT), and upper neck extensors (UNE) (**Figure 15**). Prior to electrode placement the area of interest

was shaven, and cleansed with 70% isopropyl alcohol. Electrode sights were landmarked as follows: SCM – 2/3 of the distance between the mastoid process and the suprasternal notch (Falla et al., 2002; Almosnino et al., 2009); UT – 50% along the line from the acromion to the spine on vertebra C7, as per the SENIAM guidelines (Hermens et al., 1999); UNE – at the level of the fourth cervical vertebrae 2 cm from the midline (Gosselin et al., 2014; Murray et al., 2016). Hardware characteristics of Trigno mini sensors are presented in **Table 4**.

**Table 4:** Characteristics of Delsys Trigno mini sensors

Bandwidth	20 ± 5Hz, > 40dB/dec 450 ± 50Hz, >80 dB/dec
Inter-electrode distance	10mm
Maximum sampling rate	1926 samples/sec
Actual sampling rate	1922 samples/sec
Resolution	16bits
Range	± 11mV

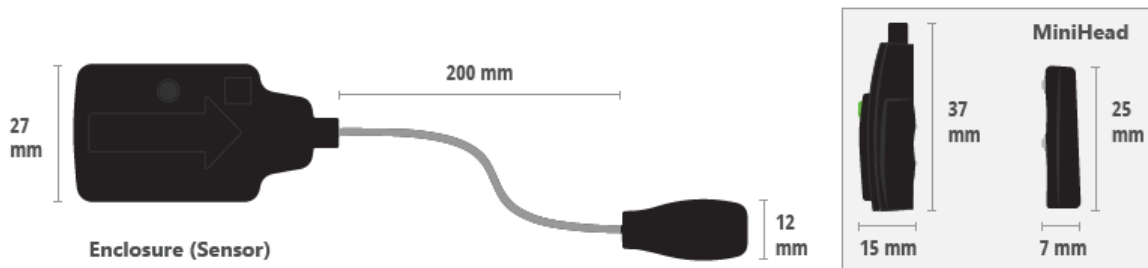


**Figure 14:** Diagram of the Delsys Trigno mini sensors



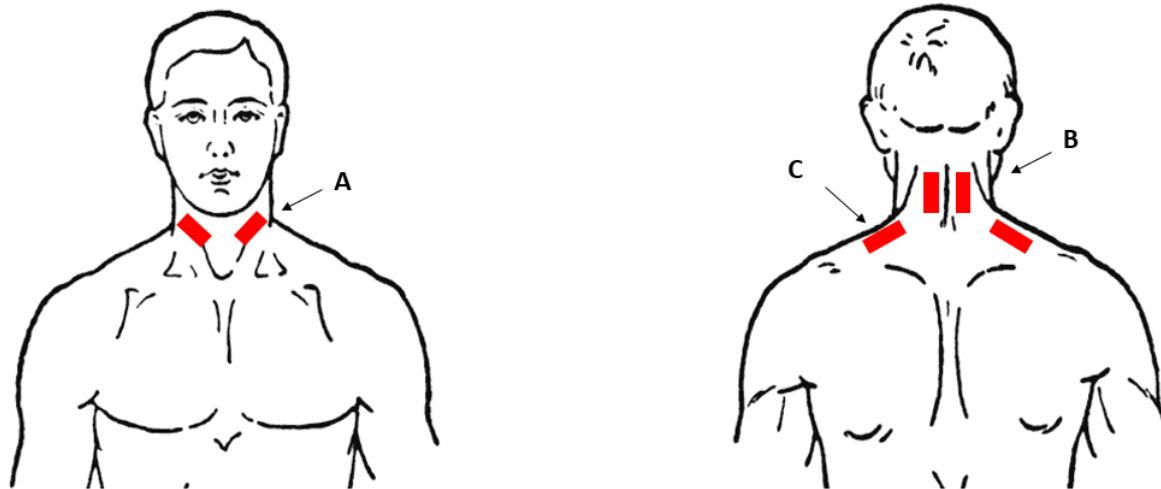


**Figure 15:** EMG electrode placement A) sternocleidomastoid B) Upper neck extensors C) Upper trapezius

### 3.2.2 Motion Capture

Participants were instrumented with six reflective markers and one rigid body on their trunk. Markers were placed on the following bony landmarks: suprasternal notch, zyphoid process, C7, T10, and left and right acromion (**Figure 16**). A rigid body was placed on their chest to ensure that the trunk was tracked and all markers could be filled during processing. Five additional passive markers were placed on the helmet in the following locations: the ears in line with the external acoustic meatus, top of the head, posterior helmet, and anterior helmet (**Figure 17**). Kinematics were collected at 80Hz using a twelve camera Vicon passive optoelectric capture system (Vicon, Centennial, CO, USA). The collection space was calibrated at least one hour prior to participants' arrival and the global coordinate system was set according to ISB standards with +X forwards, +Y upwards, and +Z to the right (Wu et al., 2002).

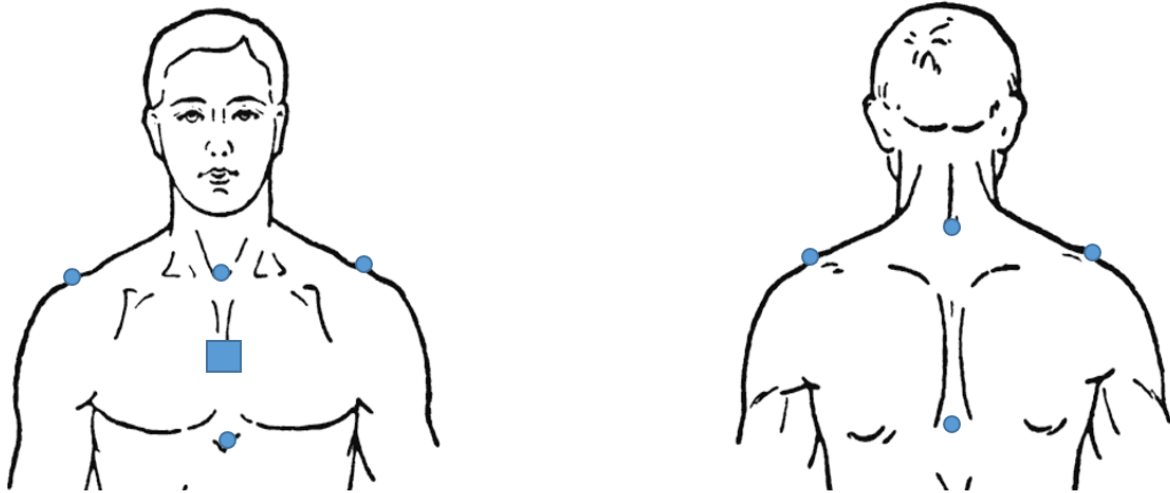


**Figure 16:** Reflective marker placement on the participant

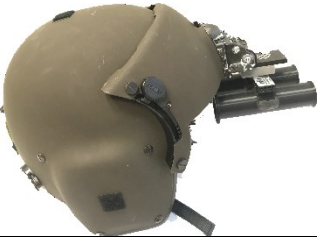









**Figure 17:** Reflective marker placement on the Gentex HGU-56/P helmet

### 3.2.3 Head supported mass

Four operationally relevant helmet configurations were tested: helmet alone (hOnly), helmet and NVGs (hNVG), helmet, NVGs and traditional CW (hCW), and the helmet, NVGs, and a CW liner (hCWL) (**Table 5**). A genuine Gentex HGU-56/P helmet weighing 1.43 kg was used. Mock NVGs were used with the interior optics removed. Mock NVGs weighed 0.55 kg. In each NVG condition (hNVG, hCW, and hCWL) a battery pack (0.23kg) was attached to the back of the helmet, as would be required when wearing real NVGs. A laser pointer was affixed to the top of the NVGs so that the laser lined up in the centre of the participants field of vision. The traditional CW was a lead block weighing 0.66 kg with Velcro on the back so it could be easily be attached to the posterior of the helmet. The modified CWL also weighed 0.66 kg and was molded to the interior of the helmet, evenly distributed across the posterior of the helmet, effectively reducing the moment arm but keeping the mass the same compared to a traditional CW.

**Table 5:** HSM conditions and associated mass and relative moment of inertia. **A)** Gentex HGU-56P helmet **B)** 3D printed NVGs **C)** Mock NVGs **D)** battery pack **E)** traditional CW **F)** counterweight liner

Helmet condition		Total Mass (kg)	Relative moment of Inertia
Assembled Helmet	Accessories		
hOnly	<div style="display: flex; justify-content: space-around; align-items: center;"> <div style="text-align: center;"> <b>A</b>   </div> <div style="text-align: center;"> <b>B</b>   </div> </div>	1.43	Low
hNVG	<div style="display: flex; justify-content: space-around; align-items: center;"> <div style="text-align: center;"> <b>C</b>   </div> <div style="text-align: center;"> <b>D</b>   </div> </div>	2.21	Moderate
hCW	<div style="display: flex; justify-content: space-around; align-items: center;"> <div style="text-align: center;"> <b>E</b>   </div> <div style="text-align: center;"> <b>D</b>   </div> </div>	2.81	High
hCWL	<div style="display: flex; justify-content: space-around; align-items: center;"> <div style="text-align: center;"> <b>F</b>   </div> <div style="text-align: center;"> <b>D</b>   </div> </div>	2.81	Moderate

### 3.2.4 VTAS

A 3D-visual target acquisition system (VTAS) was developed by Derouin and Fischer in 2017. This system provides a consistent and objective way to elicit rapid head movements and measure performance. It consists of round solar panels (6V 100mA, 100mm diameter, Sundance Solar, Hopkinton NH) arranged in pairs. Each solar panel is enclosed in a 3D printed target holder with a 20mm aperture, surrounded by three multi-colour (RGB) LEDs. The laser pointer attached to the helmet interacts with the solar panels changing the LEDs from red to blue, indicating that the target has been hit (**Figure 18**). Once the laser remained in contact with the target for a dwell time of 300ms the LEDs turned green, indicating a successful acquisition and signaling to move to the next target. Participants go back and forth between two targets in a prescribed trajectory as many times as possible in 20 seconds. Three trajectories were tested in this experiment: yaw, pitch, and off-axis (top right to bottom left). Each trajectory was tested considering two amplitudes to simulate a small ROM (e.g., akin to the operational configuration of a day flight where peripheral vision enables a wider field-of-view) and larger ROM (e.g., akin to the operational configuration of a night flight where field-of-view is restricted and thus greater neck ROM is required). The small amplitudes required the participant to move their head through an arc of 35° and the large amplitudes required the participant to move through an arc of 70° (**Figure 19**), where these distances were chosen based on comfort zones defined by Forde et al. (2011). The solar panels were connected to the Vicon system through a 14bit A/D box. VTAS data were collected at 2000Hz, syncing with the EMG and motion capture data.

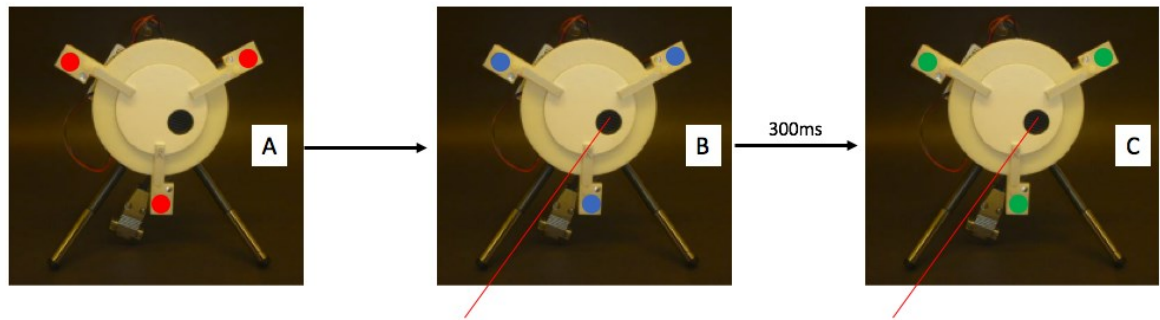


**Figure 18:** Solar panel interaction with the laser pointer. A) target is active but has not been hit with the laser pointer; B) target has been hit with the laser pointer; C) laser pointer has been on target for at least 300ms indicating a successful acquisition

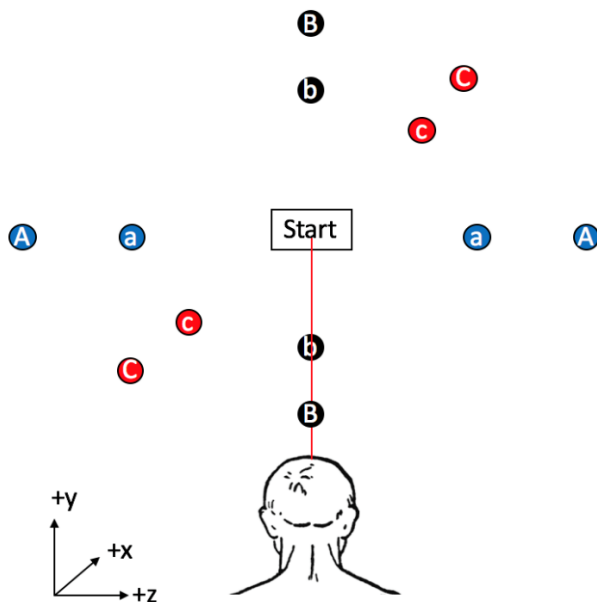


**Figure 19:** VTAS target set-up A – yaw 70°; a – yaw 35°; B – pitch 70°; b – pitch 35°; C – off-axis 70°; c – off-axis 35°

### 3.3 Experimental design

A cross-sectional repeated measures design was used. Independent variables included: HSM condition, target amplitude, and target direction. Dependent variables include integrated EMG to provide a measure of total muscular effort, a co-contraction ratio (CCR), and peak EMG

during starting and acquiring phases. HSM conditions were block randomized and target direction and amplitude were randomized within each block. Each condition was completed three times resulting in 18 trials within each HSM condition (three directions x two amplitudes x three repeats). Participants were required to perform the VTAS task for 20 seconds while data was collected for 30 seconds. At least 30 seconds of rest was given between trials. At least 5 minutes of rest was given between helmet conditions to prevent any fatigue.

### **3.4 Protocol**

Data collection took approximately two hours per participant (**Figure 20**). Upon arrival in the laboratory participants read a letter of information and provided written consent. A demographics form was filled out with the participant's height, weight and age. Anthropometrics of the head, neck, and trunk were also taken (**Table 3**). The participant was then fitted with a small, medium or large Gentex HGU-56/P helmet and all adjustable straps and pads were configured so the helmet did not slide on the head. The skin was then prepped for EMG placement. All electrodes and wires were taped down to secure them and to ensure they did not move during collection. Participants then performed a short neck and shoulder warm up including shoulder shrugs, arm circles, and neck flexion and extension before they performed maximum voluntary contractions (MVCs). MVCs provide a reference so muscle activity can be normalized to a percentage of participants' maximum, allowing for comparison between muscles as well as provide better clinical significance. Firm resistance was given against neck flexion, extension, arm at 90° flexion, and arm at 45° flexion (Harms-Rindahl et al., 2007; Murray et al., 2016; Boettcher, Ginn, & Cathers, 2008). Each MVC was performed twice with a minimum of 2 minutes between each exertion to prevent fatigue. A quiet trial was then recorded. Passive markers were placed on the participant as outlined in **Figure 17**.

Participants sat in a car seat facing the VTAS system. A 4-point harness system was used to secure the participants waist and shoulders to the chair. This seating arrangement was chosen to resemble a Griffon helicopter pilot seating as closely as possible (**Figure 20**).



**Figure 20:** Comparison of study seating vs. real seating. A – Car chair with 4-point harness used in study; B – Pilot seat inside a Griffon Helicopter

Next, participants were suited with the helmet and time was taken to ensure that the laser pointer lined up directly in the centre of their field of vision. A 30-second static calibration was then collected. Since this is a novel task, participants were given six familiarization trials (one in each trajectory) with just the helmet on (hOnly) to become acquainted with the system. Before each trail began, participants were told which trajectory they would be acquiring. They were directed to start looking at the solar panel on the left for yaw and off-axis trajectories and the top for pitch trajectories. When the lights turned red participants began the scanning task with the direction to “acquire as many targets as possible in the 20s”.



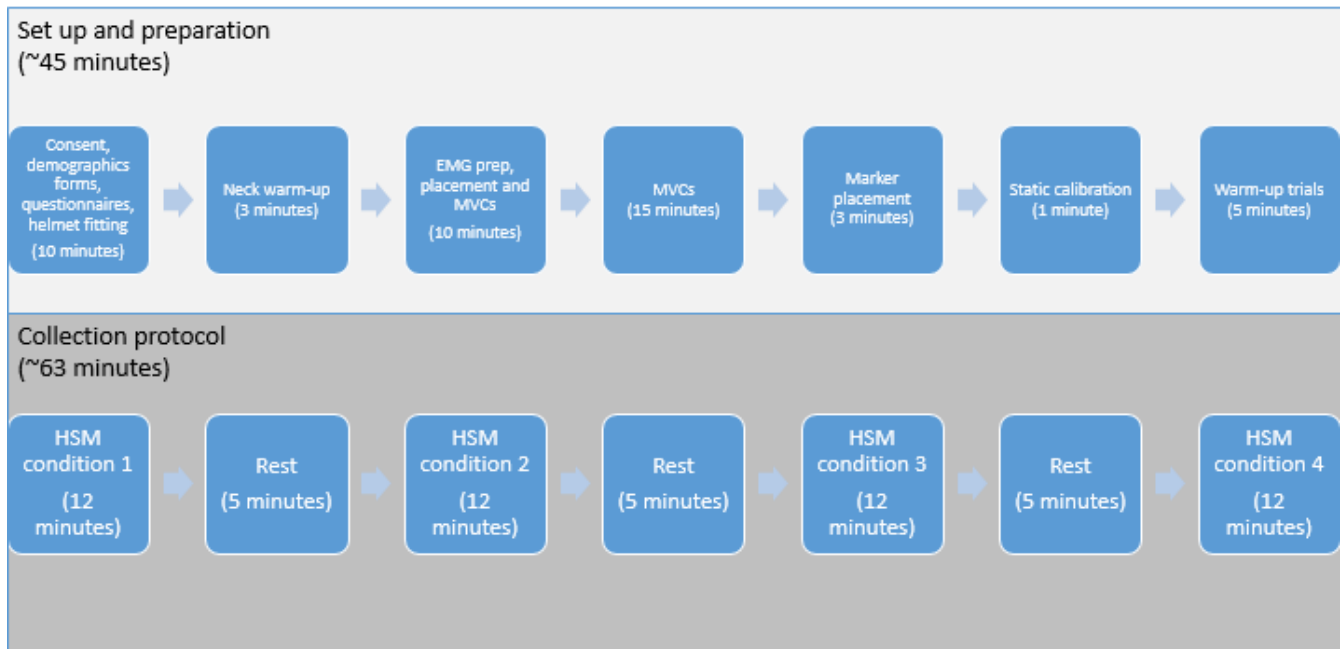


**Figure 21:** Depiction of study protocol and approximate time allocation

### 3.5 Processing

For the purposes of this thesis only yaw and pitch trajectories are considered. The third repetition of each trial was analyzed to control for any familiarization effects. If an error occurred that affected the utility of the data in the third trial, data from the second trial was instead. In this case, errors were defined using the VTAS and occurred when participants acquired the same solar panel two or more times in a row.

#### 3.5.1 VTAS

VTAS data was imported into Matlab (Mathworks Inc., USA) and was used to determine a number of performance measures. **Figure 21** provides a sample of data obtained from the VTAS. Performance measures include: Average target acquisition time (TAT) - the average time it takes (in seconds) to get from one successful acquisition to the next successful acquisition; honing time (HT) – the average time it takes (in seconds) from the first time the target is hit

(blue) to a successful acquisition (green); error – number of times the target is hit (blue) minus number of successful acquisitions (green); and acquisitions – number of successful acquisitions in a trial. The first frame (leading edge) of each successful acquisition (green) was also used to identify turns (i.e. turning right vs. left, and looking up vs. down).

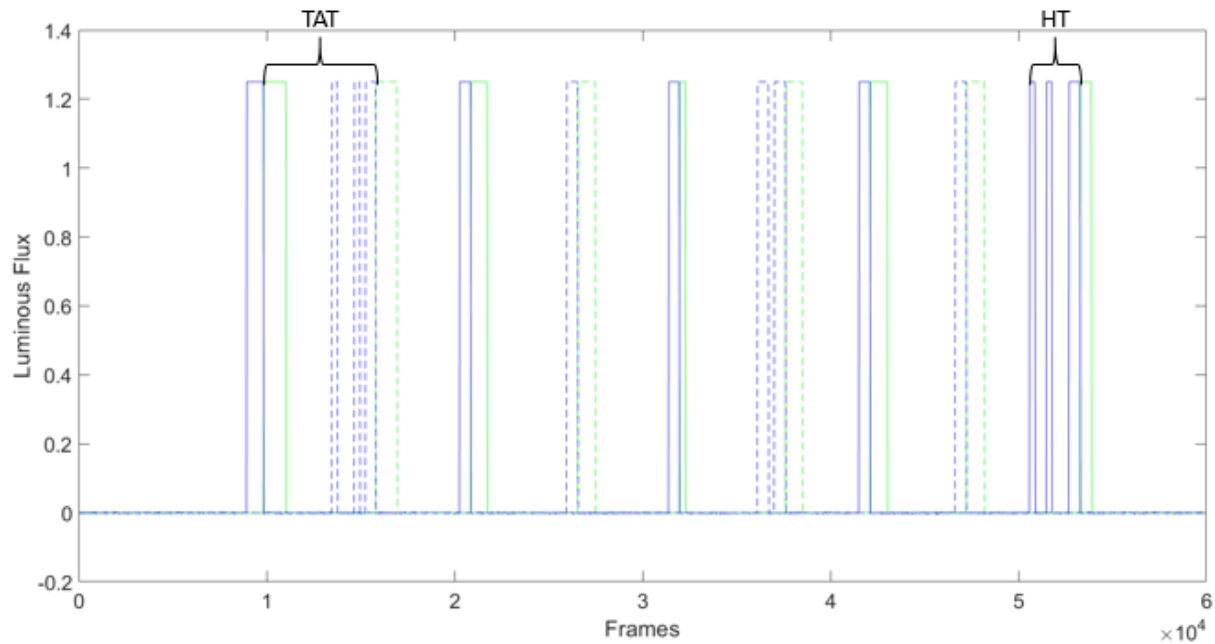


**Figure 22:** Example VTAS data with labels depicting TAT (time to acquire target – time from one acquisition the next) and HT (honing time – time from the blue to green)

### 3.5.2 Kinematics

Motion capture data were visually inspected, labeled and gap filled in Nexus 2.0. Labeled and filled data were then imported into Matlab R2018a (Mathworks Inc., USA) and dual passed through a low pass, second order Butterworth filter with an effective cutoff of 6Hz (Pezzack, Norman, & Winter, 1997). A local coordinate systems (LCS) of the head and trunk were created according to Wu (2005) (**Figure 23**) (Further analysis shown in Appendix A).

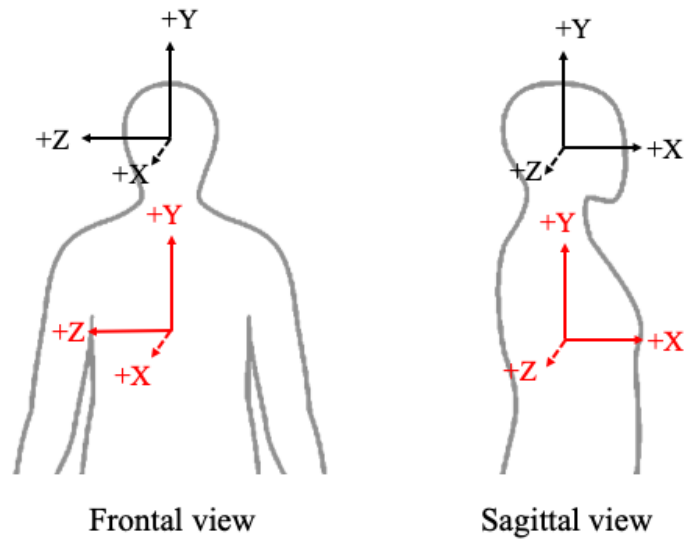


**Figure 23:** Local coordinate systems of the head (black) with the origin between the centre of the ears, and trunk (red) with the origin between T10 and the zyphoid process

Euler angles were used to determine the motion of the head relative to the trunk. A ZYX rotation matrix was used to follow International Society of Biomechanics recommendations for intervertebral motion (Wu, 2002). Position data was then differentiated using finite differentiation (Pezzack, Norman, & Winter, 1997) to get velocity (deg/s) and differentiated again to get acceleration (deg/s<sup>2</sup>).

$$\omega = \frac{\theta(t + 1) - \theta(t)}{\Delta t}$$

$$\alpha = \frac{\omega(t + 1) - \omega(t)}{\Delta t}$$

Data were then shifted to account for the phase shift introduced through finite differentiation.

### 3.5.3 Operationalizing events

Trials were segmented based on VTAS and kinematic data. First, a *turn* from one target to the other was identified, defined using the instant the VTAS turned green (a successful target acquisition) on one target to the instant it turned green on the subsequent target. Turns were considered as left and right (in yaw trajectories), or up and down (in pitch trajectories). Further, each turn was segmented into two phases. *Starting* was defined from when the target was acquired (green), until the instant of peak angular velocity when approaching the subsequent target. *Acquiring* was defined from the instant of peak angular velocity to when the VTAS turns green at the subsequent target. **Figure 24** depicts key events used to segment data, and **Figure 25** shows the phases over laid on sample EMG data. Further visualization of cutting turns can be seen in Appendix B.

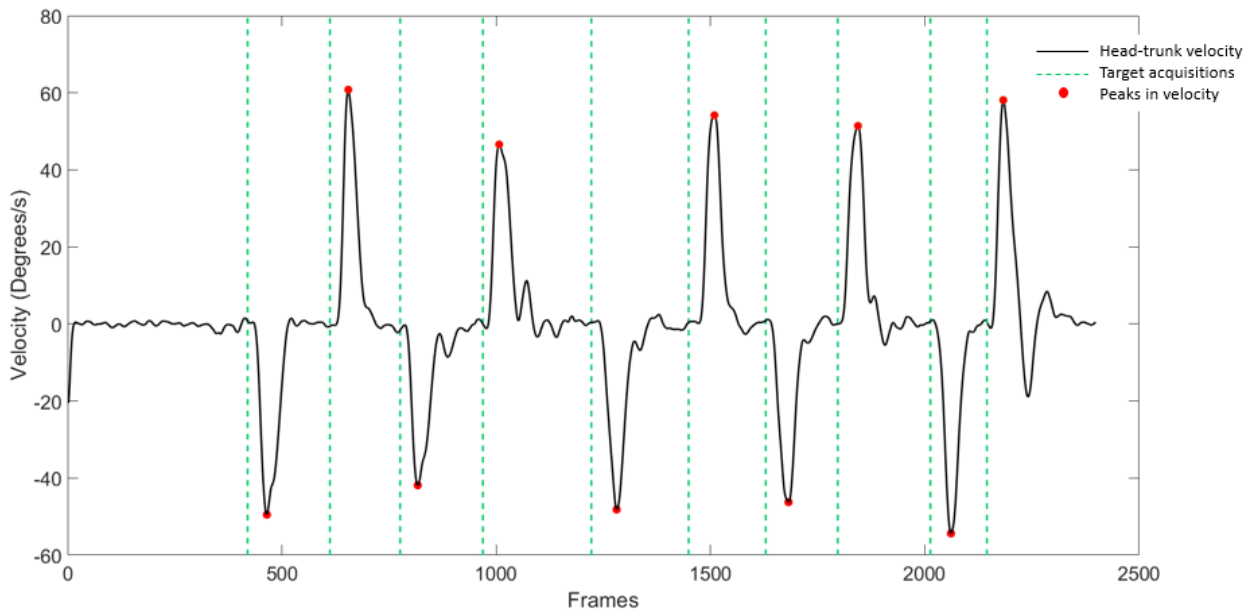


**Figure 24:** An example of operationalizing events based on kinematics and VTAS data in the yaw trajectory. The black trace is head-trunk angular velocity (deg/s) about the z-axis with peaks in velocity indicated with red dots. Green dashed lines indicate where targets have been acquired.

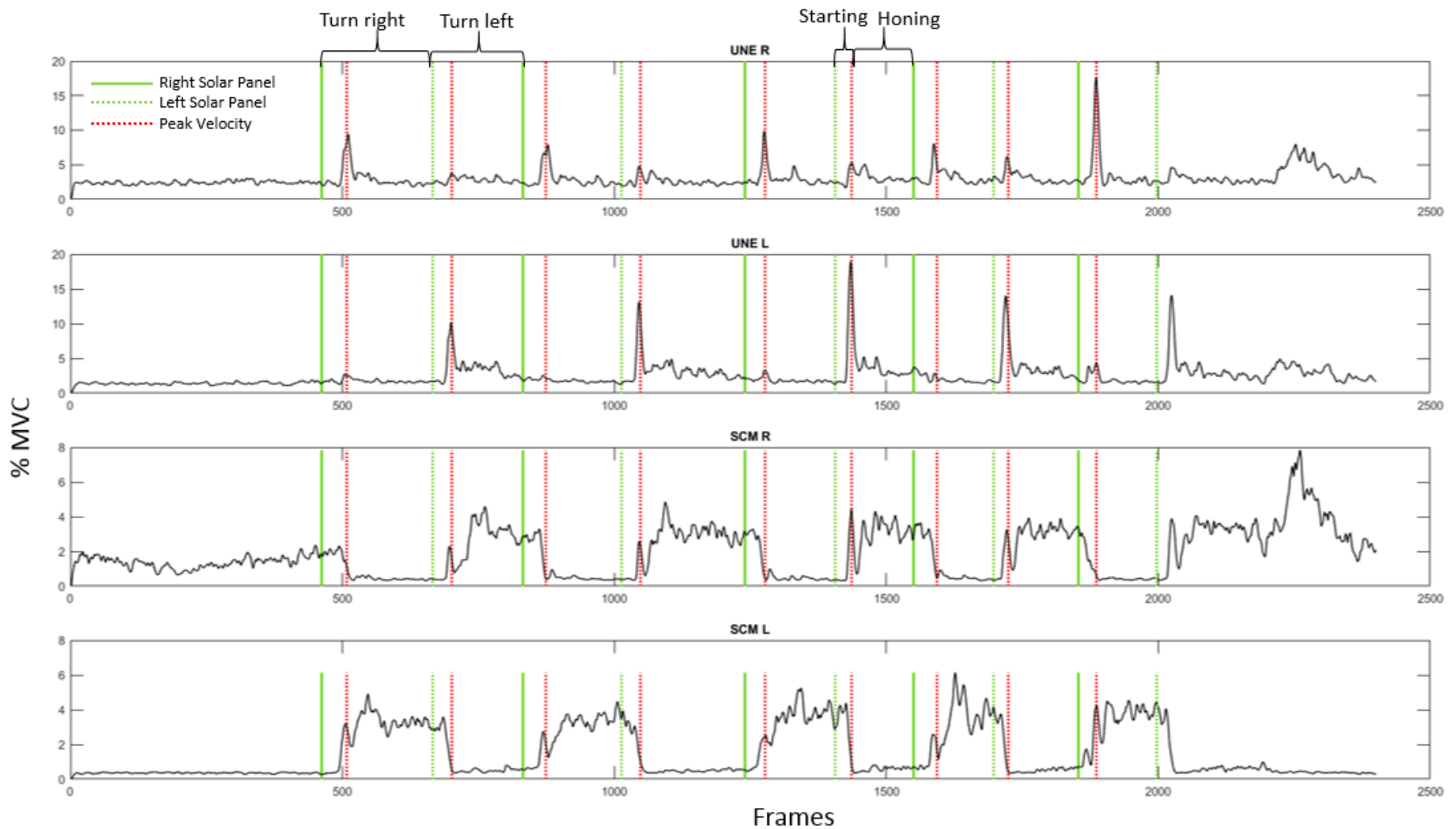


**Figure 25:** Example of operationalizing events (turn left, turn right, starting, and honing) for UNER, UNEL, SCML, and SCMR in the yaw trajectory

### 3.5.4 EMG

EMG data were imported and processed in Matlab. Quiet trial data was averaged and removed from the raw EMG signals. EMG was then de-trended and DC bias was removed. Next, data were high pass filtered at an effective cutoff of 30 Hz using a dual pass, second order Butterworth filter to remove any contamination from heartrate (Drake and Callaghan, 2006). Data were then full wave rectified, and filtered using a single pass, second order Butterworth filter with a 4Hz cutoff (McKinnon, 2012). To normalize EMG signals to each individual, the maximum from MVC trials was taken. Trials were normalized by dividing the signal by the specific muscle's maximum and multiplying by 100%.

$$\text{Normalized EMG} = \frac{EMG}{MVC \text{ maximum}} \times 100\%$$

The Delsys system has an EMG output delay of 48 milliseconds, meaning EMG data at frame one were collected 48ms earlier. Therefore, EMG data were shifted forwards by 96 frames at the start of the trial to account for this output delay. Data were then down sampled to 80Hz to sync with VTAS and kinematic data.

In some cases, EMG sensors were perturbed by the helmet. This mainly occurred in the UNE sensors when the participant was looking up in the pitch trajectory, in which case normalized EMG greatly exceeded 100%. To remove non-biological signals, but also preserve as much data as possible, if the maximum EMG in a turn exceeded 100% the outcome measure was not reported for that turn/phase. In some cases, all turns in a trial exceeded 100%, and therefore no data were reported for that muscle in that trial. After all turns exceeding 100% MVC had been

removed 1.5% of data in the pitch trajectory was missing and 0.8% of the data in the yaw trajectory was missing. In total nine participants in the pitch direction and five participants in the yaw direction contained at least one missing data point. To retain as much data as possible and as large a sample size as possible, if participants had one or two missing data points, data were filled using mean imputation (Waljee, 2013). In total eight data points were filled in the pitch trajectory and three data points were filled in the yaw trajectory, resulting in a minimum of 26 participants in the pitch trajectory and 27 in yaw. Where dependent measures consider muscles independently (i.e. iEMG and peak EMG), all muscles without missing data for a participant were used.

### 3.6 Dependant Measures

#### 3.6.1 Co-contraction

Co-contraction was calculated for each turn. The co-contraction ratio (CCR) for these events were calculated using the methods described by Cheng, Lin, and Wang (2008). This method was deemed to be the most appropriate as it was developed for cervical musculature co-contraction during different speeds of head movement. CCR is calculated as follows:

$$CCR = \frac{\Sigma NAIEMG_{antagonists}}{\Sigma NAIEMG_{total}}$$

where: *NAIEMG* is the normalized average integrated EMG, calculated as:

$$NAIEMG = \frac{IEMG}{maxEMG \times T}$$

where:  $iEMG$  is the integration of the filtered EMG signal (not normalized to MVCs),  $maxEMG$  is the maximum EMG signal as found in the MVCs, and  $T =$  the length of the turn, in frames.

$\Sigma NAIEMG_{antagonists}$  refers to the sum of the antagonist muscles which were predefined and differ based on the trajectory (**Table 6**).  $\Sigma NAIEMG_{total}$  refers to the sum of all muscles. After the CCRs were determined for each turn in each condition, turns were averaged to provide two average CCRs for each trial (left and right for yaw trajectories, or up and down for pitch trajectories).

**Table 6:** Agonist and antagonist pairs for different head movements

Trajectory	Movement	Agonist	Antagonist
Yaw	Turn left	SCM right	SCM left
		UNE left	UNE right
Pitch	Extend neck	SCM left	SCM right
		UNE right	UNE left
Pitch	Flex neck	UNE left	SCM left
		SCM right	UNE right

### 3.6.2 Muscular effort

For total muscular effort, integrated EMG ( $iEMG$ ) was calculated for SCML, SCMR, UNEL, and UNER in each condition. First, each trial was segmented into turns and the sum of the integrated EMG ( $iEMG$ ) signal for each muscle was found:

$$iEMG = \int_a^b \alpha(x) dx \approx \sum_{n=0}^{N-1} (\alpha_n + \alpha_{n+1})(\Delta\alpha)_n$$



Turns were averaged resulting in average iEMG left and right muscle activity for yaw conditions, and average iEMG up and down muscle activity for pitch conditions. Because iEMG can be influenced by the length of each turn (TAT), mean EMG was also calculated for each turn. This measure was used to supplement iEMG and provide more insight into total muscular demand.

### **3.6.3 Peak EMG**

Peak EMG were found for each muscle during four phases: starting left, acquiring left, starting right, and acquiring right for yaw conditions, and starting up, acquiring up, starting down, and acquiring down for pitch conditions. Peak EMG were found for each phase in each trial and then phases were averaged, providing an average maximum muscular activity required to start and stop the head under each condition, for each muscle.

### **3.6.4 Mean velocity**

Mean velocity was calculated for each turn. Within a trial turns were averaged providing a mean velocity left and right in the yaw trajectory and a mean velocity up and down in the pitch trajectory.

## **3.7 Statistical analysis**

Three-factor repeated measures analyses of variance (ANOVAs) were used to assess the potential influence of direction (two levels: up and down in the pitch trajectory, or left and right in the yaw trajectory), amplitude (two levels: near and far), and HSM condition (four levels: hOnly, hNVG, hCW, and hCWL). Trajectory was not considered as an independent factor. As a result, separate ANOVA models were used for each trajectory (yaw and pitch). For co-contraction (research question 1) eight three-way within participant repeated measures ANOVAs

( $\alpha=0.05$ ,  $\beta=0.08$ ) were used to detect differences in the following dependent variables: CCR left, CCR right, CCR up, and CCR down. For total muscular demand (research question 2), three-way ANOVAs were used to assess iEMG and mean EMG in each muscle. Finally, for peak EMG (research question 3), three-way ANOVAs were used to assess  $EMG_{max}$  during starting and acquiring phases for each muscle. The same process was used for mean velocity as well as performance measures (TAT, HT, error, and number of targets acquired). Main effects were assessed and pairwise comparisons were made where necessary using Bonferroni corrections. All data were analyzed using SPSS Version 25.0 (IBM Cor, Armonk, NY). Statistical significance was set at  $\alpha = 0.05$ .

## 4. Results

It was found that bilateral UT were not meaningfully active and did not meaningfully contribute to head movements (**Appendix C**). Therefore, for the purpose of this thesis only bilateral SCM and UNE are considered.

### 4.1 Research Question 1: Co-Contraction Ratio

#### *HSM Condition*

There was no main effect of HSM condition on CCR in the pitch trajectory (**Figure 26**), however there was a significant effect of condition on CCR in the yaw trajectory,  $F(3,78) = 8.992, p \leq 0.001, \eta_p^2 = 0.257$  (**Figure 27**). Pairwise comparisons of the effect of condition in the yaw trajectory are presented in **Table 6** below and suggest increased CCR for the counter-weighted conditions (CW and CWL). To support the analysis of CCR an additional analysis was performed on  $\text{NAIEMG}_{\text{antagonists}}$  and  $\text{NAIEMG}_{\text{agonists}}$  to determine if there was agonist or antagonist activity driving changes in the CCR. There was a main effect of condition on  $\text{NAIEMG}_{\text{agonists}}$  in the yaw trajectory ( $F(3,78) = 5.342, p = 0.002, \eta_p^2 = 0.170$ ), however there was no main effect of condition on any other NAIEMG measures (**Figure 27**).

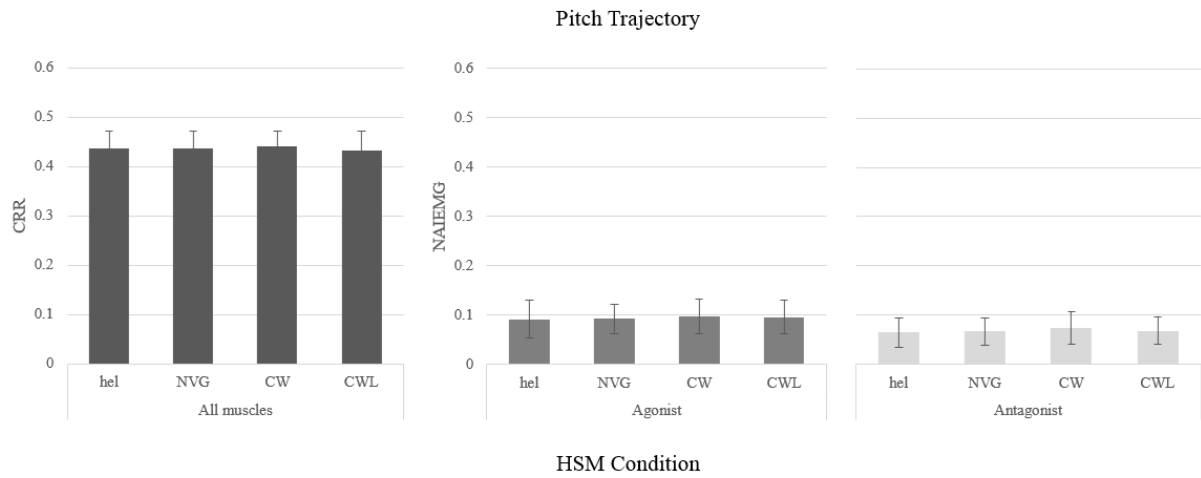


**Figure 26:** Average CCR and NAIEMG ( $\pm$  1SD) for each HSM condition in the pitch trajectory

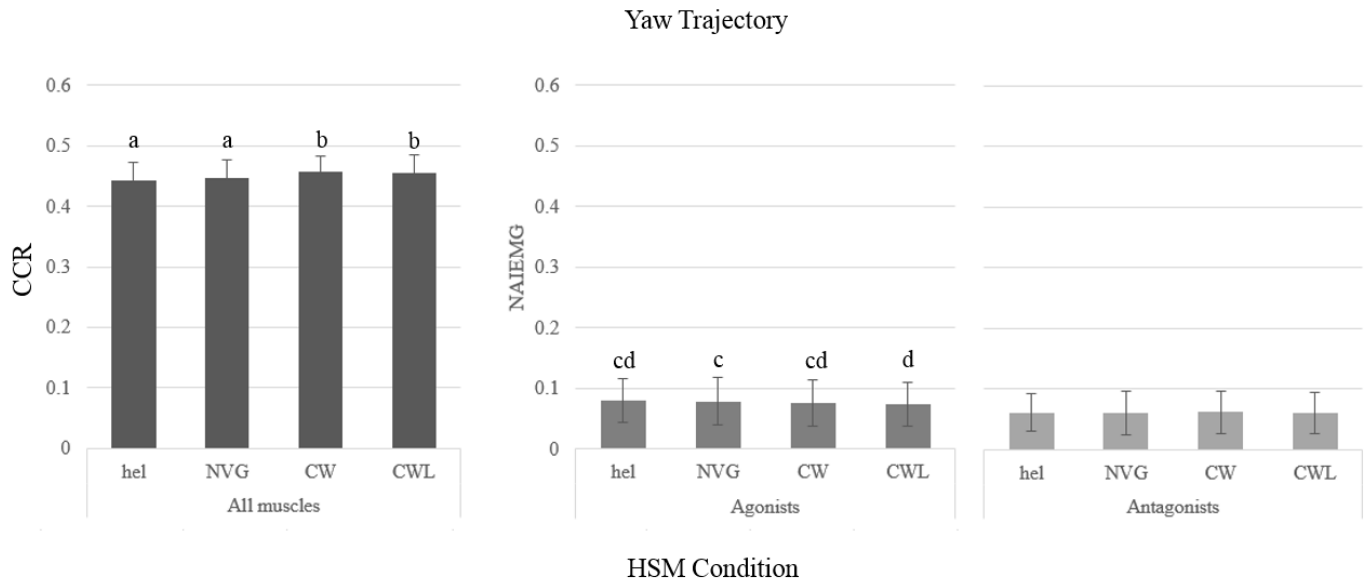


**Figure 27:** Average CCR and NAIEMG ( $\pm$  1SD) at each HSM condition in the yaw trajectory. Different letters indicate statistical difference between conditions

**Table 6:** Pairwise comparisons for the effect of HSM condition on CCR. \* Indicates significant differences

(I) HSM Condition	(J) HSM Condition	CCR Mean Difference (I-J)	Std. Error	<i>p</i>	95% Confidence Interval for Difference	
					Lower Bound	Upper Bound
hOnly	NVG	-0.004	0.003	1.000	-0.013	0.005
	<b>CW</b>	<b>-0.015</b>	<b>0.004</b>	<b>0.003*</b>	<b>-0.026</b>	<b>-0.004</b>
	<b>CWL</b>	<b>-0.013</b>	<b>0.004</b>	<b>0.013*</b>	<b>-0.024</b>	<b>-0.002</b>
hNVG	Hel	0.004	0.003	1.000	-0.005	0.013
	<b>CW</b>	<b>-0.011</b>	<b>0.004</b>	<b>0.022*</b>	<b>-0.021</b>	<b>-0.001</b>
	<b>CWL</b>	<b>-0.009</b>	<b>0.003</b>	<b>0.016*</b>	<b>-0.016</b>	<b>-0.001</b>
hCW	<b>Hel</b>	<b>0.015</b>	<b>0.004</b>	<b>0.003*</b>	<b>0.004</b>	<b>0.026</b>
	<b>NVG</b>	<b>0.011</b>	<b>0.004</b>	<b>0.022*</b>	<b>0.001</b>	<b>0.021</b>
	CWL	0.002	0.003	1.000	-0.007	0.011
hCWL	<b>Hel</b>	<b>0.013</b>	<b>0.004</b>	<b>0.013*</b>	<b>0.002</b>	<b>0.024</b>
	<b>NVG</b>	<b>0.009</b>	<b>0.003</b>	<b>0.016*</b>	<b>0.001</b>	<b>0.016</b>
	CW	-0.002	0.003	1.000	-0.011	0.007

### *Amplitude*

There was a main effect of amplitude on CCR in the pitch trajectory ( $F(1,25) = 38.448, p \leq$

$0.001, \eta_p^2 = 0.606$ ) and in the yaw trajectory ( $F(1,26) = 110.557, p \leq 0.001, \eta_p^2 = 0.810$ ).

Pairwise comparisons revealed that CCR was significantly lower for far amplitudes compared to near in both pitch and yaw trajectories (**Figure 28**).

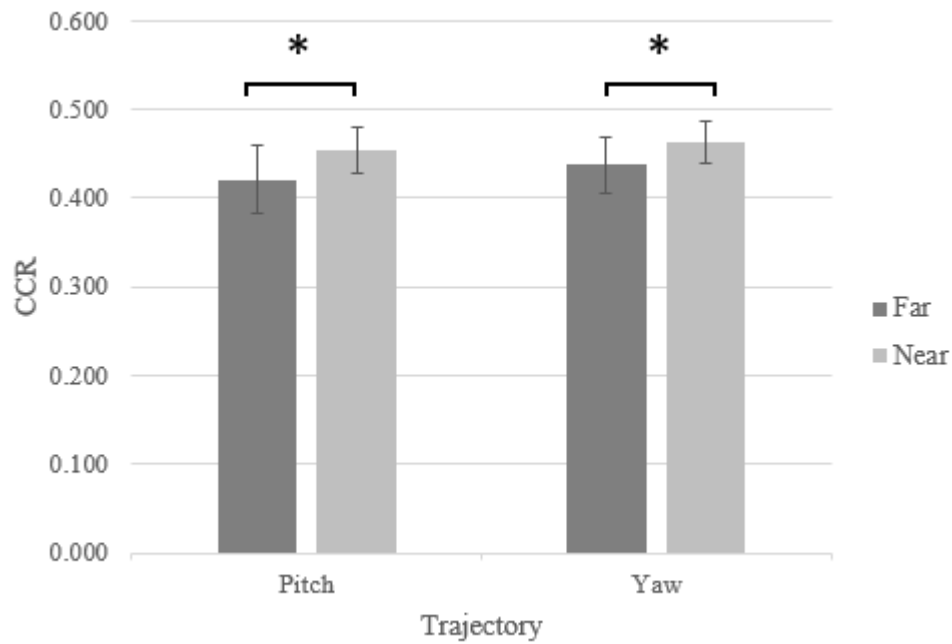


**Figure 28:** The effect of amplitude on CCR  $\pm$  1SD in both the pitch and yaw trajectories. \* Indicates significant differences

### *Interactions*

There was a significant amplitude by condition interaction effect in the yaw trajectory ( $F(3,75) = 6.068, p = 0.001, \eta_p^2 = 0.189$ ). Post hoc testing revealed that the effect of condition was amplified at the far amplitudes (**Figure 29**). More specifically, differences in HSM condition were only seen at far amplitudes (**Table 7**).

**Table 7:** Mean differences of the condition by amplitude interaction effect on CCR

Amplitude	Condition (I)	Condition (J)	Mean Difference in CCR (I-J)	Sig.	95% Confidence Interval for Difference	
					Lower Bound	Upper Bound
Far	hOnly	hNVG	-0.01	0.41	-0.02	0.00
		<b>hCW</b>	<b>-.022*</b>	<b>0.00</b>	<b>-0.04</b>	<b>-0.01</b>
		<b>hCWL</b>	<b>-.023*</b>	<b>0.00</b>	<b>-0.04</b>	<b>-0.01</b>
	hNVG	hOnly	0.01	0.41	0.00	0.02
		<b>hCW</b>	<b>-.013*</b>	<b>0.03</b>	<b>-0.03</b>	<b>0.00</b>
		<b>hCWL</b>	<b>-.014*</b>	<b>0.00</b>	<b>-0.02</b>	<b>0.00</b>
	hCW	<b>hOnly</b>	<b>.022*</b>	<b>0.00</b>	<b>0.01</b>	<b>0.04</b>
		<b>hNVG</b>	<b>.013*</b>	<b>0.03</b>	<b>0.00</b>	<b>0.03</b>
		hCWL	0.00	1.00	-0.01	0.01
	hCWL	<b>hOnly</b>	<b>.023*</b>	<b>0.00</b>	<b>0.01</b>	<b>0.04</b>
		<b>hNVG</b>	<b>.014*</b>	<b>0.00</b>	<b>0.00</b>	<b>0.02</b>
		hCW	0.00	1.00	-0.01	0.01
Near	hOnly	hNVG	0.00	1.00	-0.01	0.01
		hCW	-0.01	0.13	-0.02	0.00
		hCWL	0.00	1.00	-0.01	0.01
	hNVG	hOnly	0.00	1.00	-0.01	0.01
		hCW	-0.01	0.22	-0.02	0.00
		hCWL	0.00	1.00	-0.01	0.01
	hCW	hOnly	0.01	0.13	0.00	0.02
		hNVG	0.01	0.22	0.00	0.02
		hCWL	0.01	0.93	-0.01	0.02
	hCWL	hOnly	0.00	1.00	-0.01	0.01
		hNVG	0.00	1.00	-0.01	0.01
		hCW	-0.01	0.93	-0.02	0.01

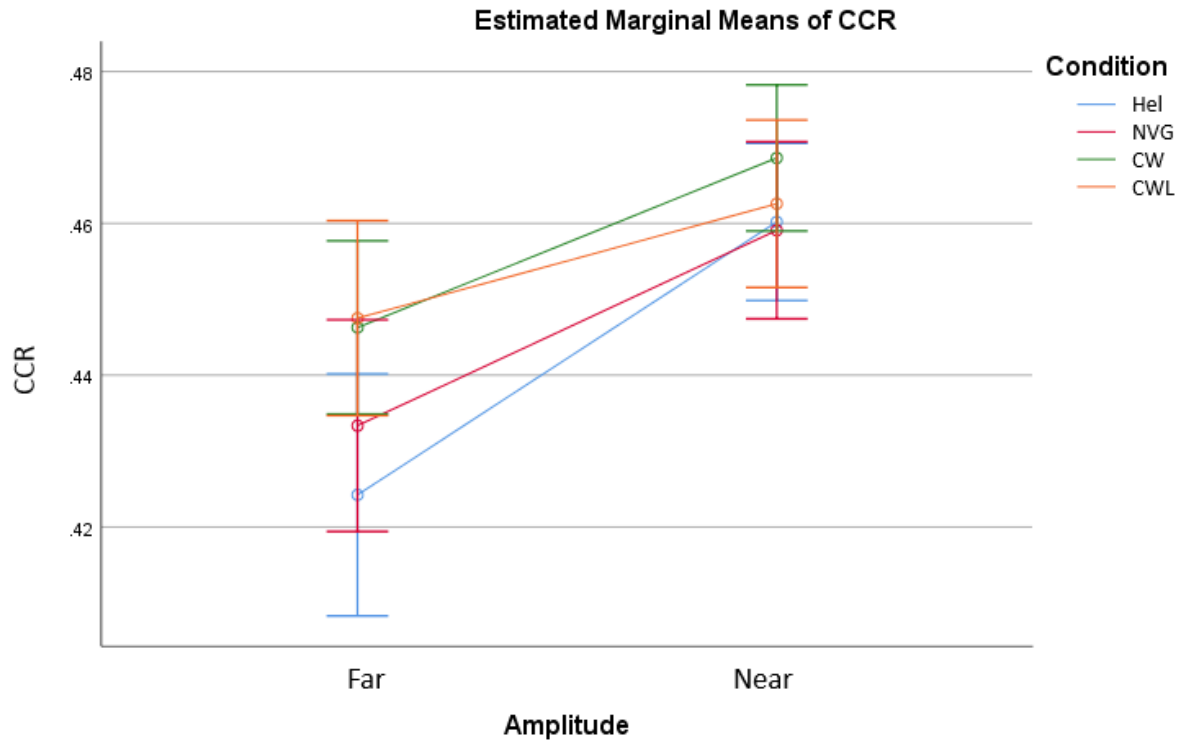


**Figure 29:** Amplitude by HSM condition interaction on CCR in the yaw trajectory. Error bars represent 95% confidence intervals. \* Indicates statistical significance

## 4.2 Research Question 2: Total Muscular Demand

### 4.2.1 Integrated EMG

The Shapiro-Wilk test for normality was significantly ( $p \leq 0.05$ ) non-normal for integrated EMG data. Therefore, data was log transformed to meet the assumption of normalcy.  $p$  and  $F$  values are reported from the normal log transformed data, however, to aid in interpretation means and mean differences are reported from the non-transformed data.



## Amplitude

In the pitch trajectory, there was a significant main effect of amplitude on iEMG in the SCML ( $F(1,29) = 287.928, p \leq 0.001, \eta_p^2 = 0.908$ ), SCMR ( $F(1,28) = 397.011, p \leq 0.001, \eta_p^2 = 0.934$ ), UNEL ( $F(1,26) = 620.296, p \leq 0.001, \eta_p^2 = 0.961$ ), and UNER ( $F(1,25) = 434.894, p \leq 0.001, \eta_p^2 = 0.942$ ). Similar results were seen in the yaw trajectory, where there was a main effect of amplitude on SCML ( $F(1,29) = 190.109, p \leq 0.001, \eta_p^2 = 0.868$ ), SCMR ( $F(1,28) = 174.856, p \leq 0.001, \eta_p^2 = 0.862$ ), UNEL ( $F(1,27) = 249.428, p \leq 0.001, \eta_p^2 = 0.902$ ), and UNER ( $F(1,26) = 300.946, p \leq 0.001, \eta_p^2 = 0.921$ ). Pairwise comparisons revealed that far conditions had significantly ( $p \leq 0.001$ ) higher integrated EMG compared with near conditions for all muscles (Figure 30).

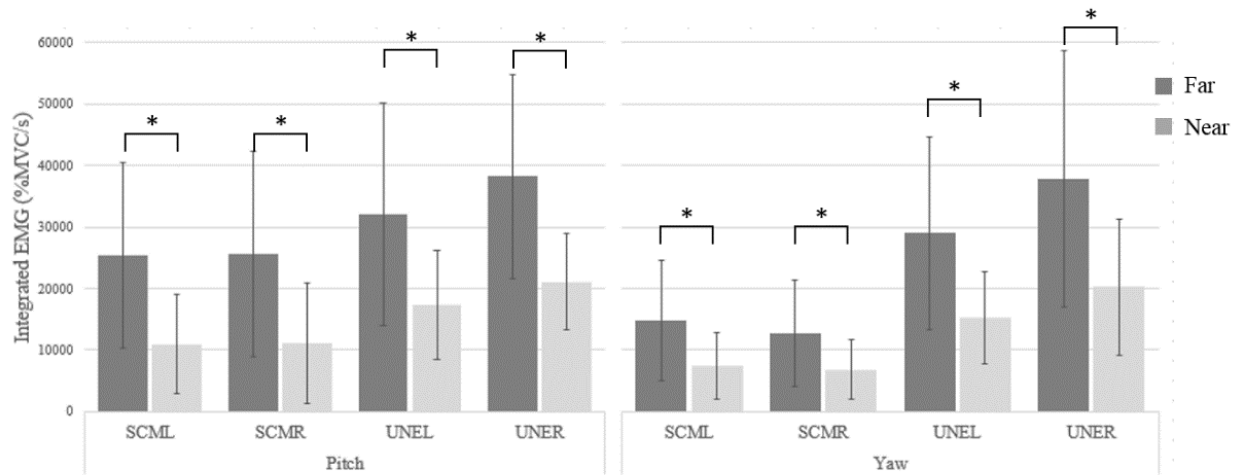


**Figure 30:** The effect of amplitude on integrated EMG  $\pm$  1SD in both the pitch and yaw trajectories. \* Indicates statistical significance

## Condition

Where Mauchly's test indicated that the assumption of sphericity had been violated, Greenhouse-Geisser corrected values were used. In the pitch trajectory, condition had a

significant effect on iEMG for SCML ( $F(2.336,67.752) = 4.635, p = 0.005, \eta_p^2 = 0.138$ ) and SCMR ( $F(2.33,65.292) = 3.473, p = 0.020, \eta_p^2 = 0.110$ ). There was no main effect of condition on iEMG for UNEL or UNER. In the yaw trajectory there was a significant main effect of condition on for SCML ( $F(2.010,58.290) = 3.596, p = 0.017, \eta_p^2 = 0.110$ ), and SCMR ( $F(2.120,59.364) = 4.018, p = 0.010, \eta_p^2 = 0.125$ ). There was also no main effect of condition for UNEL or UNER. No significant mean differences could be detected post hoc for SCML in the yaw trajectory. However, pairwise comparisons of SCML and SCMR in the pitch trajectory as well as SCMR in the yaw trajectory revealed differences between hNVG and hCW (Figures 31 & 32)

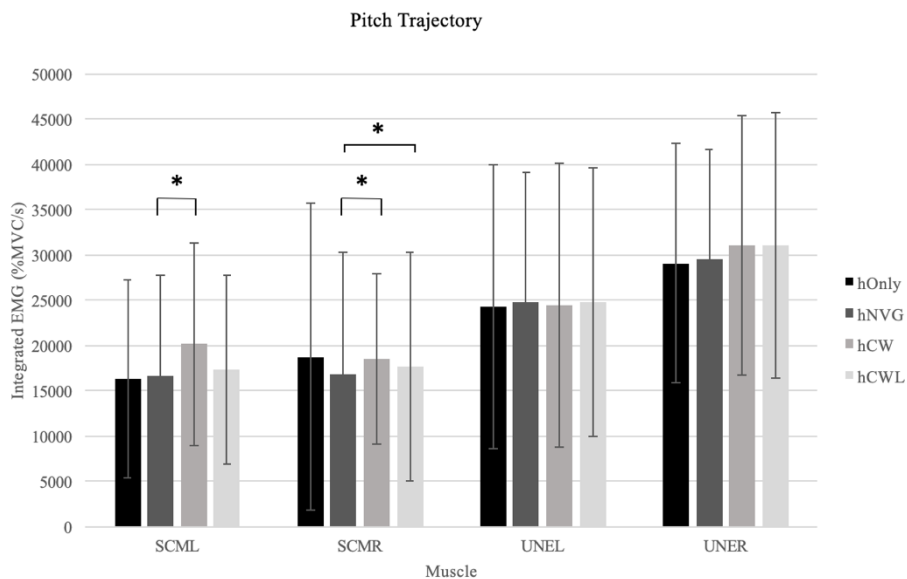


**Figure 31:** Mean differences in iEMG ± 1SD for each muscle between HSM conditions in the pitch trajectory. \* indicates significant differences

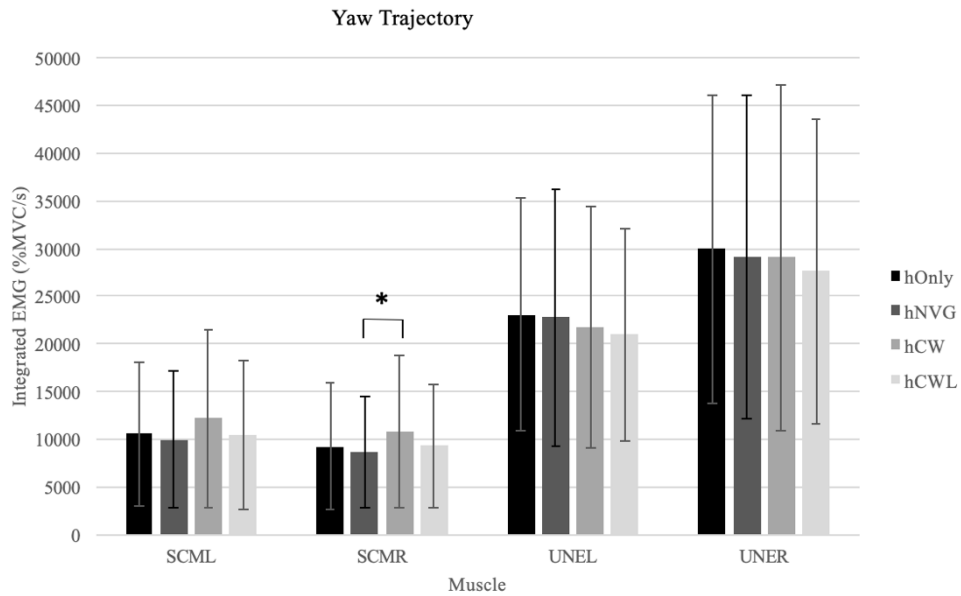


**Figure 32:** Mean differences in iEMG  $\pm$  1SD for each muscle between HSM conditions in the yaw trajectory. \* Indicates significant differences

### *Interaction effects*

There was no significant amplitude by condition interaction effects or direction by condition by amplitude interaction effects on iEMG data.

## **4.2.2 Mean EMG**

### *Amplitude*

There was a main effect of amplitude on mean EMG for all muscles in pitch and yaw trajectories (**Table 8**). Pairwise comparisons revealed that mean EMG was significantly higher for far amplitudes compared to near amplitudes (**Figure 33**).

**Table 8:** Main effects of amplitude on mean EMG for each muscle in the pitch and yaw trajectories

Trajectory	Muscle	Degrees of Freedom	F	<i>p</i>	$\eta_p^2$
Pitch	SCML	1,29	61.979	$\leq 0.001^*$	0.681
	SCMR	1,28	58.412	$\leq 0.001^*$	0.676
	UNEL	1,26	53.133	$\leq 0.001^*$	0.671
	UNER	1,25	42.338	$\leq 0.001^*$	0.629
Yaw	SCML	1,29	74.465	$\leq 0.001^*$	0.720
	SCMR	1,28	27.414	$\leq 0.001^*$	0.495
	UNEL	1,27	40.300	$\leq 0.001^*$	0.599
	UNER	1,26	68.706	$\leq 0.001^*$	0.725

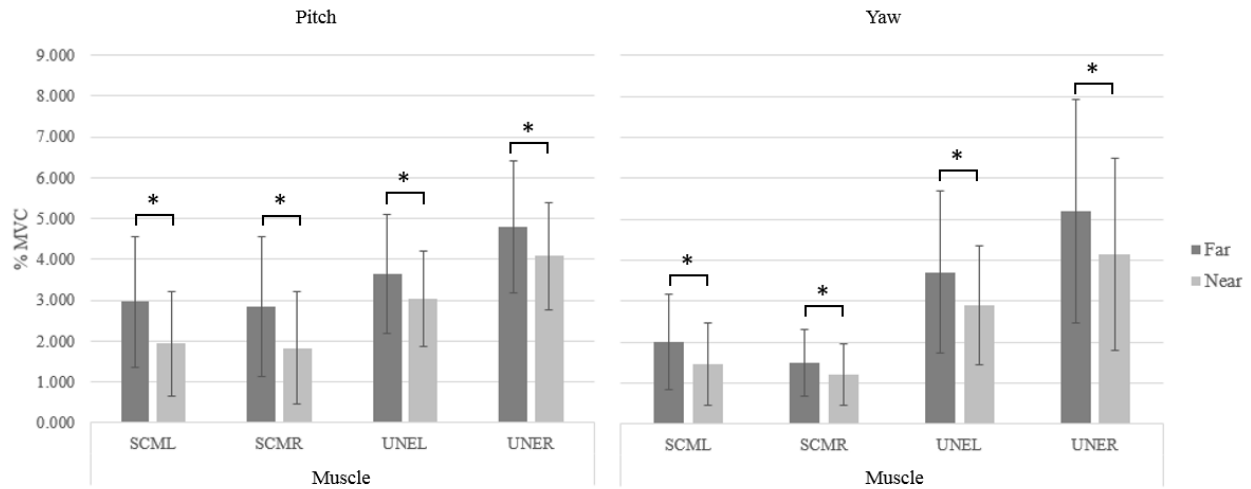


**Figure 33:** The effect of amplitude on mean EMG  $\pm$  1SD in all muscles in both the pitch and yaw trajectories. \* Indicates significant differences

### HSM Condition

In the pitch trajectory, there was a main effect of condition on mean EMG in SCML ( $F(3,87) = 4.022, p = 0.018, \eta_p^2 = 0.122$ ), UNEL ( $F(3,78) = 5.099, p = 0.003, \eta_p^2 = 0.164$ ), and UNER ( $F(3,75) = 4.406, p = 0.015, \eta_p^2 = 0.150$ ). In the yaw trajectory there was a main effect of condition on SCMR ( $F(1.652,46.245) = 3.538, p = 0.045, \eta_p^2 = 0.112$ ), and UNEL ( $F(2.322,62.702) = 7.450, p = 0.001, \eta_p^2 = 0.216$ ). In a number of cases mean differences could

not be determined post hoc (SCML and SCMR). Pairwise comparisons are shown in **Figures 34** and **35** below.

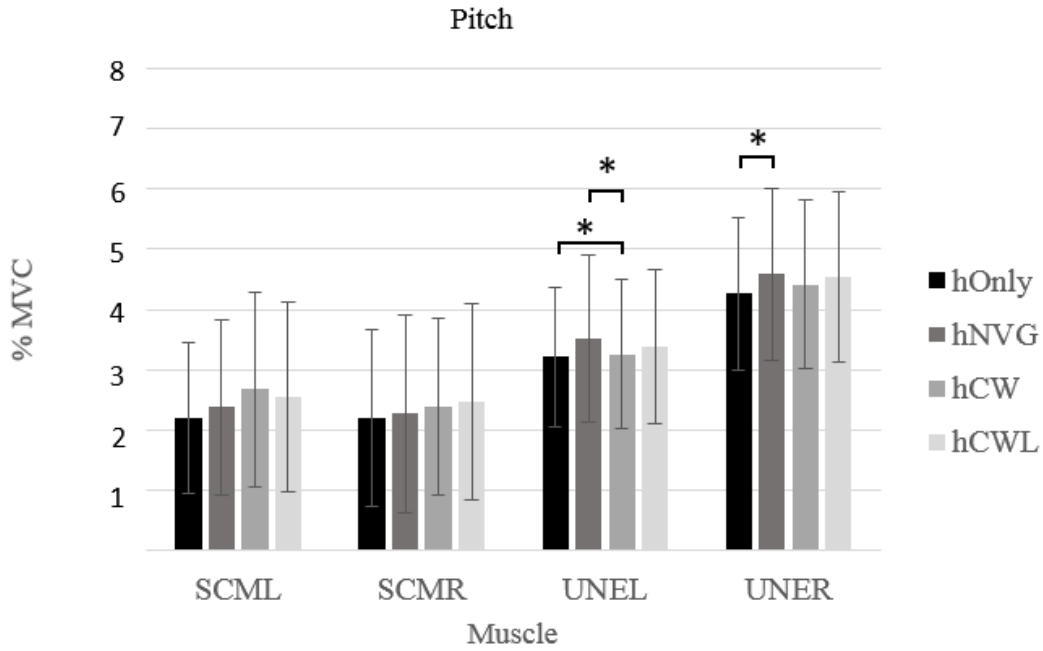


**Figure 34:** The effect of HSM condition on mean EMG  $\pm$  1SD in the pitch trajectory

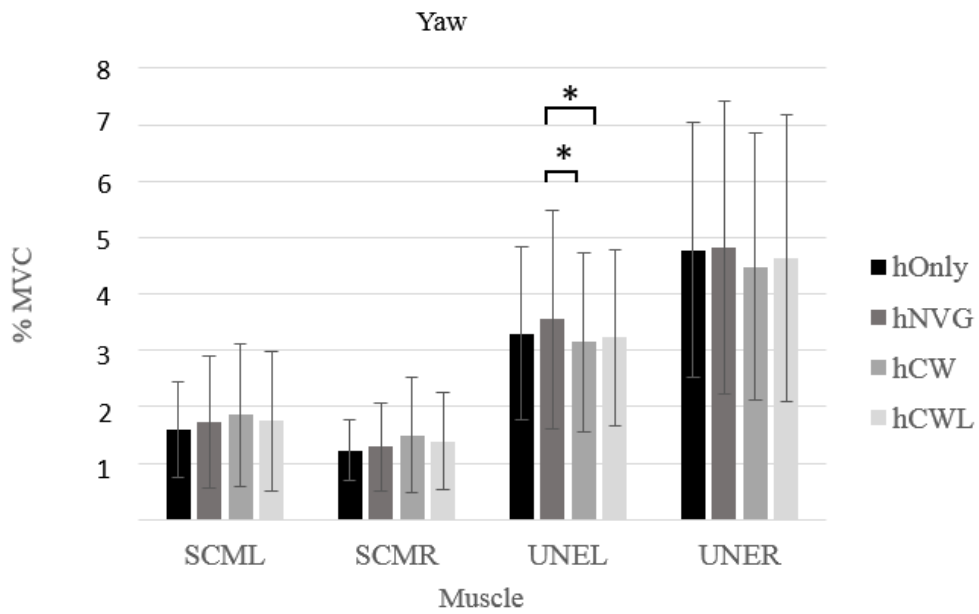


**Figure 35:** The effect of HSM condition on mean EMG  $\pm$  1SD in the yaw trajectory

### 4.3 Research Question 3: HSM and Peak Muscular Activation

#### *HSM Condition*

There was a main effect of condition on peak SCML during starting in the pitch trajectory ( $F(3,87) = 3.128, p = 0.030, \eta_p^2 = 0.097$ ). Due to a small effect size pairwise differences could not be detected. There was no main effect of HSM condition on peak EMG in any other muscles in either trajectory.

#### *Amplitude*

Amplitude had a main effect on peak EMG in both trajectories for all muscles and phases. Pairwise comparisons revealed that in all cases peak EMG was higher in the far condition compared to the near condition. Mean differences are reported in **Table 9**.

#### *Interactions*

In the yaw trajectory, there was a significant amplitude x condition interaction effect on velocity in the starting phase for peak SCML ( $F(3,87) = 3.288, p = 0.024$ ), SCMR ( $F(3,87) = 2.950, p = 0.037$ ), and UNEL ( $F(3,87) = 3.642, p = 0.016$ ), as well as in the stopping phase for peak SCML ( $F(3,87) = 2.717, p = 0.050$ ). There was not significant power to observe significant post hoc differences (**Figure 36**).

**Table 9:** The effect of amplitude on peak muscular activation

Trajectory	Phase	Muscle	Degrees of freedom	<i>F</i>	<i>p</i>	$\eta_p^2$	Mean difference (% MVC)
Pitch	Starting	SCML*	1,29	105.471	$\leq 0.001$	0.784	3.894
		SCMR*	1,29	102.458		0.779	3.601
		UNEL*	1,28	44.205		0.612	3.406
		UNER*	1,27	55.418		0.672	3.880
	Acquiring	SCML*	1,29	56.638	$\leq 0.001$	0.661	2.461
		SCMR*	1,28	52.126		0.651	2.462
		UNEL*	1,28	50.995		0.662	4.041
		UNER*	1,26	36.331		0.592	4.555
Yaw	Starting	SCML*	1,29	55.014	$\leq 0.001$	0.655	1.248
		SCMR*	1,29	50.181		0.634	1.205
		UNEL*	1,29	93.249		0.763	2.224
		UNER*	1,28	49.644		0.639	3.318
	Acquiring	SCML*	1,29	62.515	$\leq 0.001$	0.683	1.214
		SCMR*	1,29	14.601		0.335	1.488
		UNEL*	1,27	38.106		0.585	2.601
		UNER*	1,26	50.357		0.659	3.305

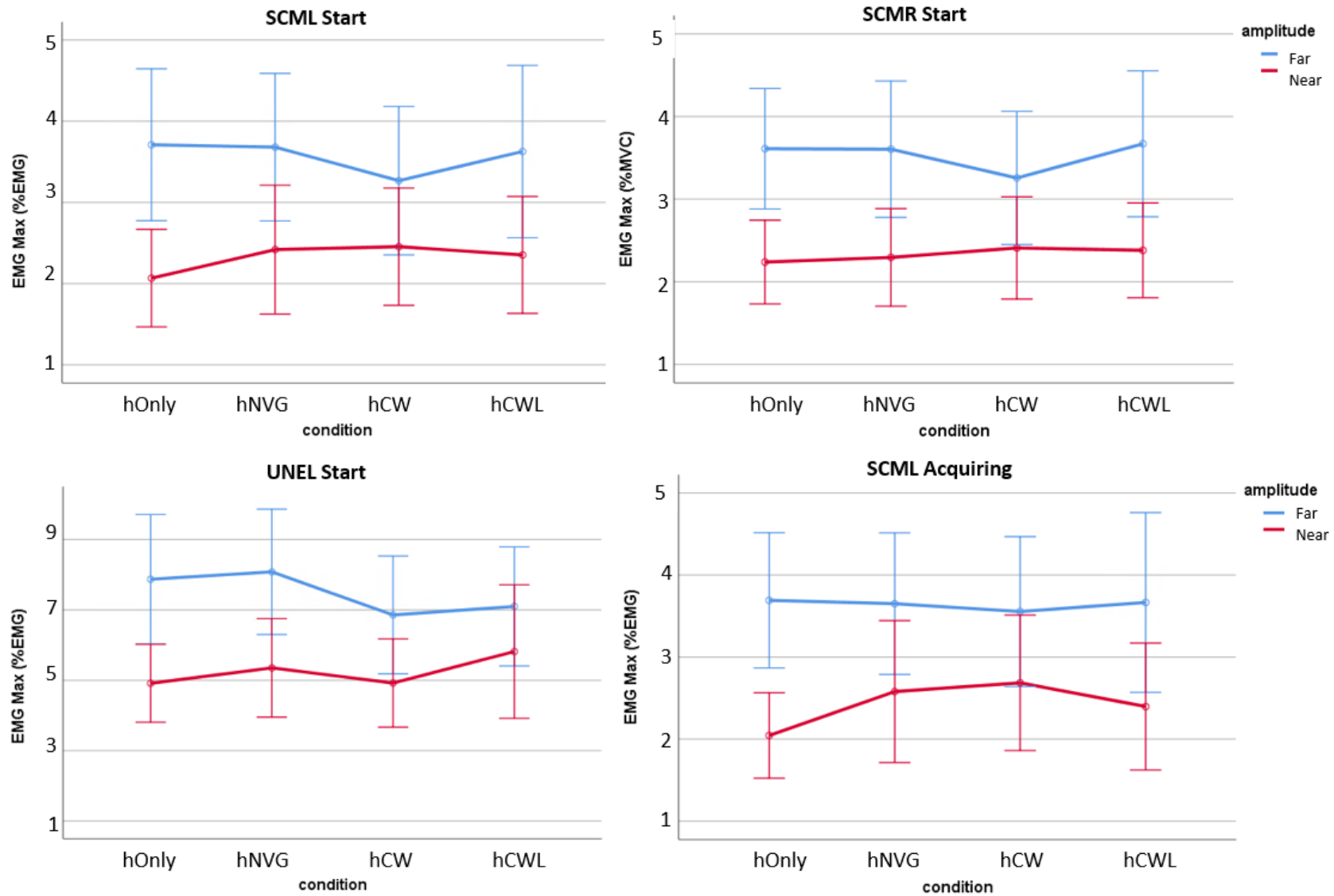


**Figure 36:** Amplitude by condition interactions for starting in the SCML, SCMR and UNEL, and acquiring in the SCML



### 4.3 Kinematics

#### *Amplitude*

Amplitude had a main effect on mean velocity in both pitch ( $F(1,29) = 284.650, p \leq 0.001, \eta_p^2 = 0.908$ ) and yaw ( $F(1,29) = 489.440, p \leq 0.001, \eta_p^2 = 0.944$ ). Pairwise comparisons revealed that average velocity in far amplitudes was  $\sim 7^\circ/s$  faster compared to near amplitudes (Figure 37).

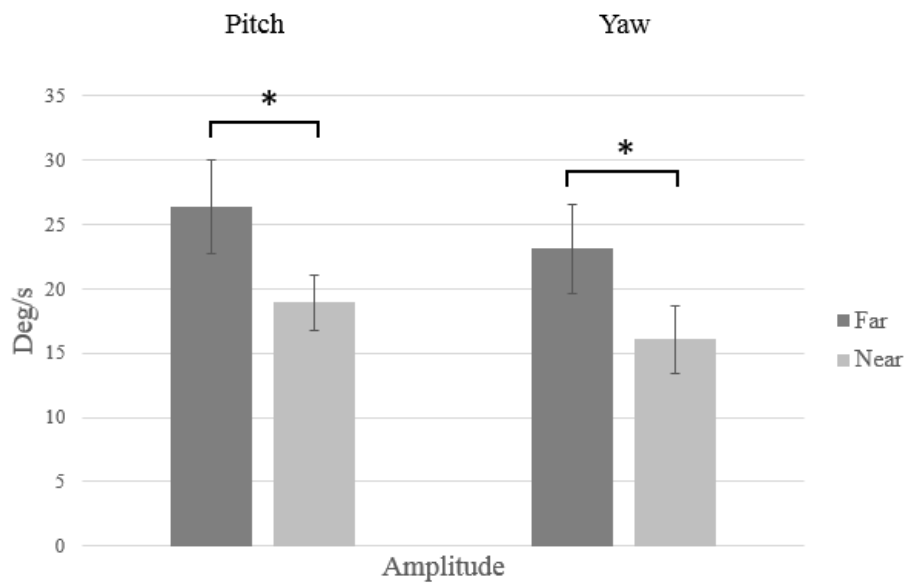


**Figure 37:** The effect of amplitude on mean velocity in the pitch and yaw trajectories

#### *HSM Condition*

HSM condition had a main effect on mean velocity in the yaw trajectory ( $F(3,87) = 10.917, p \leq 0.000, \eta_p^2 = 0.273$ ). Pairwise comparisons determined that hCW was significantly

slower than the other three conditions, however these differences were small, with the largest difference only 2 deg/s between hNVG and hCW (Figure 38).

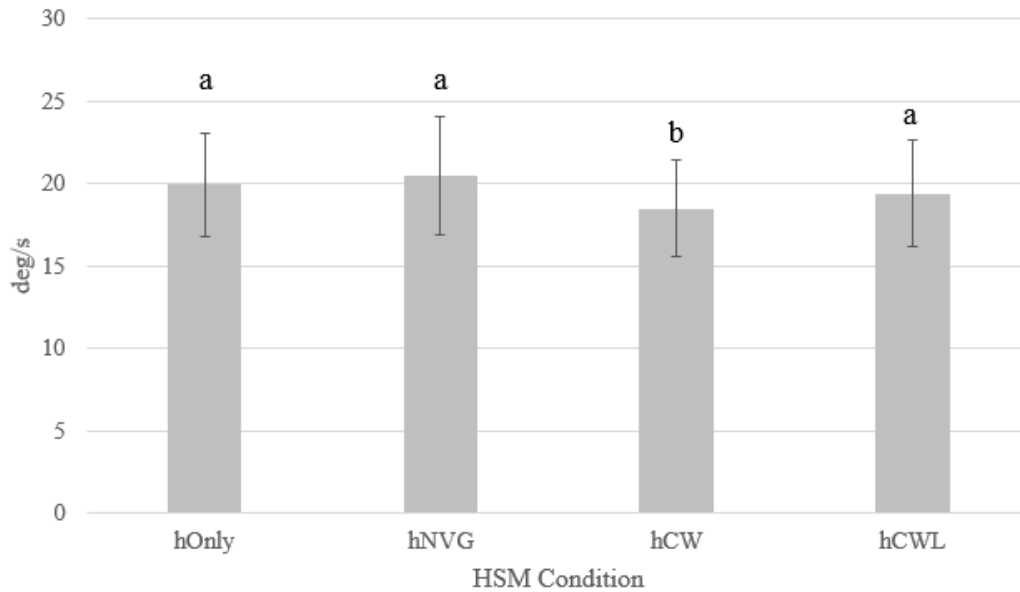


**Figure 38:** The effect of HSM condition on mean velocity in the yaw trajectory

### *Interactions*

There was a significant amplitude by condition interaction effect in the yaw trajectory ( $F(3,87) = 3.126, p = 0.030, \eta_p^2 = 0.097$ ). Post hoc testing indicated that the effect of HSM condition was amplified at far amplitudes (Figure 39). Specific differences can be seen in Table 10).

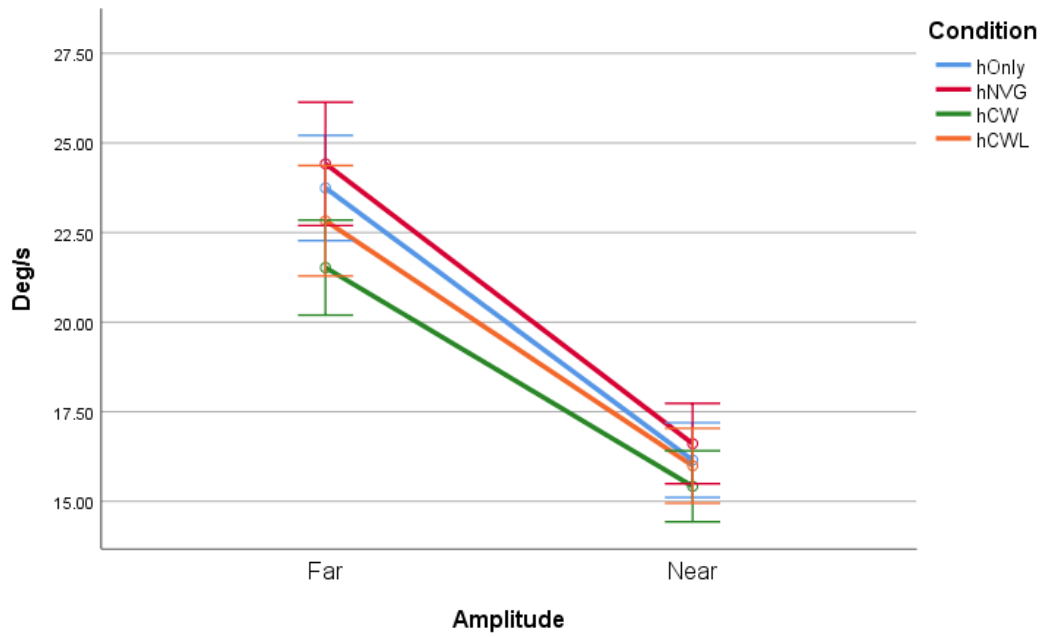


**Figure 39:** Amplitude by condition interaction effect on mean velocity in the yaw trajectory. Error bars represent 95% confidence interval

**Table 10:** Amplitude by condition interaction for mean velocity in the yaw trajectory

Amplitude	Condition(I)	Condition(J)	Mean Difference (I-J)	Std. Error	Sig	95% Confidence Interval for Difference	
						Lower Bound	Upper Bound
Far	hOnly	hNVG	-0.67	0.62	1.000	-2.42	1.07
		<b>hCW</b>	<b>2.22*</b>	<b>0.56</b>	<b>0.003</b>	<b>0.64</b>	<b>3.81</b>
		hCWL	0.92	0.78	1.000	-1.3	3.13
	hNVG	hOnly	0.67	0.62	1.000	-1.07	2.42
		<b>hCW</b>	<b>2.89*</b>	<b>0.56</b>	<b>0.000</b>	<b>1.31</b>	<b>4.48</b>
		hCWL	1.59	0.69	0.174	-0.37	3.54
	hCW	<b>hOnly</b>	<b>-2.22*</b>	<b>0.56</b>	<b>0.003</b>	<b>-3.81</b>	<b>-0.64</b>
		<b>hNVG</b>	<b>-2.89*</b>	<b>0.56</b>	<b>0.000</b>	<b>-4.48</b>	<b>-1.31</b>
		hCWL	-1.31	0.57	0.171	-2.91	0.3
	hCWL	hOnly	-0.92	0.78	1.000	-3.13	1.3
		hNVG	-1.59	0.69	0.174	-3.54	0.37
		hCW	1.31	0.57	0.171	-0.3	2.91
Near	hOnly	hNVG	-0.46	0.28	0.673	-1.26	0.34
		hCW	0.73	0.26	0.055	-0.01	1.47
		hCWL	0.16	0.25	1.000	-0.56	0.88
	hNVG	hOnly	0.46	0.28	0.673	-0.34	1.26
		<b>hCW</b>	<b>1.19*</b>	<b>0.26</b>	<b>0.001</b>	<b>0.44</b>	<b>1.94</b>
		hCWL	0.62	0.27	0.170	-0.14	1.38
	hCW	hOnly	-0.73	0.26	0.055	-1.47	0.01
		<b>hNVG</b>	<b>-1.19*</b>	<b>0.26</b>	<b>0.001</b>	<b>-1.94</b>	<b>-0.44</b>
		hCWL	-0.57	0.21	0.066	-1.17	0.02
	hCWL	hOnly	-0.16	0.25	1.000	-0.88	0.56
		hNVG	-0.62	0.27	0.170	-1.38	0.14
		hCW	0.57	0.21	0.066	-0.02	1.17

## 4.4 Performance Measures

### Amplitude

In the pitch trajectory, there was a main effect of amplitude on TAT ( $F(1,29) = 292.016$ ,  $p \leq 0.000$ ,  $\eta_p^2 = 0.910$ ). Similar results were seen in the yaw trajectory, where there was a main effect of amplitude on TAT ( $F(1,29) = 152.816$ ,  $p \leq 0.000$ ,  $\eta_p^2 = 0.840$ ). Pairwise comparisons revealed TAT was significantly longer for far conditions compared to near conditions (**Figure 40**). Full results of performance measures can be found in Appendix D.

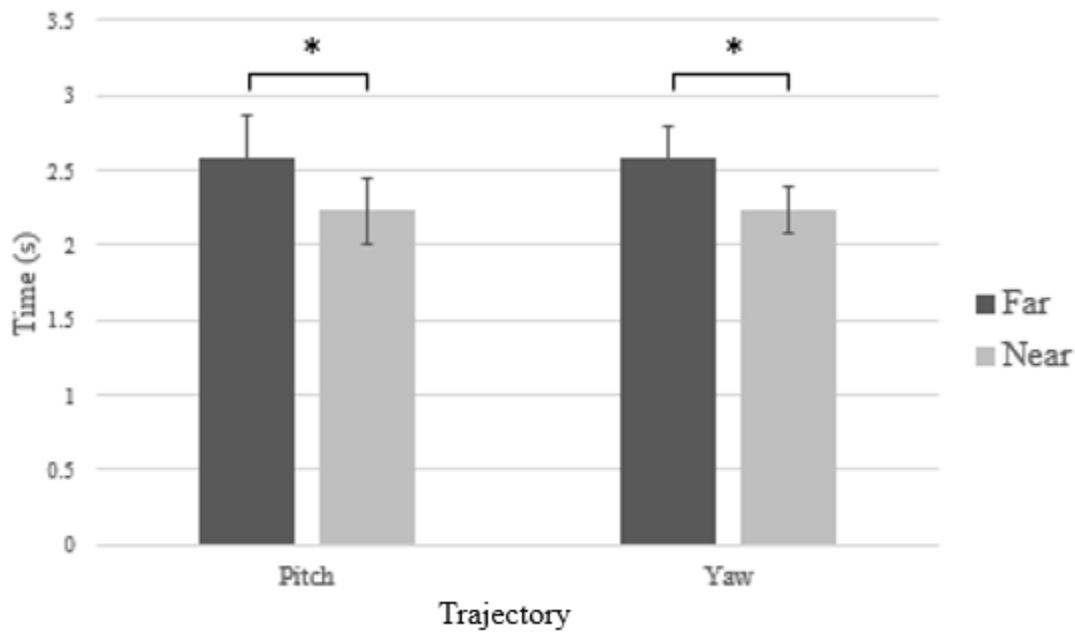


**Figure 40:** The effect of amplitude on TAT (time to acquire target)

## 5. Discussion

### 5.1 Key Findings

The objective of this study was to probe how increased mass, moment of inertia, and posture interpedently affect neck function using a novel dynamic target acquisition task. Main findings were threefold: (1) A larger range of motion increased neck muscle activity across all EMG-related outcome measures (2) Increased mass resulted in a modest increase in co-contraction (3) Moment of inertia had minimal effects on peak muscle activity required to stop and start the head. Overall, the current results suggest that the restricted field of view, causing increased range of motion, and increased muscular demand may be a dominant causal pathway by which NVGs lead to neck trouble. However, as a secondary pathway, evidence also demonstrated that increased mass resulted in increased co-contraction. Sustained increased co-contraction requirements have implications with respect to cumulative loading or Cinderella hypothesis-based injury models.

### 5.2 Co-Contraction

Hypothesis one postulated that an increase in mass would increase co-contraction. It was proposed that an increase in mass would increase the potential energy of the system, thereby requiring increased co-contraction to stabilize the head across the entire scanning task (**Figure 1**). Significant differences in co-contraction were found between counter-weighted conditions (hCW and hCWL) and non-counter-weighted conditions (hOnly and hNVG) in the yaw trajectory (**Figure 27**), supporting this hypothesis. The increase in co-contraction is important because it may lead to increased loading in the cervical spine, reducing stress bearing capacity and eventually lead to a cumulative loading injury (**Figure 1**). Alternatively, the increased co-

contraction may require prolonged recruitment of type one fibres, eventually resulting in an injury via the Cinderella hypothesis (**Figure 1**).

While the results indicate an increase in co-contraction with increased mass, these results should be interpreted with caution as mean differences were no greater than  $0.015 \pm 0.004$ , or a 0.15% change in CCR, to which the clinical significance is not known. Further, a significant increase was only seen in the yaw trajectory, and no pattern in agonist ( $\text{NAIEMG}_{\text{agonist}}$ ) or antagonist ( $\text{NAIEMG}_{\text{antagonist}}$ ) activity were found. Comparatively, Callaghan (2014) reported muscle co-activation during sustained static postures, under different helmet conditions, and found no helmet mass main effects. One explanation for small changes despite increased load may be due to the complexity of the neck musculature and load sharing (Thuresson et al., 2003; Murray et al., 2016). Because only two muscles were assessed in this study, it is unknown what the contributions of the deep cervical stabilizers are. It is possible that this study, as well as previous studies, have underestimated the increase in co-contraction due to the inability to access a number of deep neck muscles. Although the changes seen in this study were small, these differences may be amplified during vibration, with increased mass (for example, while also wearing a chemical threat mask or heads up display unit), or over time as pilots become fatigued. Therefore, the data suggest the plausibility of a mass-related destabilization effect resulting in increases co-contraction, with the possibility of these effects being amplified in real flight scenarios.

Although no hypothesis directly linked CCR and amplitude, there were main effects of amplitude on CCR. CCR was significantly greater for near amplitudes in both the yaw and pitch trajectories, however, these differences were small (**Figure 28**). Further highlighting the importance of amplitude is an interaction effect between amplitude and condition where

significant differences in CCR between HSM conditions (hOnly, hNVG < hCW, hCW) only existed at far amplitudes (**Figure 29**). Interestingly, mean velocity was also significantly higher during far amplitudes, approximately  $\sim 7$ deg/s faster compared to near amplitudes (**Figure 36**). This is important to note because these results align with Cheng et al. (2008) and may explain the CCR findings. Cheng et al. (2008) assessed the effect of speed on neck muscle co-contraction using the CCR. They determined that CCR was significantly higher in slow and medium speeds (3.0-13.1°/s), compared to fast speeds (23.0-32.1°/s). They attribute these differences to control strategies, one being a feedback loop for slow and controlled movements, and the second being a feed-forward loop for fast movements. The feed-forward loop for fast movements is also known as an anticipatory mechanism, which increases agonistic activity, but does not increase antagonistic activities required to stabilize the spine (Ebadzadeh et al., 2005). Although lower antagonistic activity reduces the resistance to motion, supporting the potential for increased velocity, a lack of co-contraction may provide less protection against innocuous perturbations, increasing injury risk (McGill et al., 2003). While the CCR findings in the current study were similar to that of Cheng et al. (2008) for a range of velocities, relationships between CCR and injury risk are still unknown. As hypothesized in research question one, elevated HSM led to increased co-contraction which may increase injury risk. Future research should continue to probe CCR as a potentially relevant indicator of risk and to highlight underlying neuromuscular control strategies.

Mean EMG data also supports the Cinderella hypothesis (Hagg, 1991) as a possible injury pathway. As hypothesized in **Figure 1**, increased mass was thought to lead to increased co-contraction, which may have implications in a cumulative loading or Cinderella hypothesis injury pathway. While muscle activity appears to be relatively low, previous work has shown



sustained muscle activity as low as 5% MVC can cause localized fatigue and ischemic muscular pain (Sjogaard et al., 1986). In this case, individuals mean muscle activity ranged from 0.4-17.7% in the pitch trajectory and from 0.3-16.5% in the yaw trajectory. However, averaged across participants and trajectories, mean muscle activity ranged from 1-6% MVC. Comparatively, Murray et al. (2016) found sustained UNE activity of ~10% during a sortie. Callaghan (2014) also found mean EMG to range from 0.6-12.9% MVC during slow head movements and static holds. It is possible that the low, sustained activity will overwork type 1 fibres, resulting in fibre injury, and eventually neck pain (Hagg, 1991). Because of the range of muscle activity seen, we cannot disregard the potential effects of the Cinderella Hypothesis, and the effects this sustained muscle activity may have over time.

### **5.3 Total muscular effort**

Target amplitude was varied to assess the effects of range of motion. All outcome measures were substantially influenced by target amplitude. In general, muscular activity was higher for far conditions compared to near. Specifically, total muscular activity (iEMG) was significantly higher for far amplitudes compared to near for all muscles. It is important to note that TAT was also significantly longer (by ~0.34s) for far amplitudes (**Figure 39**), influencing the iEMG measure. For this reason, average (mean) EMG was also assessed as a measure to represent the construct of total muscular effort. Mean EMG was also significantly higher for far amplitudes compared to near, with a mean difference between 1.2-4.5% (**Table 7**). Therefore, the results provide support for hypothesis 2a, that an increase in range of motion would increase total muscular demand. An increase in total muscular demand may have implications regarding overexertion injuries (**Figure 1**). Interestingly, there was no interaction effect of condition or

amplitude for iEMG or mean EMG, such that hypothesis 2b was rejected; differences in total muscular demand under different HSM condition were not dependent on amplitude.

Posture and range of motion have long been understood as influential factors when considering the effects of helmets and HSM on neck trouble (Forde et al., 2011; Thuresson et al., 2003; Knight & Baber, 2007; McKinnon, 2016). In fact, in a 2004 report offering recommendations to reduce flight-related neck pain suggested moving the control display unit to a point further up to reduce extreme forward flexion (Adam, 2004). Further, Forde et al. (2011) determined that a key difference between day flying (without NVGs) and night flying (with NVGs) was time spent in extreme postures at night. They determined that loading is increased in part by the mass of the helmet and NVG system, but more significantly by time spent in non-neutral postures. Interestingly, while Harms-Ringdahl et al. (2007) agreed extreme postures increase in the load moment of the C7-T1 segment and are likely a causal factor in neck trouble, they found no significant increase in muscle activity during sustained extreme flexion and extension. They proposed that this finding may suggest that when holding very extreme flexion positions the load moment is balanced by passive connective tissue structures such as joint capsules and ligaments. Our findings support previous work that suggest range of motion is a risk factor for neck trouble during a dynamic, rapid scanning task, as it increases total muscular demand. However, more detailed musculoskeletal modeling is required to probe how the load moment might be balanced via active and passive tissues.

## **5.4 Peak muscular activity**

Hypothesis three postulated that an increase in moment of inertia would increase peak muscular activity required to stop and start the head. The results suggested that there was no

difference in peak muscular activity between HSM conditions, with the exception of SCML starting in the pitch trajectory. These results suggest that increased moment of inertia does not have a pronounced effect on peak muscle activity, refuting hypothesis three.

It is interesting that despite increasing helmet mass by over 50%, and changing the moment of inertia of the helmet, peak neck muscle activity to stop and start did not significantly change during the rapid reciprocal scanning. Few authors have assessed the effect of HSM on neck muscle activity during dynamic movements in laboratory or in flight and found similar results. In one laboratory study, Callaghan (2014) assessed the effects of no helmet, helmet only, helmet with NVGs and helmet with CW on neck muscle activity during static and slow-moving tasks. Of the 315 statistical comparisons done to determine the effect of helmet condition on muscular activation, including mean, median, peak root mean square (RMS), and amplitude probability distribution function (APDF), only six main effects of head supported mass were found. They concluded that helmet condition had little effect on neck muscular responses. Murray et al. (2016) found similar results when recording EMG during a cruising flight, and concluded that added NVGs resulted in less than a 1% difference in mean muscle activity. Finally, Thuresson et al. (2007) found small, but significant, differences in total muscle activity when wearing NVGs and NVGs and a CW compared to helmet only. However, these differences were not present when position and individual muscles were considered.

A number of factors may influence this phenomenon. First, some authors suggest it is due to the non-linear relationship between force and muscle activity (Murray et al., 2016; Thuresson et al., 2003). This was demonstrated by Schuldt and Harms-Ringdahl (1988), who demonstrated that a force up to 40% of maximum could be produced by a muscle activity level between 10-15% MVC. They determined that muscle activity required to produce the same force can differ

based on neck position, which this study supports with hypothesis two. Further, it is likely that the load is shared amongst a number of muscles in the neck acting synergistically. Because only two muscles were assessed in this study, it is unknown what the contributions of the deep cervical stabilizers are. It is possible that other muscles in the neck are contributing more to stop and start the head, however we did not capture it with the UNE and SCM muscles.

Interestingly, peak EMG was influenced by target amplitude. Our findings align with others who found peak EMG to range from 1.5-19.6% MVC (McKinnon, 2016). These results suggest that a possibly pathway of injury may be increased range of motion causing an increase in muscle forces required to stop and start the head, resulting in an overexertion injury over time. One possible explanation for this pathway may be due to the increased angular velocity at farther amplitudes (**Figure 36**). To generate higher velocity requires higher muscle activity, and likewise, to stop the head from a faster velocity likely also requires higher muscle activities. To further probe this hypothesis, future work should assesses muscle activity required to stop and start the head at known and controlled speeds to determine if peaks in muscle activity is due to increased range of motion, or increased velocity.

## **5.5 Implications and suggestions**

The results of this study provide useful information to both pilots and potential helmet designers as it highlights potential mediating factors within plausible neck injury pathways. The original pathways of injury hypothesized at the start of this study have been revised based on the results of this study (**Figure 41**). Pathways that were probed and deemed to be important are highlighted with red arrows. The main results suggest that increased range of motion may be the most influential factor resulting in higher neck muscle activity, which may in turn, increase risk

of injury. Interestingly, while it was hypothesized that an increase in range of motion would increase muscular demand, it was also found to have effects on peak EMG and co-contraction, further demonstrating the importance of range of motion. However, it is important to note that increased range of motion also increased mean velocity, which potentially may be the driving factor causing difference in some outcome measures. While the main focus for many years has been the weight and shift in centre of mass caused by added head supported devices, our results suggest that such efforts may be less efficacious relative to a focus on overcoming the field-of-view restriction. That is not to say that mass and moment of inertia are not important factors to consider, rather designers should consider all factors with the largest consideration on postural requirements.

There are many suggestions to decrease range of motion of pilots that include both the helmet system, as well as the environment. The largest factor that will influence range of motion is increasing the field of view of NVGs. Transparent NVGs have been suggested to increase the field of view (Knight & Barbar, 2007). Further, with advancing technologies such as virtual reality headsets, the possibility of 3-D displays and fully immersive binocular displays streaming real-world images may completely remove the need for pilots to wear heavy and view restricting goggles. Other factors that should be addressed include cockpit design, which as many authors have pointed out, is not ergonomically favorable (Fischer et al., 2013; Forde et al., 2011). Rearrangement of controls and screens may decrease postural demands both during day and night flying. However, short term solutions may include educating pilots to remain in neutral postures as much as possible and reducing flying time wearing NVGs.

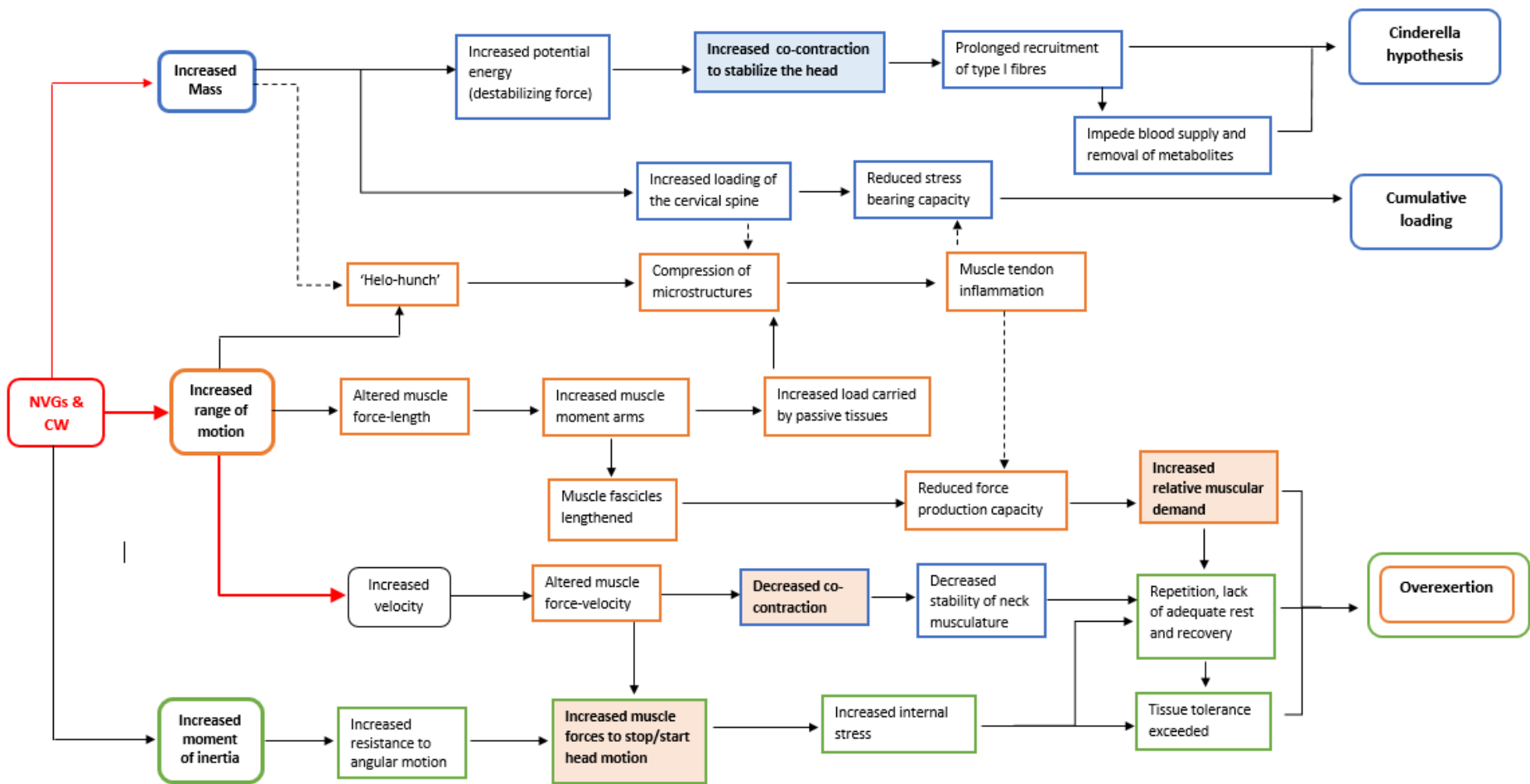


**Figure 41:** Updated potential causal pathways of injury. Highlighted boxes indicate findings from the current study.

## 5.6 Limitations

### *Surface EMG*

Several limitations must be taken into consideration when interpreting the results of this study. First, surface EMG of the neck is susceptible to large amounts of cross-talk due to the small size and number of muscles in the neck (Thuresson et al, 2005). Care was taken in placement of electrodes to try to mitigate these effects. Noise was also problematic, likely due to physical contact between the helmet and EMG sensors and potential cable artifact from the Delsys mini sensor to the base. For this reason, 7 to 13 out of 64 trials were removed for three participants in the yaw trajectory and four participants in the pitch trajectory. Further, surface electrodes are subject to sliding over the muscle. While great care was taken to tape electrodes to the skin to prevent movement, the nature of the muscles in the neck, specifically the sternocleidomastoid muscles, make it difficult to control in fully rotated or fully flexed positions. Finally, only two muscles are assessed in this study, SCM and UNE. While these are amongst the most common observed in HSM studies and were determined to be the primary movers in the yaw and pitch trajectories assessed, deeper cervical stabilizing muscles may also have a very important role in rapid neck movements and stabilization of different HSM conditions.

### *Simulating a Flight*

This study tried to simulate a number of flight-like characteristics, such as amplitudes for near and far scanning (Forde et al., 2011), the helmet and NVGs, and the chair and harness. However, there are characteristics that differ from a real flight and may be important to consider. First, our study population was healthy, young adults. Active aircrew are noted to have

degenerative spine changes and therefore their response to a scanning task may differ from a healthy population (Murray et al., 2016).

Importantly, these results should be interpreted relative to the length of a military sortie, which can be up to 3.5 hours (Murray et al., 2016; Harrison et al., 2007). In the present study participants were given ample rest time to prevent fatigue from occurring, however many authors have noted that fatigue may be a factor leading to neck trouble in pilots (Thuresson et al., 2005; Tack et al., 2014; Harrison et al., 2009). As of now, it is unknown whether the results from this study would remain the same over a longer duration. Another large factor is that during flight pilots are subject to vibration, a factor that many authors have suggested may be contributing to neck pain and reduced performance (Shanahan & Reading, 1984; Fischer et al., 2013; Smith, 2002). Vibration has been found to largely affect the head in pitch motion, and increase the load (Butler, 1992). It is hypothesized that vibration will amplify the results seen in this study. However, it is of great interest to determine how vibration influences muscle activity and performance under these different target amplitudes and HSM conditions.

### *VTAS*

The VTAS was used to elicit reciprocal, rapid head movements. However, it is important to note participants were performing a novel task, which has the ability to induce a learning effect. To mitigate these effects all participants were given practice trials to familiarize themselves with the system and helmet. Further, previous pilot work with the VTAS system has shown three repetitions is adequate to get repeatable results from participants.



## 5.7 Future Directions

First, to confirm our conclusions and to improve external validity, it is critical to understand the effects of vibration on the outcome measures assessed. Additionally, it would be interesting to extend the protocol to examine the effect of prolonged exposure to HSM, as akin to a real sortie or search and rescue mission. To address the differences in velocity between amplitudes, future work should control for speed and determine the effects of speed and amplitude independently. Finally, it would be interesting to have experienced pilots take part in the study to determine if their experience wearing helmets and NVGs, as well as any potential neck strength or degeneration affects the results. These steps would all help confirm the findings of this study and improve external validity.

Further, non HSM questions about participant motivation, performance, and control strategy arose from this study. It would be interesting to look at correlations between participant performance and muscle activity to determine if performance or motivation was a confounding factor. Along these lines, it would be interesting to assess control strategies and determine if individuals can be categorized by strategy. Because the VTAS is based on Fitt's Law, participants were forced to sacrifice speed for accuracy and vice-versa. It is possible that neck muscle activity may exhibit different patterns for individuals that prioritized speed, versus individuals that prioritized accuracy. Although these factors do not directly link to understanding the cause of neck trouble, they would be interesting to understand with regard to use of the VTAS system in understanding other motor control paradigms.

## 6. Conclusions

This study was novel in that it pragmatically probed the effects of mass, moment of inertia, and range of motion on neck muscle activity and performance in a dynamic scanning task. It was designed to purposely probe factors that may give insight into pathways by which donning NVGs might influence neck trouble. The main outcome from this study was that range of motion had the greatest influence on neck muscle activity and performance, relative to added mass and altered moment of inertia. We can suggest that an increased range of motion will increase muscular demand required for a scanning task, potentially leading to an overexertion injury (Kumar, 2001). Further, increased range of motion was also found to increase peak muscle forces required to stop and start the head, possibly contributing to an overexertion injury. It is important to note that velocity may also be a contributing factor when considering the differences between near and far amplitudes in this study. There was also evidence to support hypothesis one based on increased co-contraction with increased mass in the yaw trajectory. Further, mean EMG values were over a 5% limit (Sjogaard et al., 1986), further adding to the possibility of a cumulative load injury, or an injury due to the Cinderella hypothesis (Kumar, 2001; Hagg, 1991). In conclusion, when considering how to reduce neck pain in injury in helicopter pilots, designers should first consider ways in which field of vision can be increased and postural demands can be lowered, followed by decreasing the total mass of the helmet.

## References

- Adam, J. (2004). Results of NVG-induced neck strain questionnaire study in CH-146 Griffon aircrew. DRDC-TR-2004-153.
- Alem, N. M., Meyer, M. D., & Albano, J. P. (1995). Effects of Head Supported Devices on Pilot Performance During Simulated Helicopter Rides U . S . Army Aeromedical Research Laboratory, (95).
- Altizer, L. (2003). Strains and Sprains. *Orthopaedic Nursing*, 22(6), 404-409.
- Ang, B., & Harms-Ringdahl, K. (2006). Neck pain and related disability in helicopter pilots: A survey of prevalence and risk factors. *Aviation, Space, and Environmental Medicine*, 77(7), 713-719.
- Aydog, S.T., Turbedar, E., Demirel, A.H., Tetik, O., Akin, A., & Doral, M.N. (2004). Cervical and lumbar spinal changes diagnosed in four-view radiographs of 732 military pilots. *Aviation, Space, and Environmental Medicine*, 75(2), 154-157.
- Barazanji, K. W., Alem, N. M., & Aeromedical, U. S. A. (n.d.). Tolerance of females to head-supported devices during simulated helicopter vibration, (Mvc).
- Barrett, J. (2016). An EMG-Driven cervical spine model for the investigation of joint kinetics: With application to a helicopter pilot population. (Masters Dissertation). The University of Waterloo, Waterloo, CA.
- Bogduk, N., & Mercer, S. (2000). Biomechanics of the cervical spine. I: Normal kinematics. *Clinical Biomechanics*, 15(9), 633–648.
- Bogduk, N., & Yoganandan, N. (2001). Biomechanics of the cervical spine Part 3: Minor injuries. *Clinical Biomechanics*, 16(4), 267–275.
- Boettcher, C.E., Ginn, K.A., & Cathers, I. (2009). Standard maximum isometric voluntary contraction tests for normalizing shoulder muscle EMG. *Journal of Orthopaedic Research*, 26(12), 1591-1597.
- Butler, B.P. (1992). Helmeted head and neck dynamics under whole body vibration. (Doctoral dissertation). The University of Michigan, Michigan, US.
- Butler, B.P., & Alem, N.M. (1997). Long-duration exposure criteria for head-supported mass. USAARL Report no. 97-34. Fort Rucker, AL.
- Callaghan, J.P., Dickerson, C., Laing, A., Joseph, C., McKinnon, C., & Noguchi, M. (2014). The influence of neck posture and helmet configuration on neck muscle demands. DRDC-RDDC-2014-C188

- Chafe, G.S., Farrell, P.S. (2016). Royal Canadian Air Force CH-146 Griffon aircrew 2014 spinal musculoskeletal trouble survey. DRDC-RDDC-2016-R179
- Cheng, C.H., Lin, K.H., & Wang, J.L. (2008). Co-contraction of cervical muscles during sagittal and coronal neck motions at different movement speeds. *European Journal of Applied Physiology*, *103*, 647-654.
- Cheverud, J., Gordon, C.C., Walker, R.A., Jacquish, C., Kohn, L., Moore, A., Yamashita, N. (1990). 1988 Anthropometric survey of US army personnel: Correlation coefficients and regression equations. Part 1 statistical techniques, landmark, and measurement definitions. Report from United States Army Natick Research, Natick, MA 01760-5000
- Choi, H., & Vanderby, R. Electromyographic measurement and analysis of neck loads. Presented at the 43rd Annual meeting of the Orthopaedic Research Society, San Francisco, California, February 9–13, 1997.
- Cote, P., Cassidy, J.D., & Carroll, L. (1998). The Saskatchewan Health and Back Pain Survey: the prevalence of neck pain and related disability in Saskatchewan adults. *Spine*, *23*(15), 1689-1698.
- Craig, J., Task, L., Filipovich, D. (1997). Development and evaluation of the Paranormic Night Vision Goggle. Air Force Research Laboratory Wright-Patterson, AFB, OH. ASC97-0507.
- Ebadzadeh M., Tondu, B., & Darlot, C. (2005). Computation of inverse functions in a model of cerebellar and reflex pathways allows to control a mobile mechanical segment. *Neuroscience*, *133*(1), 29:49.
- Eckersley, C.P., Cox, C.A., Ortiz-Paparoni, M.A., Lutz, R.H., Sell, T.C., & Bass, C.R. (2018). A pain in the neck: A modeling analysis for design limitations of head supported mass. 2018 Ohio State University Injury Biomechanics Symposium.
- Falconer, K., & Winter, D.A. (1985). Quantitative assessment of co-contraction at the ankle joint in walking. *Electroencephalography and Clinical Neurophysiology*, *25*(2-3), 135-149.
- Falla, D. (2004). Masterclass: Unravelling the complexity of muscle impairment in chronic neck pain. *Manual Therapy*, *9*(1), 125-133.
- Falla, D., Dall’Alba, P., Merletti, R., & Jull, G. (2002). Location of innervation zones of sternocleidomastoid and scalene muscles – a basis for clinical and research electromyography applications. *Clinical Neurophysiology*, *113*(1), 57-63.
- Farrell, P., Tack, D.W., Nakaza, E.T., Bray-Miners, J. (2014). Combined task and physical demands analyses towards a comprehensive human work model. *Proceedings of the Human Factors and Ergonomics Society 58<sup>th</sup> Annual Meeting*, *58*(1).

- Farrell, P., Tack, D.W., Nakaza, E.T., & Bray-Miners, J. (2016). Helicopter aircrew cumulative neck loads from integrated task and physical demands analysis. *Proceedings of the Human Factors and Ergonomics Society 2016 Annual Meeting*, 60(1).
- Fischer, S.L., Stevenson, J.M., Albert, W.J., Harrison, M.F., Bryant, T., Beach, T.A.C., Reid, S.A., & Coffey, B. (2013). Near-term ideas to address aircrew helmet systems-induced neck pain. DRDC-CR-2013-039.
- Forde, K.A., Albert, W.J., Harrison, M.F., Neary, J.P., Croll, J., & Callaghan, J.P. (2011). Neck loads and posture exposure of helicopter pilots simulated day and night flights. *International Journal of Industrial Ergonomics*, 41(2), 128-135.
- Gosselin, G., & Gagan, M.J. (2014). The effects of cervical muscle fatigue on balance – A study with elite amateur rugby league players. *Journal of Sports Science Medicine*, 13(2), 329-337.
- Girolami, M., Ghermandi, R., Ghirelli, M., Gasbarrini, A., & Boriani, S. (2017). Anatomy of the subaxial cervical spine. In S. Boriani, L. Presutti, A. Gasbarrini, & F. Mattioli (Eds.), *Atlas of craniocervical junction and cervical spine surgery* (17-26). Switzerland: Springer International Publishing.
- Hagg, G.M. (1991). Human muscle fibre abnormalities related to occupational load. *European Journal of Applied Physiology*, 83(1), 159-165.
- Harms-Ringdahl, K., Ekhold, J., Schuldt, K., Nemeth, G., & Arborelius, U.P. (1986). Load moments and myoelectric activity when the cervical spine is held in full flexion and extension. *Ergonomics*, 29(12), 1539-1552.
- Harrison, M.F., Neary, P.J., Albert, W.J., Veillette, D.W., McKenzie, N.P., & Croll, J.C. (2007). Physiological effects of night vision goggle counterweights on neck musculature of military helicopter pilots. *Military Medicine*, 172(8), 864-870.
- Harrison, M.F., Neary, P.J., Albert, W.J., Kuruganti, U., Croll, J.C., Chancey, V.C., & Bumgardner, B.A. (2009). Measuring neuromuscular fatigue in cervical spinal musculature of military helicopter aircrew. *Military Medicine*, 174(1), 1183-1189.
- Hermens, H.J., Freriks, B., Merletti, R., Haag, G.G., Stegeman, D., Blok, J., Rau, G., & Disselhorst-Klug, C. (1999). SENIAM 8: European Recommendations for Surface ElectroMyoGraphy, deliverable of the SENIAM project. Roessingh Research and Development b.v., 1999, ISBN: 90-75452-15-2.
- Hodgson, J.A., Pozos, R.S., Feith, S.J., & Cohen, B.S. (1997). Neck and back strain profiles of rotary-wing female pilots. Naval Health Research Centre San Diego, California. MIPR Number: 95MM5559.

- Jonsson, H, Bring, G., Rauchning, W., & Sahlstedt, B. (1991). Hidden cervical spine injuries in traffic accident victims with skull fractures. *Journal of Spinal Disorders*, 4(3), 251-263.
- Kumar, S. (2001). Theories of musculoskeletal injury causation. *Ergonomics*, 44(1), 17-47.
- Landau, D.A., Chapnick, L., Yoffe, N., Azaria, B., Goldstein, L., & Atar, E. (2006). Cervical and lumbar MRI findings in aviators as a function of aircraft type. *Aviation, Space, and Environmental Medicine*, 77(11), 1158–1161.
- Manoogian, S.J., Kenney, E.A., & Duma, S.M. (2006). A literature review of musculoskeletal injuries to the human neck and the effects of head-supported mass worn by soldiers. USAARL No. CR-2006-01, Fort Rucker, AL.
- Marieb, E. N. Human anatomy & physiology. Menlo Park (CA): Benjamin/ Cummings Publishing Company, Inc.; 1998.
- McGill, S.M., Grenier, S., Kavcic, N., & Cholewicki, J. (2003). Coordination of muscle activity to assure stability of the lumbar spine. *Journal of Electromyography and Kinesiology*, 13(4), 353-359.
- McKinnon, C.D., Dickerson, C.R., Laing, A.C.T., & Callaghan, J.P. (2016). Neck muscle activity during simulated in-flight static neck postures and helmet mounted equipment. *Occupational Ergonomics*, 13(3-4), 119-130.
- Meyer, A.J., Patten, C., & Fregly, B.J. (2017). Lower extremity EMG-driven modeling of walking with automated adjustment of musculoskeletal geometry. *PLOS One*. Doi: <https://doi.org/10.1371/journal.pone.0179698>.
- Moroney, S.P., Schultz, A.B., & Miller, J.A.A. (1988). Analysis and measurement of neck loads. *Journal of Orthopaedic Research*, 6(5), 713-720.
- Murray, M., Lange, B., Chreiteh, S.S., Olsen, H.B., Nornberg, E.B., Sogaard, K., & Sogaard, G. (2016). Neck and shoulder muscle activity and posture among helicopter pilots and crew members during military helicopter flights. *Journal of Electromyography and Kinesiology*, 27(1). 10-17.
- Paddan, G.S., & Griffin, M.J. (1988). The transmission of translational seat vibration to the head. 1. Vertical seat vibration. *Journal of Biomechanics*, 21(1), 191-197.
- Panjabi, M.M., Cholewicki, J., Nibu, K., Grauer, J., Babat, L.B., & Dvorak, J. (1998). Critical load of the human cervical spine: an in vitro experimental study. *Clinical Biomechanics*, 13(1), 11-17.
- Parkinson, R.J., & Callaghan J.P. (2007). The role of load magnitude as a modifier of the cumulative load tolerance of porcine cervical spinal units: progress towards a force weighting approach. *Theoretical Issues in Ergonomics Science*, 8(3), 171-184.

- Patwardhan, A.G., Havey, R.M., Ghanayem, A.J., Diener, H., Meadem K.P., Dunlap, B. & Hodges, S.D. (2000). Load-carrying capacity of the human cervical spine in compression is increased under a follower load. *SPINE*, 25(12), 1548-1554.
- Phillips, A.S. (2011). The scope of back pain in navy helicopter pilots. (Naval postgraduate school thesis). Monterey, California.
- Pozzo, T., Berthoz, A., & Lefort, L. (1989). Head kinematic during various motor tasks in humans. *Progress in Brain Research*, 80(1), 377-383.
- Salmon, D.M., Harrison, M.F., & Neary, J.P. (2011). Neck pain in military aircrew and the role of exercise therapy. *Aviation, Space, and Environmental Medicine*, 82(1), 978-987.
- Shannon, S.G., & Mason, K.T. (1997). U.S. Army Aviation Life Support Equipment Retrieval Program: Head and neck injury among night vision goggle users in rotary-wing mishaps. USAARL Report No. 98-02. Fort Rucker, AL.
- Shanahan, D.F., & Reading, T.E. (1984). Helicopter pilot back pain: A preliminary study. *Aviation, Space, and Environmental Medicine*, 55(2), 117-121.
- Smith, S.D. (2004). Collection and characterization of pilot and cockpit buffet vibration in the F 15 Aircraft. *SAFE Journal*, 30(1), 208-218.
- Smith, S.D., & Smith, J.A. (2006). Head and helmet biodynamics and tracking performance in vibration environments. *Aviation, Space, and Environmental Medicine*, 77(4), 388-397.
- Sjogaard, G., & Jensen, B.R. (2006). Low level static exertions. in W.S. Marras, & W. Karwowski (Eds.), *Fundamentals and assessment tools for occupational ergonomics* (2 ed., pp. 14.1-14.13). Boca Raton, FL: CRC Press. Occupational ergonomics handbook, Vol. [1]
- Swartz, E.E., Floyd, R.T., & Cendoma, M. (2005). Cervical spine functional anatomy and the biomechanics of injury due to compressive loading. *Journal of Athletic Training*, 40(3), 155-161.
- Tack, D.W., Bray-Miners, J., Nakaza, E.T., Osborne, A., & Mangan, B. (2014). Griffon helicopter neck strain project. DRDC-RDDC-2014-C228. Defence Research Council of Canada
- Thuresson, M., Ang, B., Linder, J., & Harms-Ringdahl, K. (2003). Neck muscle activity in helicopter pilots: Effect of position and head-mounted equipment. *Aviation, Space, and Environmental Medicine*, 74(5), 527-532.
- Thuresson, M., Ang, B., Linder, J., & Harms-Ringdahl, K. (2005). Mechanical load and EMG activity in the neck induced by different head-worn equipment and neck postures. *Industrial Ergonomics*, 35(1), 13-18.

- Thomae, M.K., Porteous, J.E., Brock, J.R., Allen, G.D., & Heller, R.F. (1998). Back pain in Australian military helicopter pilots: A preliminary study. *Aviation, Space, and Environmental Medicine*, 69(5), 468-473.
- Van den Oord, M.H.A.H., De Loose, V., Meeuwssen, T., Sluiter, J.K., & Frings-Dresen, M.H.W. (2010). Neck pain in military helicopter pilots: Prevalence and associated factors. *Military Medicine*, 175(1), 55-60.
- Van Mameren, H., Drukker, J., Sanches, H., & Beursgens, J. (1990) Cervical spine motion in the sagittal plane (I) range of motion of actually performed movements, an X-ray cinematographic study. *European Journal of Morphology*, 28, 47-68.
- Vasavada, A.N., Li, S., & Delp, S.L. (1998). Influence of muscle morphometry and moment arms on the moment-generating capacity of human neck muscles. *SPINE*, 23(4), 412-422.
- Waljee, A.K., Mukherjee, A., Singal, A.G., Zhang, Y., Warren, J., Calis, U., Marrero, J., Zhu, J., & Higgins, P.D.R. (2013). Comparison of imputation methods for missing laboratory data in medicine. *British Medical Journal Open*, (3) e002847.
- Wickes, S., Scott, J., & Greeves, J. (2005). Epidemiology of flight-related neck pain in Royal Airforce (RAF) aircrew. *Aerospace and Environmental Medicine*, 76(3), 389.
- Wikstrom, B.O. (1993). Health effects of long-term occupational exposure to whole-body vibration: a review. *International Journal of Industry Ergonomics*, 14(4), 273-292.
- Winter, D.A. (2009). Biomechanics and motor control of human movement. John Wiley & Sons.
- Wu, G., et al. (2002). ISB recommendation on definitions of joint coordinate system of various joints for the reporting of human joint motion--part I: ankle, hip, and spine. International Society of Biomechanics. *Journal of Biomechanics*, 35(4), 543-548.
- Wu, G., et al. (2005). ISB recommendation on definitions of joint coordinate systems of various joints for the reporting of human joint motion--Part II: shoulder, elbow, wrist and hand. *Journal of Biomechanics*, 38(5), 981-992.
- Yoganandan, N., Kumaresan, S., Pintar, F.A. (2001). Biomechanics of the cervical spine part 2: Cervical spine soft tissue responses and biomechanical modeling. *Clinical Biomechanics*, 16(1), 1-27.
- Yughdtheswari, M., & Reddy, R.S. (2012), Effect of dorsal neck muscle fatigue on postural control. *Indian Journal of Physiotherapy and Occupational Therapy*, 6(2), 147-149.



## Appendix A: More on kinematic processing

### A.1 Defining local coordinate systems

Head LCS:

$O_h$ : The point directly between the two ear markers

$Y_h$ : A vector from the centre of the head to the top of the head

$Z_{h\text{ temp}}$ : The centre of the head to the right ear

$X_h$ :  $Y_h$  cross  $Z_h$

$Z_h$ :  $X_h$  cross  $Y_h$

Thorax LCS (Wu, 2005):

$O_t$ : Suprasternal notch

$Y_t$ : The line connecting the midpoint between the xiphoid process and T8 and the midpoint between the suprasternal notch and C7, pointing upward

$Z_{t\text{ temp}}$ : The line perpendicular to the plane formed by the suprasternal notch, C7, and the midpoint between the suprasternal notch and T8, pointing to the right

$X_t$ :  $Y_t$  cross  $Z_t$

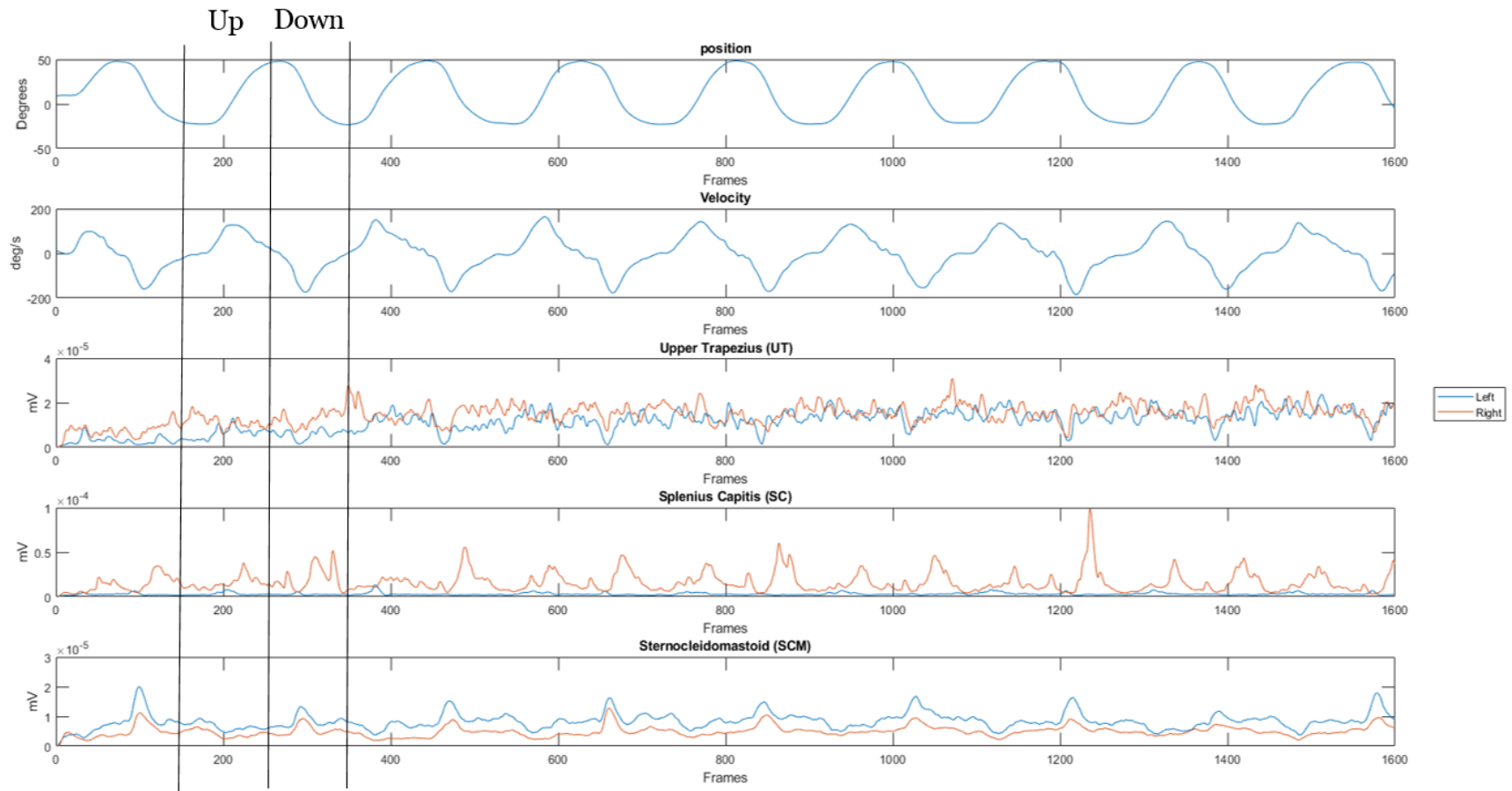
$Z_t$ :  $X_t$  cross  $Y_t$

### A.2 ZYX Rotation Matrix

$$\begin{bmatrix} C_1 C_2 & C_1 S_2 S_3 - S_1 C_3 & S_1 S_3 + C_1 S_2 C_3 \\ S_1 C_2 & S_1 S_2 S_3 + C_1 C_3 & S_1 S_2 C_3 - C_1 S_3 \\ -S_2 & C_2 S_3 & C_2 C_3 \end{bmatrix}$$

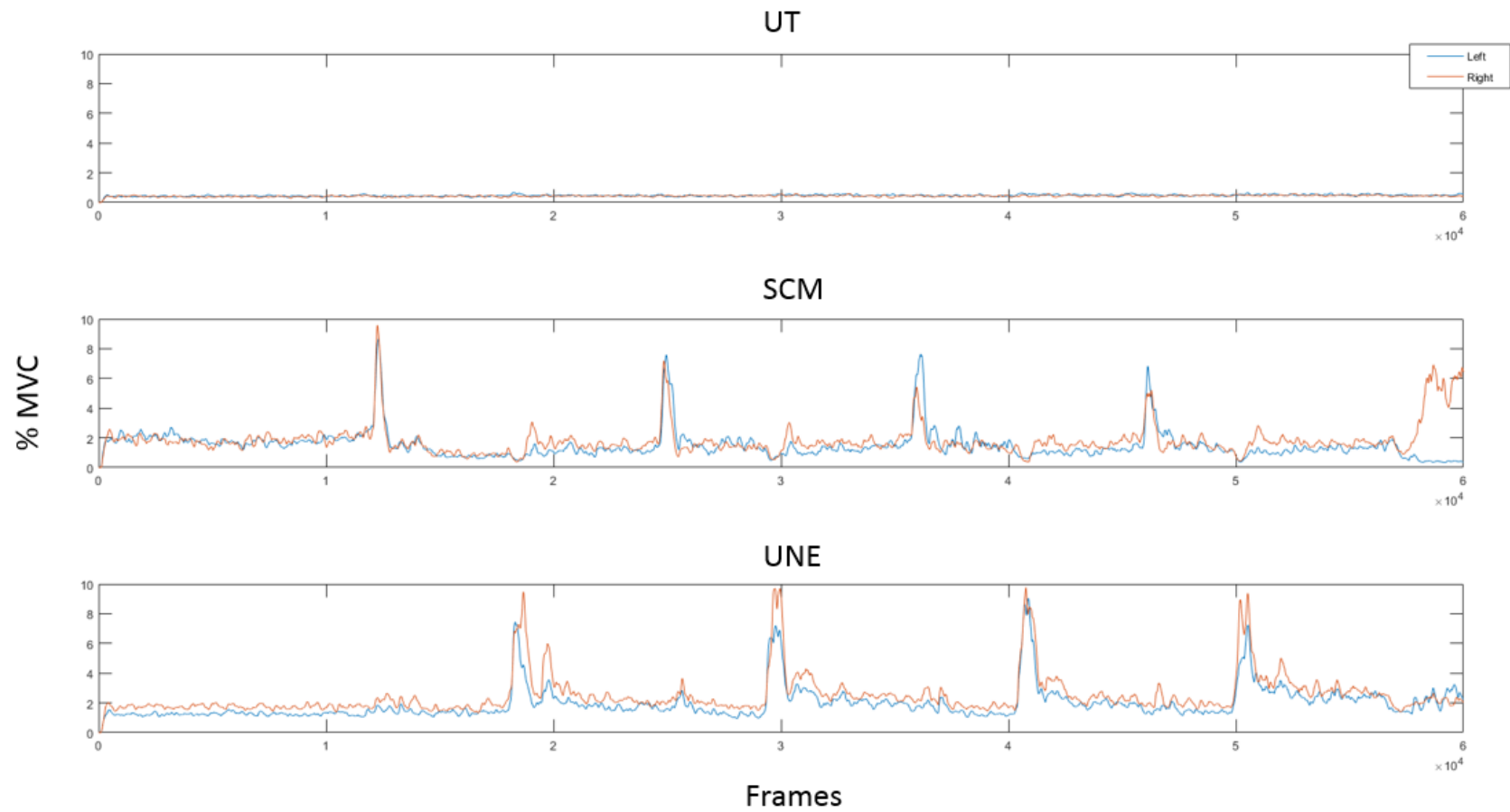
Where C = cos and S = sin

## Appendix B: Visualization of cutting turns



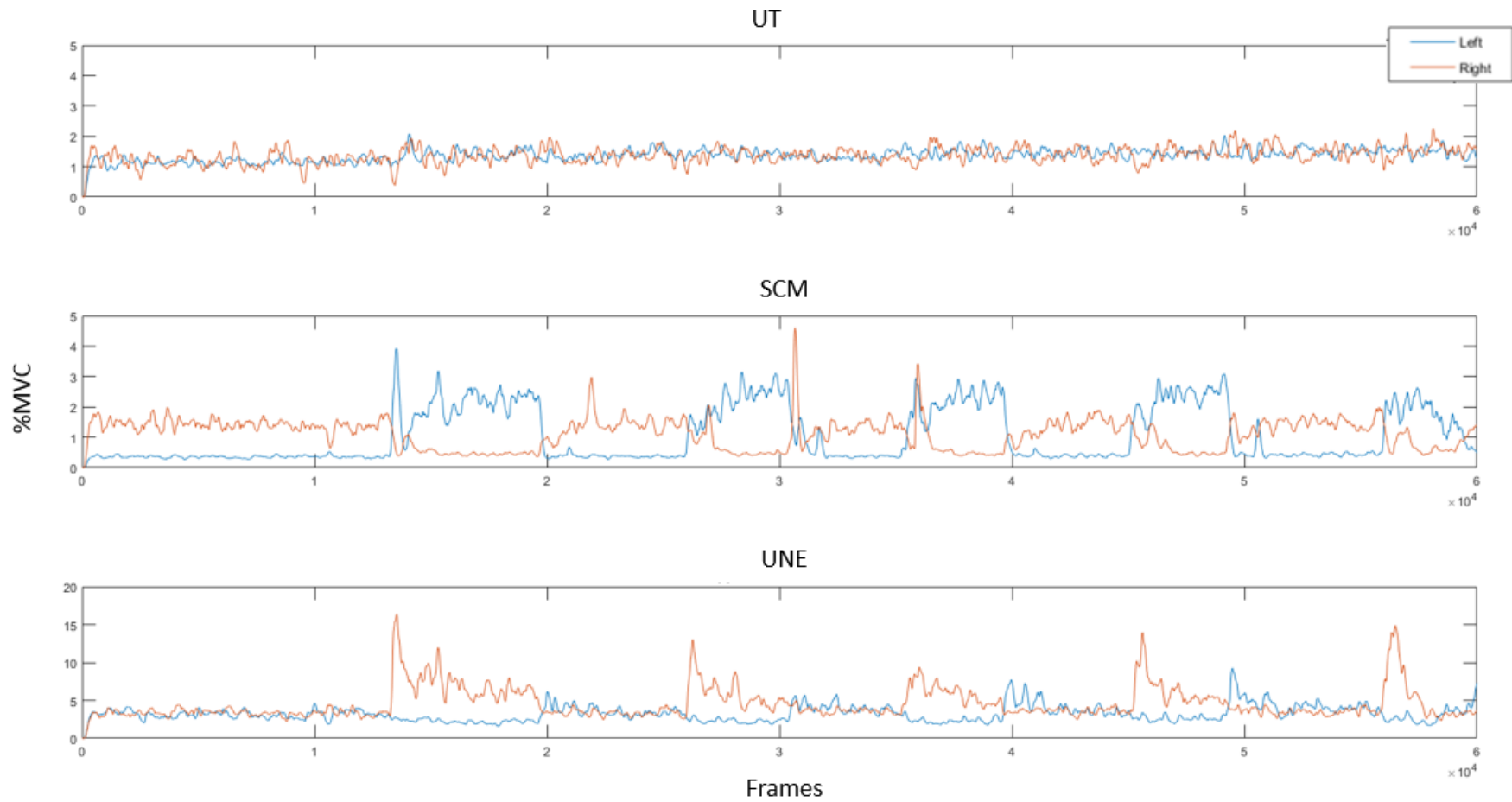
Appendix B: Example of using peak velocity to cut EMG data into up and down turns

## Appendix C-1: Upper trapezius example - pitch



Appendix C-1: An example of upper trap activity during a pitch trial

## Appendix C-2: Upper trapezius example - yaw



Appendix C-2: An example of upper trap activity during a yaw trial

## Appendix D: Full Performance Measures

### Amplitude

In the pitch trajectory, there was a main effect of amplitude on TAT ( $F(1,29) = 292.016$ ,  $p \leq 0.000$ ,  $\eta_p^2 = 0.910$ ), HT ( $F(1,29) = 16.175$ ,  $p \leq 0.000$ ,  $\eta_p^2 = 0.358$ ), and number of targets acquired ( $F(1,29) = 229.503$ ,  $p \leq 0.000$ ,  $\eta_p^2 = 0.888$ ). Similar results were seen in the yaw trajectory, where there was a main effect of amplitude on TAT ( $F(1,29) = 152.816$ ,  $p \leq 0.000$ ,  $\eta_p^2 = 0.840$ ), HT ( $F(1,29) = 6.008$ ,  $p = 0.021$ ,  $\eta_p^2 = 0.172$ ) and number of targets acquired ( $F(1,29) = 133.092$ ,  $p \leq 0.000$ ,  $\eta_p^2 = 0.821$ ). Pairwise comparisons revealed TAT and HT were significantly longer for far conditions compared to near conditions. Number of targets acquired and error rate were both significantly higher in near conditions (**Figures 42 & 43**)

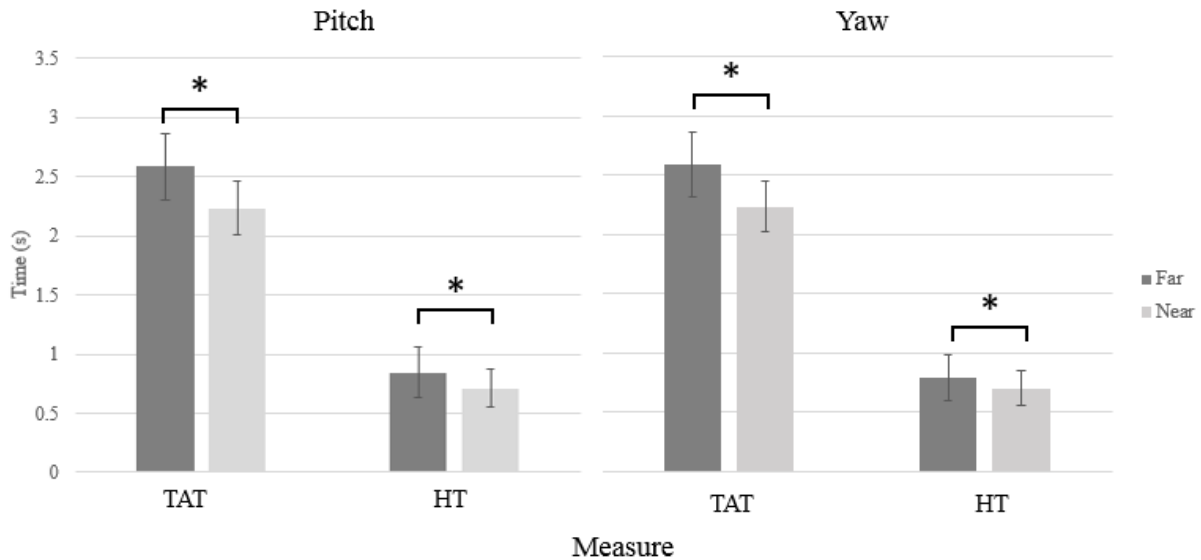


**Figure 42:** The effect of amplitude on TAT (time to acquire target) and HT (honing time) in the pitch and yaw trajectories

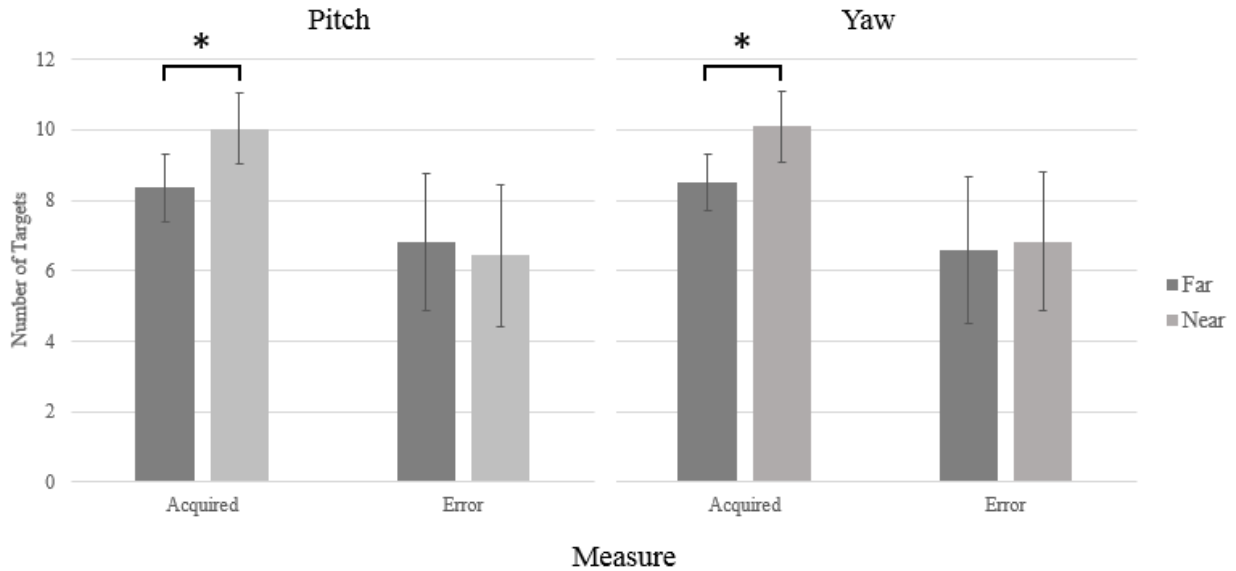


**Figure 43:** The effect of amplitude on number of targets acquired and error rate in the pitch and yaw trajectories

### *HSM Condition*

There was a main effect of condition in the pitch trajectory on TAT ( $F(3,87) = 3.211, p = 0.027, \eta_p^2 = 0.100$ ), and number of targets acquired ( $F(3,87) = 5.938, p = 0.001, \eta_p^2 = 0.170$ ). Similarly, in the yaw condition there was a main effect of condition on TAT ( $F(3,87) = 6.667, p \leq 0.000, \eta_p^2 = 0.187$ ), and number of targets acquired ( $F(3,87) = 9.783, p \leq 0.001, \eta_p^2 = 0.252$ ). Pairwise comparisons were not powered to detect differences in TAT in the pitch direction. In the yaw trajectory, TAT was significantly different in hNVG compared to hOnly and hCW, however it was not different from hCWL (**Figure 44**). For number of targets acquired, hNVG and hCW were significantly different and had a mean difference of 0.73s in the pitch trajectory. In the yaw trajectory, hCW was significantly lower than all other conditions, with a maximum difference of 0.88s.

### Interactions

There was no significant condition by amplitude interaction effects for any performance measures.

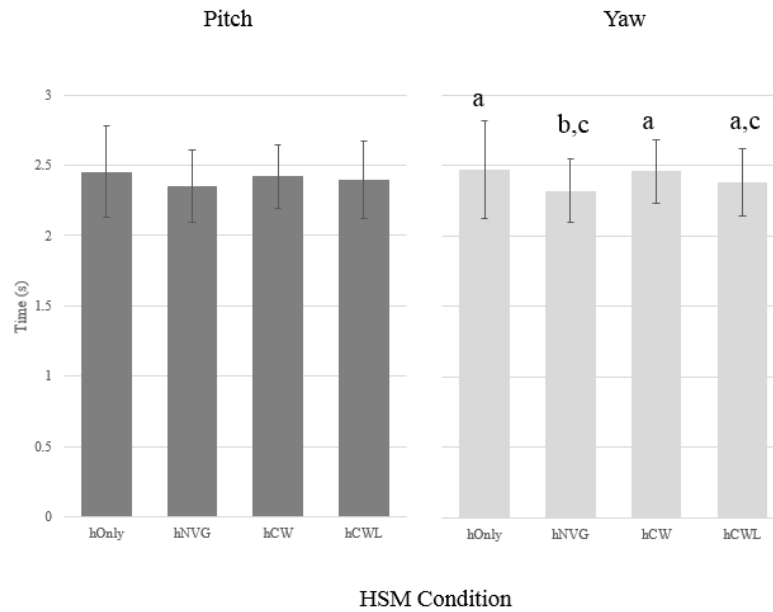


**Figure 44:** The effect of HSM condition on TAT (time to acquire target) in the pitch and yaw trajectories. Different letters indicate conditions are significantly different.